



Universität für Bodenkultur Wien

Department Wasser-Atmosphäre-Umwelt (WAU)

Institut für Meteorologie (BOKU-Met)

Vorstand: O. Univ.-Prof. Dr. Helga Kromp-Kolb

Betreuer: Ao. Univ.-Prof. Mag. Dr. Philipp Weihs

FERNERKUNDLICHE UNTERSUCHUNG VON
TROCKENSTRESS UND SCHÄTZUNG VON
VEGETATIONSPARAMETERN FÜR LAND- UND
FORSTWIRTSCHAFTLICHE ANWENDUNGSGEBIETE

Dissertation
zur Erlangung des Doktorgrades
an der Universität für Bodenkultur Wien

Eingereicht von
Mag. Katja Richter

Wien, Juni 2009

Danksagung

Die vorliegende Dissertation entstand teilweise im Rahmen des Projekts "Crop Drought Stress Monitoring by Remote Sensing" (DROSMON) an der Universität für Bodenkultur, Wien, Österreich, das vom österreichischen Fonds zur Förderung der wissenschaftlichen Forschung (FWF, Projekt Nr. P17647-N04) finanziert wurde. Im Weiteren wurde sie durch das „Participatory multi-Level EO-assisted tools for Irrigation water management and Agricultural Decision-Support“ (PLEIADeS) Projekt der Universität Federico II di Napoli, Italien, finanziert.

Mein besonderer Dank gilt Prof. Dr. Philipp Weihs für die gute durchgehende Betreuung der Arbeit. Im Weiteren gilt mein Dank Rita Linke, Pablo Rischbeck, Prof. Werner Schneider, Josef Eitzinger, Franz Suppan und allen anderen Kollegen des DROSMON Projekts für ihre große Unterstützung. Insbesondere bedanke ich mich bei Prof. Guido D'Urso, der mir Rahmen und Ideen für die Weiterführung der Dissertation gegeben hat. Großer Dank gilt auch Clement Atzberger und Wim Timmermans für die gute Zusammenarbeit und ihre motivierende Mitarbeit an den gemeinsamen Publikationen.

Außerdem danke ich Frédéric Baret und den Kollegen des INRA, Avignon, für die Bereitstellung der verwendeten Reflexionsmodelle und den wissenschaftlichen Austausch.

Vielen Dank aber im Besonderen an meine Familie, die guten Freunde und Francesco.

Abstract

The availability of high spatial and temporal resolution optical remote sensing data allows the estimation of biophysical parameters for a wide territorial coverage. This is of essential importance for ecological, hydrological, climatic and other applications, giving the basis for a sustainable management of agricultural and forestry resources.

The present studies analysed the use of physically based approaches for the quantification of the Leaf Area Index (LAI) and other important vegetation characteristics. Comparisons with traditional empirical models, using vegetation indices, are performed.

Furthermore, the relevance of canopy reflectance models for precision farming applications, such as the detection of drought stress zones, monitoring of vegetation growth and dynamic and energy balance modelling, is highlighted. The models were validated and moreover, the physiological reaction of plants to drought stress and recovery was analysed by means of optical leaf reflectance field and laboratory measurements. Additionally, the configuration of the forthcoming ESA Sentinel-2 mission was tested in an operative perspective.

The remotely sensed and ground based data used in the studies were acquired, amongst others, in the framework of the “Crop Drought Stress Monitoring by Remote Sensing” (DROSMON) project of the University of Natural Resources and Applied Life Sciences, Vienna.

Summarizing the results of all studies, it could be shown that optical remote sensing is a valuable tool rather for estimating structural changes of the canopy (such as LAI) than for an early drought stress detection. The physically based estimation of surface parameters could be performed for a wide range of conditions, i. e. for different geographical locations, sensors and vegetation types, and in a satisfyingly accurate way using turbid medium modelling schemes.

The method is therefore recommended for an operational quantification of biophysical products or for the determination of medium or longer term drought stress in agricultural and forestry applications.

Keywords: vegetation parameters, LAI, model inversion, drought stress, optical remote sensing

Kurzfassung

Der Einsatz fernerkundlicher Methoden ermöglicht die flächenhafte Bestimmung biophysikalischer Vegetationsparameter in hoher räumlicher und zeitlicher Auflösung. Diese stellen bedeutende Informationen u. a. für die Bereiche der Ökologie, Hydrologie und Klimatologie dar und schaffen somit die Basis für ein nachhaltiges Management in Land- und Forstwirtschaft.

Die vorliegenden Studien analysierten die Verwendung physikalisch basierter Modelle für die Quantifizierung von Blattflächenindex (LAI) und anderer Vegetationsparameter im Vergleich zu empirischen Ansätzen. Insbesondere wurde die Bedeutung von Bestandesreflexionsmodellen für wichtige Precision Farming-Anwendungen wie Trockenstresszonierung, Beobachtung des Wachstums und der Dynamik der Vegetation und Energiebilanzmodellierung aufgezeigt. Im Weiteren wurde die Konfiguration zukünftiger Satelliten (Sentinel-2) hinsichtlich ihrer Eignung für operative Anwendungen getestet. Die Modelle wurden evaluiert und außerdem die physiologische Reaktion der Pflanzen auf Trockenstress und Erholung anhand spektraler Signale auf Blattebene untersucht.

Die in den Studien verwendeten hyper- und multispektralen Sensordaten und Bodenmessungen wurden im Rahmen des „Crop Drought Stress Monitoring by Remote Sensing“ (DROSMON) Projekts der Universität für Bodenkultur, Wien und verschiedener anderer Feldkampagnen erhoben.

Zusammenfassend konnte gezeigt werden, dass die Fernerkundung vom sichtbaren bis zum mittleren Infrarotbereich eine Eignung eher für die Erkennung struktureller Veränderungen des Bestands, z. B. LAI, als für die Trockenstressfrüherkennung aufweist. Die physikalisch basierte Schätzung von Vegetationsparametern kann mit zufriedenstellender Genauigkeit und auch unter diversen Bedingungen, d. h. in unterschiedlicher geographischer Lage, für eine Reihe von Sensortypen und verschiedene Vegetationsarten, durch Inversion von homogenen Turbid Medium-Modellen durchgeführt werden.

Die verwendeten Methoden werden daher für eine operative Quantifizierung von biophysikalischen Vegetationsparametern bzw. für die Bestimmung von mittel- und langfristigem sowie potentiellstem Trockenstress in Land- und Forstwirtschaft sehr empfohlen.

Schlüsselwörter: Vegetationsparameter, Blattflächenindex, Modellinversion, Trockenstress, optische Fernerkundung

Inhaltsverzeichnis

1	Einleitung	6
1.1	Bedeutung der Fernerkundung für Land- und Forstwirtschaft	6
1.2	Schätzung von Vegetationsparametern	7
1.3	Fernerkundliche Bestimmung von Trockenstress	9
2	Überblick über die Publikationen	10
2.1	Thematischer Zusammenhang zwischen den Publikationen	11
2.2	Schlussfolgerung und Ausblick	15
3	Literaturverzeichnis	17
4	Publikationen	20
4.1	Publikation I	20
4.2	Publikation II	39
4.3	Publikation III	52
4.4	Publikation IV	71
4.5	Publikation V	94
5	Anhang (Bestätigung der Publikation I)	106
6	Lebenslauf/CV	107

1 Einleitung

Zur Einführung wird ein Überblick zum großen Themenfeld der fernerkundlichen Untersuchungen in Land- und Forstwirtschaft gegeben, in das die vorliegende Dissertation einzuordnen ist. Die in den Studien bearbeitete Thematik analysiert die Fernerkundung als Mittel für Untersuchungen von Trockenstress und insbesondere zur Schätzung von Vegetationsparametern für land- und forstwirtschaftliche Anwendungsbereiche.

1.1 Bedeutung der Fernerkundung für Land- und Forstwirtschaft

Vegetation hat die Eigenschaft, elektromagnetische Strahlung in bestimmten Wellenlängenbereichen zu reflektieren, zu absorbieren, zu transmittieren und auch zu emittieren. Dies wird von der Fernerkundung, die als berührungsfreie Erfassung und Messung von Objekten der Erdoberfläche definiert ist (Barrett and Curtis, 1976), ausgenutzt. Für fernerkundliche Beobachtungen werden einerseits passive Sensoren eingesetzt, die entweder die von der Erdoberfläche oder Atmosphäre reflektierte Solarstrahlung (z. B. anhand Multispektralscanner) messen oder die Wärmestrahlung von Objekten (z. B. anhand Thermalkameras) untersuchen. Die zweite Möglichkeit sind aktive Aufnahmesysteme, wobei die Rückstreuung von Objekten, z. B. anhand Radar- oder Lasersystemen, gemessen wird.

Fernerkundliche Aufnahmen von flugzeug- oder satellitenbasierten Plattformen eröffnen den besonderen Vorteil der wiederholten großflächigen Erfassung von Gebieten. Dies bringt eine hohe Kosteneffizienz gegenüber arbeits- und zeitintensiven bodengebundenen Messungen.

Die hier vorliegende Arbeit konzentriert sich auf die multi- und hyperspektrale optische Fernerkundung, wobei die Wellenlängenbereiche des sichtbaren Lichts, des nahen Infrarots (IR) und teilweise des mittleren IR genutzt werden, um die räumliche und die zeitliche Dynamik der terrestrischen Biosphäre zu erfassen.

In land- und forstwirtschaftlichen Forschungs- und Anwendungsbereichen wird die Fernerkundung eingesetzt, um anhand des spektralen Reflektionsverhaltens verschiedene Pflanzenspezies zu unterscheiden und biophysikalische Vegetationsparameter zu bestimmen. In der praktischen Anwendung kann die fernerkundliche Bestimmung von biophysikalischen Parametern ein nachhaltiges landwirtschaftliches Management unterstützen und somit das Ertragspotential von Anbauflächen deutlich erhöhen. Eine große Bedeutung hat in dieser Hinsicht bereits das sogenannte „Precision Farming“ (Präzisionslandwirtschaft) erlangt, wobei z. B. Dünge- und Pflanzenschutzmittel nicht mehr einheitlich, sondern räumlich differenziert, je nach Bedarf auf einer Anbaufläche eingesetzt werden (SCHUELLER 1992). Ein weiteres Anwendungsbeispiel sind Programme zur Bewässerungsberatung (DE MICHELE et al. 2009), für die Informationen über die kleinräumliche Verteilung und die zeitliche Veränderung bestimmter Vegetationsparameter Voraussetzung sind.

Auch im Forstbereich wird anhand fernerkundlicher Kartierung von Baumarten und Waldstruktur, Baumvitalität bzw. Baumschäden zu einer nachhaltigeren Bewirtschaftung beigetragen (FRANKLIN 2001, ATZBERGER 2003).

In den letzten Jahrzehnten wurde eine große Anzahl neuer Satelliten gestartet (ESA 2008). Dennoch war es bis heute trotz großer technischer Fortschritte nicht möglich, hohe räumliche mit hoher zeitlicher Auflösung zu verbinden. Somit sind Daten von räumlich hochauflösenden Sensoren (d. h. 10-30 m, z. B. Landsat TM, SPOT) nur in mäßiger zeitlicher Auflösung verfügbar (d. h. 15-30 Tage), während Daten mit niedriger räumlicher Auflösung (250-1000 m, z. B. Aqua/Terra MODIS, SPOT/VGT) viel häufiger zugänglich sind (ein bis drei

Tage) (BSAIBES et al. 2009). Eine Lösung ist die Kombination verschiedener Sensoren, was aber oft zu Schwierigkeiten in der Vergleichbarkeit der abgeleiteten Produkte durch sensorspezifische Charakteristiken (z. B. räumliche und spektrale Auflösung, spektrale Responsfunktionen, u. a.) führt (SOUDANI et al. 2006). Eine weitere Möglichkeit bietet die Datenfusion von Sensoren verschiedener räumlicher und zeitlicher Auflösung, z. B. von MERIS und Landsat. Hierbei werden anhand Spectral Unmixing Techniken die häufig verfügbaren Daten von MERIS auf die höhere geometrische Genauigkeit von Landsat gerechnet (ZURITA-MILLA et al. 2007).

Um diese Schwierigkeiten zu erleichtern und insbesondere um den ständig steigenden Anforderungen der Nutzer entgegenzukommen, wurden bereits neue Missionen gestartet oder sind für die nahe Zukunft geplant. Eine wichtige Rolle spielen dabei die Sentinel-Satelliten des Global Monitoring for Environment and Security (GMES) Programms der European Space Agency (ESA). Für die operative Beobachtung der Landbedeckung und Landnutzung ist der multispektrale Sentinel-2 Sensor vorgesehen, der ab dem Jahr 2012 Daten in mittlerer räumlicher Auflösung (10–60 m) in 13 Spektralkanälen (im Wellenlängenbereich des sichtbaren Lichts bis zum mittleren IR) liefern soll (MARTIMORT 2007).

Mit der durch die neuen Satelliten erwarteten Verbesserung der Datenlage eröffnen sich vielfältige Möglichkeiten im Bereich der Landkartierung, im Umweltmonitoring sowie für die ökologische Prozessskalierung von lokaler zu globaler Ebene (SOUDANI et al. 2006). Einerseits können bereits existierende Modelle für die Quantifizierung von biophysikalischen Vegetationsparametern evaluiert und andererseits neue Algorithmen entwickelt werden.

1.2 Schätzung von Vegetationsparametern

Charakteristika und raumzeitliche Verteilungsmuster von biophysikalischen Vegetationsparametern helfen wichtige Prozesse und Wechselwirkungen des Systems Boden – Pflanze - Atmosphäre zu beschreiben und sind daher bedeutende Eingangsgrößen für ökologische, hydrologische, klimatische und andere Modellansätze (RUNNING et al. 1989, ATZBERGER 2000).

Der wohl am intensivsten in ökologischen Feld- und Modellierungsstudien untersuchte biophysikalische Vegetationsparameter ist der Blattflächenindex („leaf area index“, LAI), der als die (einseitige) Oberfläche sämtlicher grüner Blätter bzw. Nadeln über einer bestimmten Bodenfläche definiert ist (BSAIBES et al. 2009). Der Blattflächenindex kann in verschiedenen räumlichen Skalen gemessen, analysiert und modelliert werden. Eine besondere Schlüsselrolle spielt der LAI für die Beschreibung des Vegetationszustands. Er ist somit ein wichtiger Indikator für Prozesse des Bodenwasserhaushalts, z. B. der Verdunstungsleistung des Bestands, der Interzeption oder der aerodynamischen Verhältnisse (ASNER et al. 2003). Der Parameter wird in einer Vielzahl von physiologischen, klimatologischen und biochemischen Studien benötigt. Zum Beispiel ermöglicht die Bestimmung von LAI mittels fernerkundlichen Methoden die Einführung der räumlichen Dimension in die Wachstumsmodellierung (GUERIF and DUKE 1998). Des Weiteren ist LAI einer der wichtigsten Eingangsparameter für Energiebilanzmodelle (KUSTAS and NORMAN 1996).

Die Bestimmung des LAI oder anderer Parameter, wie z. B. Blattchlorophyllgehalt (C_{ab}), mittlerer Blattwinkel (ALA), Bedeckungsgrad (fCover) oder ein Bodenfaktor (α_{soil}) aus spektralen Signaturen ist jedoch kein einfaches Verfahren, da ebenso eine Vielzahl von anderen Parametern (V) sowie einige Randbedingungen (θ) das Spektrum der Vegetation (ρ_λ) beeinflussen (ATZBERGER 2003):

$$\rho_\lambda = f(V_1, \dots, V_n, \theta)$$

Prinzipiell gibt es zwei Gruppen von Optionen für die Bestimmung der Vegetationsparameter aus spektralen Signalen (ATZBERGER 2003):

- 1 Empirisch-statistische Verfahren.
- 2 Inversion physikalisch basierter Modelle.

Zu (1) gehören Korrelationen zwischen Bandkombinationen verschiedener Spektralanteile (Vegetationsindizes, VIs) und den zu schätzenden Parametern (BARET and GUYOT 1991; JI and PETERS 2007), die anhand Feldkampagnen kalibriert werden müssen (DORIGO et al. 2007).

Die Anwendung von physikalisch basierten Reflexionsmodellen (2) eröffnet neue potentielle Möglichkeiten, da die Genauigkeit der Parameterschätzung durch das Einbeziehen von a-priori-Wissen sowie der gesamten spektralen Information erhöht werden kann. Es kommt einerseits zu keinem Informationsverlust durch Verhältnisbildung (wie bei VIs), und andererseits werden Randbedingungen (θ), wie z. B. Beleuchtungs- und Sichtgeometrie, berücksichtigt. Die Modelle können, basierend auf physikalischen Prinzipien, die spektrale bidirektionale Reflexion von Vegetationsbeständen berechnen. Die Modellierungsstrategien reichen von Turbid Medium-Ansätzen, über geometrisch-optische, hybride bis zu Monte Carlo Ray-Tracing, das auf der dreidimensionalen (3-D) Beschreibung des Bestands basiert (ATZBERGER 2003). Ein Überblick zu diesem Thema findet sich in der Arbeit von GOEL (1988) oder in PINTY et al. (2004). Generell gilt, je komplexer die Modellierungsstrategie, desto genauer kann die spektrale Reflexion auch modelliert werden und z. B. auch die ungleichmäßige Verteilung der Blätter / des Pflanzenbestands („clumping“) berücksichtigen. Allerdings erfordert ein sehr genaues Modell auch eine große Menge an Eingangsparametern sowie eine hohe Rechenzeit.

Für die anwendungsorientierte Forschung stellen Turbid Medium-Ansätze einen guten Kompromiss zwischen Parametrisierungsaufwand und Simulationsgenauigkeit dar. Ein Beispiel ist das bereits vielfach getestete Blatt- und Bestandesreflexionsmodell PROSPECT+SAILH (PROSAILH) (JACQUEMOUD and BARET 1990, VERHOEF 1984, VERHOEF 1985) für die Landwirtschaft oder das Zwei-Schichten Modell ACRM (KUUSK 2001) für Simulationen im Forstbereich. Das PROSAILH Modell wird bereits operativ für die Schätzung von Vegetationsprodukten eingesetzt (BARET et al. 2007).

Um aus den fernerkundlich erfassten spektralen Signalen die jeweiligen Parameter zu schätzen, ist die Inversion der Modelle notwendig. Es gibt verschiedene Arten von Inversionsstrategien, u. a.:

- „Look-up table“ (LUT) Verfahren (z. B. DARVISHZADEH et al. 2008, KOETZ et al. 2005, WEISS et al. 2000).
- Iterative numerische Minimierungen (z. B. JACQUEMOUD et al. 1995, MERONI et al. 2004).
- Künstliche Neuronale Netze (NN) (z. B. ATZBERGER 2004, SCHLERF and ATZBERGER 2006).
- Support-Vektor-Maschinen (z. B. CAMPS-VALLS et al. 2009, DURBHA et al. 2007).
- Bayes'sche Verfahren (z. B. YAO et al. 2008).

Die Methoden sollen hier nicht im Detail erklärt und diskutiert werden. Es ist aber anzumerken, dass die LUT-Strategie die wohl einfachste aber auch robusteste und gemeinsam mit den NN die effektivste Methode für operative Anwendungen darstellt (BARET and BUIS 2008). Für eine ausführliche Diskussion der wichtigsten Inversionsstrategien wird auf KIMES et al. (2000) oder BARET and BUIS (2008) verwiesen.

Eine grundlegende Schwierigkeit bei der Inversion von Reflexionsmodellen besteht darin, dass sehr unterschiedliche Parameterkombinationen zu (fast) identischen spektralen Signaturen führen können. Für das sogenannte „ill-posed“ Problem (COMBAL et al. 2002) werden in der Literatur verschiedene Lösungsansätze aufgezeigt, z.B. der Einsatz von a priori Informationen (COMBAL et al. 2002) oder die Verwendung sogenannter Objektsignaturen (ATZBERGER 2004).

1.3 Fernerkundliche Bestimmung von Trockenstress

Wassermangel, durch Klima- oder Bodeneigenschaften hervorgerufen, führt zu pflanzlichem Trockenstress und ist eines der Hauptprobleme für die weltweite landwirtschaftliche Produktion. Pflanzen reagieren entsprechend der Dauer der Trockenphase mit reversiblen (bei kurzfristigem Stress) oder irreversiblen (bei längerfristigem Stress) Veränderungen. Eine der ersten Reaktionen auf Wassermangel ist das Absinken des Turgordrucks in den Blatzellen und die Schließung der Spaltöffnungen, was zu einer Erhöhung der Blattoberflächentemperatur führt (CASA 2003). Solche Variationen der Bestandstemperatur können sehr gut mit Sensoren, die im thermalen infraroten (TIR) Bereich des elektromagnetischen Spektrums empfindlich sind, erfasst werden (z. B. GONZALEZ-DUGO et al. 2005). Mithilfe von Energiebilanzmodellen kann dann die Partitionierung der eingestrahlten Sonnenenergie in Energieflüsse fühlbarer und latenter sowie in Boden- bzw. Bestandswärmeströme simuliert werden (z. B. KUSTAS and NORMAN 1996).

Eine Schwierigkeit für die Trockenstressfrüherkennung auf operationeller Basis bzw. im Kontext von Precision Farming ist die unzureichende Verfügbarkeit von TIR Daten in hoher räumlicher Auflösung (d. h. mindestens 10–20 m). Insbesondere für sehr heterogene landwirtschaftliche Gebiete bzw. für Analysen der Inner-Feldvariabilität ist eine solche Mindestauflösung aber erforderlich.

Mittel- oder längerfristiger Trockenstress dagegen führt zu strukturellen Veränderungen der Bestandsarchitektur, z. B. Verringerung des LAI, die mithilfe Methoden der optischen Fernerkundung erfasst werden können (CASA 2003). Optische Sensoren – empfindlich im Spektralbereich des sichtbaren Lichts bis zum mittleren IR - haben gegenüber den thermalen außerdem den Vorteil der häufigen Verfügbarkeit in hoher räumlicher Auflösung.

2 Überblick über die Publikationen

Folgende fünf Publikationen wurden in der vorliegenden Dissertation zusammengefasst:

Publikation I:

Katja Richter, Clement Atzberger, Francesco Vuolo, Guido D'Urso, and Philipp Weihs (2009): Experimental assessment of the Sentinel-2 band setting for RTM-based LAI retrieval of sugar beet and maize. *Canadian Journal of Remote Sensing*, accepted for publication.

Publikation II:

Katja Richter and Wim Timmermans (2009): Physically based retrieval of crop characteristics for improved water use estimates. *Hydrology and Earth System Sciences* 13: 663-674.

Publikation III:

Katja Richter, Pablo Rischbeck, Josef Eitzinger, Werner Schneider, Franz Suppan, and Philipp Weihs (2008): Plant growth monitoring and potential drought risk assessment by means of Earth Observation data. *International Journal of Remote Sensing* 29 (17-18): 4943–4960.

Publikation IV:

Philipp Weihs, Franz Suppan, Katja Richter, Richard Petritsch, Hubert Hasenauer, and Werner Schneider (2008): Validation of forward and inverse modes of a homogeneous canopy reflectance model. *International Journal of Remote Sensing* 29 (5): 1317–1338.

Publikation V:

Rita Linke, Katja Richter, Judith Haumann, Werner Schneider, and Philipp Weihs (2008): Occurrence of repeated drought events: can repetitive stress situations and recovery from drought be traced with leaf reflectance? *Periodicum Biologorum* 110 (3): 219-229.

Kategorien und Bewertung der Zeitschriften:

Publikation I wurde in der offiziellen Zeitschrift der Canadian Remote Sensing Society, dem „Canadian Journal of Remote Sensing“ publiziert.

- Kategorie: Remote Sensing (12/14)
- Journal Impact Factor: 0.658

Publikation II wurde im “Interactive Open Access Journal of the European Geosciences Union”, dem “Hydrology and Earth System Sciences” publiziert.

- Kategorie: Geosciences, multidisciplinary (26/127), Water Resources (2/59)
- Journal Impact Factor: 2.27

Publikationen III und IV wurden in der offiziellen Zeitschrift der “Remote Sensing and Photogrammetry Society“, dem „International Journal of Remote Sensing“ publiziert.

- Kategorie: Remote Sensing (9/14), Imaging Science & Photographic Technology (5/11)
- Journal Impact Factor: 0.987

Publikation V wurde im der Zeitschrift der „Croatian Society of Natural Sciences“, im „Periodicum Biologorum“ publiziert.

- Kategorie: Biology (66/71)
- Journal Impact Factor: 0.262

2.1 Thematischer Zusammenhang zwischen den Publikationen

Im Folgenden werden die Ziele, Methoden und Ergebnisse der fünf Studien jeweils kurz vorgestellt und danach in ihrem Zusammenhang erläutert.

Publikation I

In Publikation I wurde das Potential des zukünftigen ESA Satelliten Sentinel-2 für die Schätzung des LAI von Zuckerrüben und Mais getestet. Dabei wurde untersucht, ob die Bestimmung von LAI anhand einer LUT-basierten Inversion des PROSAILH Modells mit einer Genauigkeit von $\leq 10\%$ (definiert vom GMES-Komitee) durchführbar ist. Die Studie basiert (u. a.) auf Daten der ESA AgriSAR 2006 Kampagne in Mecklenburg-Vorpommern (Deutschland), wobei hyperspektrale CASI Daten aufgenommen und entsprechend der spektralen Responsefunktion von Sentinel-2 aufbereitet wurden. Zu Validierungszwecken wurden bodengebundene LAI Messungen anhand des LAI-2000 Plant Canopy Analyzer Instruments durchgeführt. Der LUT-Ansatz wurde mit zwei weiteren Inversionsmethoden (iterative Minimierung und NN) verglichen und außerdem in einer alternativen Bandkonfiguration angewendet.

Für Zuckerrüben konnte die erforderliche Schätzungsgenauigkeit getroffen werden (8-9 %), während sie für Mais verfehlt wurde (16-22 %). Auch die alternativen Inversionsstrategien konnten keine Verbesserung der Ergebnisse erzielen. Der LUT-Ansatz erwies sich als die stabilste und robusteste Inversionsmethode. Des Weiteren wurde die günstige Position der Spektralkanäle des Sentinel-2 Sensors bestätigt.

In der Schlussfolgerung wird die verwendete Schätzungsmethode für eine operative Auswertung der Sentinel-2 Daten dennoch empfohlen, da sie einen guten Kompromiss zwischen Genauigkeit und Modellkomplexität bietet. Um den Genauigkeitsansprüchen der potentiellen Nutzer zu genügen, sollte allerdings für Feldfrüchte mit der Neigung zum „clumping“ - wie Mais im frühen Wachstumsstadium - ein komplexerer Modellansatz gewählt werden.

Publikation II

In Publikation II wird die gleiche LUT-basierte Schätzungsmethode wie in Publikation I für LAI und fCover angewendet. Zusätzlich werden die Parameter mit einem empirischen Modell, d. h. mit der Beziehung zwischen den Parametern und dem skalierten „Normalized Difference Vegetation Index“ (NDVI), bestimmt. Beide Arten von Schätzungen wurden in Kartenform als Eingangsgrößen für ein Energiebilanzmodell (TSEB) verwendet, und die simulierten Energieflüsse wurden auf Basis von Landnutzungsklassen analysiert. Die Studie stützte sich auf Daten der Messkampagne SPARC 2004 in Barrax, Spanien, wobei thermale und optische hyperspektrale Daten erhoben sowie Bodenmessungen der Parameter und Energieflüsse durchgeführt wurden.

Im direkten Vergleich mit den Bodenmessungen übertraf die physikalische die empirische Schätzungsmethode in der Genauigkeit. Für den LAI erzielte die physikalische Schätzung einen mittleren quadratischen Fehler (RMSE) von 0.79, und für fCover einen RMSE von 0.12, während das empirische Modell für LAI nur einen RMSE von 1.44 und für fCover von 0.15 erreichte. Des Weiteren konnten insbesondere für die Landnutzungsklassen mit einer hohen Vegetationsbedeckung fühlbare und latente Energieflüsse sowie der

Bodenwärmestrom realistischer mit den Eingangsparametern des physikalischen Modells simuliert werden.

Als Schlussfolgerung wird für die Energiebilanzmodellierung von Vegetationsflächen die Inversion eines physikalischen Modells für die Quantifizierung von LAI und fCover gegenüber einem empirischen Modell empfohlen. Die höhere Genauigkeit des physikalischen Modells erhöht ebenso die Präzision der Simulation von Energieflüssen und erfordert außerdem keine Kalibrierung in Abhängigkeit der Vegetationstypen.

Publikation III

In Publikation III wurde ebenso die LUT-basierte Inversionsmethode am PROSAILH Modell durchgeführt, um die räumliche Variation von Vegetations- und Bodenparametern innerhalb eines Weizenfeldes (*Triticum Durum*) aus hyperspektralen Hymap Daten zu schätzen. Die Studie wurde im Marchfeld, Österreich, im Rahmen des „Crop Drought Stress Monitoring by Remote Sensing“ (DROSMON) Projekts der Universität für Bodenkultur, Wien, durchgeführt. Im Marchfeld herrscht die Besonderheit von Sandsträngen ehemaliger Donaumäander, die die Felder durchziehen und dadurch die Wasserverfügbarkeit für die Feldfrüchte verringern.

Bodenbedingter Trockenstress innerhalb des Feldes wurde anhand von Bodenprofilmessungen nachgewiesen. Außerdem wurde die spektrale Abhängigkeit bzw. die Veränderung des Bodenspektrums bei verschiedenen Wassergehalten in einem Laborversuch untersucht. Die geschätzten biophysikalischen Parameter (LAI, ALA und C_{ab}) sowie ein Bodenfaktor (α_{soil}) wurden mittels einer Clusteranalyse gruppiert und das Weizenfeld wurde in vier verschiedene Zonen mit unterschiedlichem Trockenstressniveau unterteilt.

Im Vergleich mit der empirischen NDVI-Methode konnten keine signifikanten Unterschiede in der Zonierung erzielt werden. Dennoch brachte die physikalische Modellierung den Vorteil, dass insbesondere unter Verwendung hyperspektraler Daten bestimmte Pflanzenparameter und Bodeneigenschaften geschätzt werden konnten, die wiederum einen höheren Erklärungswert als ein einfacher Index haben. In der Schlussfolgerung wird empfohlen, mithilfe der getesteten Methodik gefährdete Trockenstresszonen innerhalb von Feldern zu orten und mithilfe eines entsprechenden Managements zu bearbeiten (bewässern). Auf diese Weise können mögliche Ernteverluste vermieden werden.

Publikation IV

Publikation IV untersuchte, ob hyperspektrale Signaturen (Hymap Sensor) von Buchenwald mit einem Bestandesreflexionsmodell für Wald (ACRM) simuliert werden können. Im Weiteren wurde mit einer iterativen Inversionsmethode der LAI bestimmt. Die Studie basiert auf Daten des Lehrforsts „Rosalia“ der Universität für Bodenkultur und wurde ebenfalls im Rahmen des DROSMON-Projekts durchgeführt. Die Blattreflexion konnte mit einem spezifischen Eingangsdatensatz sehr gut anhand des Blattreflexionsmodells PROSPECT im Vergleich zu spektralen Blattmessungen modelliert werden. Die anhand des ACRM Modells simulierten Spektren des Bestands zeigten allerdings eine erhöhte Reflexion im Vergleich zu den Hymap-Signaturen (Offset 4-77 %, entsprechend dem spektralen Bereich). Dies könnte auf fehlende Informationen über die räumliche Variation der Eingangsdaten (z. B. Blattchlorophyll- oder Blattwassergehalt) zurückzuführen sein. Der Vergleich von LAI-Felddaten und durch Modellinversion geschätzte Werte erzielte dennoch sehr gute Ergebnisse mit RMSE von 0.3 bis 0.5. Die Ergebnisse der physikalischen Schätzungsmethode wurde mit einer Auswahl empirischer Indizes verglichen, die jedoch keine höhere Genauigkeit in der Bestimmung des LAI erzielten.

Als Schlussfolgerung wird darauf hingewiesen, dass für die Modellierung der spektralen Signatur von Waldbeständen mit dem ACRM Modell ein Offset notwendig ist. Wie schon in Publikation II wird die verwendete physikalisch basierte Schätzungsmethode gegenüber empirischen Modellen für die Bestimmung von LAI sehr empfohlen.

Publikation V

In der in Publikation V vorgestellten Studie, die ebenfalls im Rahmen des DROSMON-Projekts erarbeitet worden ist, wurden zwei verschiedene Weizensorten (*Triticum Aestivum* und *Triticum Durum*) in der Klimakammer in Blüte und Reifephase unter Trockenstress gesetzt. Des Weiteren wurden Erholungsphasen (d. h. ausreichende Bewässerung) nach dem Trockenstress in der Blüte eingebaut. Physiologische Messungen (z. B. Photosyntheseraten, Blattleitfähigkeit, relativer und absoluter Blattwassergehalt) und optische Blattreflexionsmessungen wurden regelmäßig an den Testpflanzen durchgeführt, um mögliche Signale von Trockenstress bzw. der erfolgten Erholung nachzuweisen. Trockenstress führte zu einer signifikanten Reduktion der physiologischen Parameter, unabhängig von der Wachstumsphase seines Einsetzens. Ausreichende Bewässerung nach der Trockenheit in der Blüte führte wieder zu einer Normalisierung der Werte. Das war nicht für die spektrale Blattreflexion der Fall. Diese erhöhte sich nach dem Trockenstress irreversibel und signifikant über das gesamte Spektrum (400–2500 nm), allerdings mit Unterschieden zwischen den Weizensorten.

Die Anwendung spektraler Indizes führte zwar zu ausreichenden Relationen mit den physiologischen Parametern. Dennoch weisen die Indizes keine Eignung für die Trockenstressfrüherkennung bzw. den Nachweis von Trockenstress nach Erholungsphasen auf.

Im thematischen Zusammenhang beschäftigen sich die Publikationen I bis III mit der Schätzung von biophysikalischen Vegetationsparametern aus optischen multi- bzw. hyperspektralen Fernerkundungsdaten für (hauptsächlich) landwirtschaftliche Anwendungen.

Dabei steht in Publikation I die Eignung der Inversionsmethode für die LAI-Schätzung an sich bzw. auf Basis des zukünftigen Sensors Sentinel-2 im Vordergrund.

Publikationen II und III konzentrieren sich dagegen eher auf die Verwendung der geschätzten Parameter (LAI, fCover, ALA, C_{ab} und α_{soil}) als Eingangsgrößen für spezielle Anwendungsbereiche, d. h. Energiebilanzmodellierung bzw. Zonierung von Trockenstressgefährdung.

Publikation IV beschäftigt sich ebenso mit der physikalisch basierten Schätzung von LAI anhand eines Reflexionsmodells aber hierbei für Waldbestände. Im Rahmen der Studie wird zusätzlich ein weiterer essentieller Aspekt in der Arbeit mit Reflexionsmodellen untersucht: die Evaluierung des Modells, d. h. der Vergleich von simulierten mit denen eines Sensors gemessenen spektralen Signaturen. Diese Untersuchung stellt im Grunde die Voraussetzung für weitere Arbeitsschritte, wie der Modellinversion, dar. Fehler in der Parameterschätzung können bereits durch Fehler des Modells entstehen und müssen nicht erst aufgrund der Inversionsalgorithmen zustande kommen. Ein weiterer kritischer Punkt und unverzichtbare Voraussetzung für die Arbeit mit Fernerkundungsdaten wird ebenso diskutiert: die Korrektur der gemessenen Spektren auf atmosphärische Effekte.

Publikation V unterscheidet sich auf den ersten Blick thematisch etwas von den Publikationen I bis IV und wurde daher an das Ende gereiht. Dennoch liefert die Studie

wichtige grundsätzliche Erkenntnisse für die anderen Arbeiten, da darin der direkte Zusammenhang zwischen den ersten physiologischen Reaktionen der Pflanzen auf Trockenstress und den spektralen Signaturen im optischen Wellenlängenbereich auf der Blattebene untersucht wird. Es wird auf die Schwierigkeit in der Erfassung von (vergangenem) Trockenstress in diesem Spektralbereich (400-2500 nm) hingewiesen, da selbst innerhalb von Pflanzenarten Unterschiede in der Reaktion auf Wassermangel auftreten können.

2.2 Schlussfolgerung und Ausblick

Die Schätzung biophysikalischer Vegetationsparameter ist von grundlegender Bedeutung für die Erkennung von Trockenstress sowie für zahlreiche ähnliche Anwendungen, um eine nachhaltige Land- und Forstwirtschaft zu garantieren. Die Fernerkundung ist dabei das wichtigste Mittel, denn ohne Datenverfügbarkeit in guter räumlicher, spektraler und zeitlicher Auflösung wäre ein flächenhaftes Monitoring der Vegetation viel zu kosten-, zeit- und arbeitsintensiv.

Die vorliegenden Studien konzentrierten sich vor allem auf die Quantifizierung der Parameter anhand physikalisch-basierter Schätzungsmethoden. Der Informationswert spektraler Signaturen wurde dabei auf fünf verschiedenen räumlichen Skalen untersucht, von hoher zu niedriger räumlicher Auflösung:

- auf Blattebene (Publikation V).
- auf Bestandesebene (Publikation IV).
- auf Feld-Skala (Publikation III).
- für wenige Felder mit zwei verschiedenen Feldkulturen (Publikation I).
- für größere landwirtschaftliche Gebiete mit vielen verschiedenen Feldkulturen (Publikation II).

Im Vergleich zu empirischen Beziehungen (d. h. VIs) erzielte die Schätzung der biophysikalischen Parameter mittels Inversion von Bestandesreflexionsmodellen in allen Studien (I-IV) bessere bzw. zumindest gleichwertige Ergebnisse.

Die Hauptgrund für diese höhere Genauigkeit der physikalisch-basierten Algorithmen liegt in ihrer Fähigkeit Ursache-Wirkungsbeziehungen realistischer zu beschreiben. Das bedeutet, dass bei der Berechnung der spektralen Signale die Beobachtungs- und Beleuchtungsgeometrie, der Bodeneinfluss (v. a. Bodenfeuchte) und Bestandseigenschaften zum Beobachtungszeitpunkt berücksichtigt werden (DORIGO et al. 2007). Das macht diese Art von Modellen robuster als empirische Ansätze, die bei Veränderungen dieser Faktoren oftmals erneut kalibriert werden müssen (DORIGO et al. 2007).

Dennoch ist eine weitere Verbesserung der physikalischen Algorithmen notwendig, z. B. um die „ill-posed“ Problematik der Modellinversion zu lösen, auch wenn keine Zusatzinformationen durch Feldmessungen vorhanden sind. Weitere Probleme bestehen in der ungenügenden Beschreibung komplexerer Bestandsarchitekturen anhand des Turbid Medium-Konzepts bzw. in der naturgegebenen Variabilität der Vegetationsparameter, die oft zu Unsicherheiten in der Modellparametrisierung führt (BARET and BUIS 2008). Allerdings würde die Verwendung komplexerer dreidimensionaler Modelle wiederum Aufwand und Rechenzeit stark erhöhen. Diese erscheinen daher oftmals für operative Anwendungen nicht geeignet.

Häufig werden die Schätzungsfehler allein in der Modellierung gesucht, während die Genauigkeit der Feldmessungen als selbstverständlich betrachtet wird. Es gibt aber eine Vielzahl von Faktoren, die die Genauigkeit solcher bodengebundenen Messungen bestimmen. Dazu gehören Unterschiede in den Instrumenten und in Mess- und Auswertemethodiken sowie subjektive Einflüsse durch die Beobachter. Deshalb sollten Messwerte immer mit großer Sorgfalt betrachtet, hinterfragt und analysiert werden.

Für die zukünftige Arbeit wird daher die Durchführung korrekt geplanter Messkampagnen für die Evaluierung und mögliche Verbesserung der Schätzalgorithmen sehr empfohlen.

Zusammenfassend konnte im Rahmen der vorliegenden Studien gezeigt werden, dass eine physikalisch basierte Schätzung von wichtigen biophysikalischen Vegetationsparametern anhand von homogenen Turbid Medium-Modellen sehr gut und auch unter diversen Bedingungen, d. h. in unterschiedlicher geographischer Lage, für eine Reihe von Sensortypen und verschiedene Vegetationsarten, möglich ist.

Auf dieser Grundlage wurden in den vorliegenden Studien folgende neue Erkenntnisse gewonnen:

Insbesondere wurde die Eignung des zukünftigen ESA Satelliten Sentinel-2 für die LAI-Bestimmung verschiedener Feldfrüchte hinsichtlich der Anforderungen des GMES Komitees teilweise erfolgreich getestet. Es wurden Unsicherheiten in der Modellierung im Vergleich zu gemessenen hyperspektralen Fernerkundungsdaten aufgezeigt. Im Weiteren wurde der Einsatz von physikalisch geschätzten Vegetations- und Bodenparametern für die Bestimmung von längerfristigem bzw. potentiellstem Trockenstress anhand einer Zonierung der Felder analysiert. Es wurde nachgewiesen, dass kurzfristiger oder vergangener Trockenstress nur eingeschränkt anhand der optischen Fernerkundung, d. h. Blattreflexion, nachweisbar ist. Im Weiteren eigneten sich physikalisch basierte Schätzungen von LAI und fCover besser für die Bestimmung von Energieflüssen im Rahmen der Energiebilanzmodellierung als die herkömmlichen empirischen Methoden.

Die in den Studien bearbeiteten Techniken bieten einerseits die Basis für weitere wissenschaftliche Untersuchungen und können andererseits integrierte Lösungen für ein effektives und operatives Management und somit eine nachhaltige Entwicklung in Land- und Forstwirtschaft unterstützen.

3 Literaturverzeichnis

- ASNER, P.G.; SCURLOCK, J.M.O.; HICKE, J.A. (2003): Global synthesis of leaf area index observations: implications for ecological and remote sensing studies. *Global Ecol. Biogeogr.* 12: 191-205.
- ATZBERGER, C. (2000): INFORM: Ein invertierbares Forstreflexionsmodell zur fernerkundlichen Bestimmung biophysikalischer Größen. In Albertz (Hrsg.): *Photogrammetrie und Fernerkundung. Neue Sensoren – Neue Anwendungen. Publikationen der Deutschen Gesellschaft für Photogrammetrie und Fernerkundung* 8: 163-173.
- ATZBERGER, C. (2003): Möglichkeiten und Grenzen der fernerkundlichen Bestimmung biophysikalischer Vegetationsparameter mittels physikalisch basierter Reflexionsmodelle. *Photogrammetrie, Fernerkundung, Geoinformation* 1: 51– 61.
- ATZBERGER, C. (2004): Object-based retrieval of biophysical canopy variables using artificial neural nets and radiative transfer models. *Remote Sens. Environ.* 93: 53-67.
- BARET, F. and GUYOT (1991): Potentials and limits of vegetation indices for LAI and PAR assessment. *Remote Sens. Environ.* 35: 161–173.
- BARET, F.; HAGOLLE, O.; GEIGER, B. et al. (2007): LAI, fAPAR and fCover CYCLOPES global products derived from VEGETATION. Part 1: Principles of the algorithm. *Remote Sens. Environ.* 110(3): 275- 286.
- BARET, F. and BUIS, S. (2008): Estimating canopy characteristics from remote sensing observations. Review of methods and associated problems. In S. Liang (ed.): *Advances in Land Remote Sensing: System, Modeling, Inversion and Application*. Springer Netherlands, 172-301.
- BARRET, E.C. and CURTIS, L.F. (1976): *Introduction to environmental remote sensing*. London: Chapman and Hall.
- BSAIBES, A.; COURAULT, D.; BARET, F. et al. (2009): Albedo and LAI estimates from FORMOSAT-2 data for crop monitoring. *Remote Sens. Environ.* 113: 716-729.
- CAMPS-VALLS, G.; MUÑOZ-MARI, J.; GOMEZ-CHOVA, L. et al. (2009): Biophysical Parameter Estimation With a Semisupervised Support Vector Machine. *Geosci. Rem. Sens. Lett. IEEE* 6 (2): 248-252.
- CASA, R. (2003): *Multiangular remote sensing of crop canopy structure for plant stress monitoring*. Dundee, Scotland: PhD Thesis, University of Dundee.
- COMBAL, B.; BARET, F.; WEISS, M. et al. (2002): Retrieval of canopy biophysical variables from bidirectional reflectance using prior information to solve the ill-posed inverse problem. *Remote Sens. Environ.* 84: 1– 15.
- DARVISHZADEH, R.; SKIDMORE, A.; SCHLERF, M. et al. (2008): Inversion of a radiative transfer model for estimating vegetation LAI and chlorophyll in a heterogeneous grassland. *Remote Sens. Environ.* 112: 2592-2604.
- DE MICHELE, C.; VUOLO, F.; D'URSO, G. et al. (2009): The Irrigation Advisory Program of Campania Region: from research to operational support for the Water Directive in Agriculture. In: *proceedings of 33rd International Symposium on Remote Sensing of Environment, Stresa, Italy, 4-8 May 2009* (in print).

- DORIGO, W.; ZURITA-MILLA, R.; DE WIT, A. J. W. et al. (2007): A review on reflective remote sensing and data assimilation techniques for enhanced agroecosystem modeling. *Int. J. Appl. Earth Obs. Geoinf.* 9: 165–193.
- DURBHA, S. S.; KING, R. L.; YOUNAN, N. H. (2007): Support vector machines regression for retrieval of leaf area index from multi-angle imaging spectroradiometer. *Remote Sens. Environ.* 107: 348–361.
- EUROPEAN SPACE AGENCY, ESA (2008): The Earth Observation Handbook, Climate Change Special Edition 2008. www.eohandbook.com/eohb2008/earthobservation.htm (Letzter Zugriff 04.06.2009)
- FRANKLIN, S.E. (2001): Remote sensing for sustainable forest management. Boca Raton, Lewis Publishers.
- GOEL, N.S. (1988): Models of vegetation canopy reflectance, their use in estimation of biophysical parameters from reflectance data. *Rem. Sens. Rev.* 4: 1-212.
- GONZALEZ-DUGO, M.; MORAN, M.S.; MATEOS, L. et al. (2006): Canopy temperature variability as an indicator of crop water stress severity. *J. Irrig. Sci.* 24: 233-240.
- GUERIF, M. and DUKE, C. L. (1998): Calibration of the SUCROS emergence and early growth module for sugar beet using optical remote sensing data assimilation. *Eur. J. Agron.* 9: 127-136.
- KIMES, D.; KNJAZIKHIN, Y.; PRIVETTE, J.L. et al. (2000): Inversion methods for physically-based models. *Remote Sens. Rev.* 18: 381-440.
- KOETZ, B.; BARET, F.; POILVE, H. et al. (2005): Use of coupled canopy structure dynamic and radiative transfer models to estimate biophysical canopy characteristics. *Remote Sens. Environ.* 95: 115– 124.
- KUSTAS, W. P. and NORMAN, J. M. (1996): Use of remote sensing for evapotranspiration monitoring over land surfaces. *Hydrolog. Sci. J.* 41: 495–516.
- JACQUEMOUD, S. and BARET, F. (1990): PROSPECT: A model of leaf optical properties spectra. *Remote Sens. Environ.* 34: 75-91.
- JACQUEMOUD, S.; BARET, F.; ANDRIEU, B. et al. (1995): Extraction of Vegetation Biophysical Parameters by Inversion of the PROSPECT + SAIL Models on Sugar Beet Canopy Reflectance Data. Application to TM and AVIRIS Sensors. *Remote Sens. Environ.* 52: 163-172.
- KUUSK, A. (2001): A two-layer canopy reflectance model. *J. Quant. Spectrosc. Ra.* 71: 1–9.
- JI, L. and PETERS, A. J. (2007): Performance evaluation of spectral vegetation indices using a statistical sensitivity function. *Remote Sens. Environ.* 106(1): 59-65.
- MARTIMORT, P. (2007): Sentinel-2 — The optical high-resolution mission for GMES operational services. *ESA Bulletin* 131: 18–23.
- MERONI, M.; COLOMBO, R. and PANIGADA, C. (2004): Inversion of a Radiative transfer model with hyperspectral observations for LAI mapping in poplar plantations. *Remote Sens. Environ.* 92(2): 195–206.
- PINTY, B.; WIDLowski, J.L.; TABERNER, M. et al. (2004): Radiation Transfer Model Intercomparison (RAMI) exercise - results from the second phase. *J. Geophys. Res.* 109: D06210, doi:10.1029/2003JD004252.

- RUNNING, S.W.; NEMANI, R.R.; PETERSON, D.L. et al. (1989): Mapping regional forest evapotranspiration and photosynthesis by coupling satellite data with ecosystem simulation. *Ecology* 70(4): 1090-1101.
- SCHLERF, M. and ATZBERGER, C. (2006): Inversion of a forest reflectance model to estimate structural canopy variables from hyperspectral remote sensing. *Remote Sens. Environ.* 100: 281-294.
- SCHUELLER, J.K. (1992): A review and integrating analysis of spatially-variable control of crop production. *Fert. Res.* 33: 1-34.
- SOUDANI, K.; FRANCOIS, C.; LE MAIRE, G. et al. (2006): Comparative analysis of IKONOS, SPOT, and ETM+ data for leaf area index estimation in temperate coniferous and deciduous forest stands. *Remote Sens. Environ.* 102 (1): 161-175.
- VERHOEF, W. (1984): Light scattering by leaf layers with application to canopy reflectance modeling: the SAIL Model. *Remote Sens. Environ.* 16: 125-141.
- VERHOEF, W. (1985): Earth observation modeling based on layer scattering matrices. *Remote Sens. Environ.* 17: 165-178.
- WEISS, M.; BARET, F.; MYNENI, R.B. et al. (2000): Investigation of a model inversion technique to estimate canopy biophysical variables from spectral and directional reflectance data. *Agronomie* 20: 3-22.
- YAO, Y.; LIU, Q.; LIU, Q. et al. (2008): LAI retrieval and uncertainty evaluations for typical row-planted crops at different growth stages. *Remote Sens. Environ.* 112(1): 94-106.
- ZURITA-MILLA, R.; KAISER, G.; CLEVERS, J.P.G.W. et al. (2007): Spatial unmixing of MERIS data for monitoring vegetation dynamics. In: H. Lacoste & L. Ouwehand (Eds.), *Proceedings of the Envisat Symposium 2007, Montreux 23.-27 April 2007*, copyright 2007 European Space Agency, The Netherlands.

4 Publikationen

4.1 Publikation I

Experimental assessment of the Sentinel-2 band setting for RTM-based LAI retrieval of sugar beet and maize

Katja Richter, Clement Atzberger, Francesco Vuolo, Guido D'Urso, and Philipp Weihs

Canadian Journal of Remote Sensing. 2009 (In print).

Experimental assessment of the Sentinel-2 band setting for RTM-based LAI retrieval of sugar beet and maize

Katja Richter, Clement Atzberger, Francesco Vuolo, Philipp Weihs, Guido D'Urso

Abstract. The present work aimed at testing the potential of the upcoming E.O. satellite Sentinel-2 (European GMES/Kopernikus programme) for the operational estimation of the Leaf Area Index (LAI) of two contrasting agricultural crops (sugar beet and maize). Mapping of LAI was achieved by using a Look-up table (LUT) based inversion of a physically based radiative transfer model (SAILH+PROSPECT). Besides the Sentinel-2 spectral sampling, another band set described as 'ideal' for vegetation studies, has been evaluated in a comparative way. Analyses were mainly carried out using hyperspectral data acquired by the optical airborne instrument CASI during the ESA AgriSAR 2006 campaign. Additionally, data from two other experiments were tested to extend the validation database. Alternative inversion methods, i.e. an iterative optimization technique (SQP) and a neural network (NN) have been evaluated for comparison purposes. The GMES/Kopernikus defined precision of 10 % for LAI estimation, evaluated with in situ LAI measurements, was met for sugar beet (8-9 %), but not for maize (16-22%). The inversion approach and band setting had only a minor influence on the retrieval accuracy, with the only exception of the iterative optimization technique which failed to give reliable results. The results demonstrate the importance of using an appropriate radiative transfer model for each crop. For row crops with strong leaf clumping and not covering completely the soil surface, such as maize at early stage, the standard SAILH+PROSPECT does not appear suitable.

Résumé. Dans le cadre de la présente étude nous examinons le potentiel du futur satellite Sentinel-2 (programme européen GMES/Kopernikus) pour l'estimation opérationnelle de l'indice de surface foliaire (LAI) de deux cultures différentes (maïs et betterave à sucre). L'inversion du LAI a été effectuée en utilisant des tables pré-calculées par un modèle de transfert radiatif (SAILH + PROSPECT). Les mesures hyper spectrales de l'instrument aéroporté CASI faites dans le cadre de la campagne ESA AgriSAR 2006 ont été utilisées pour cette analyse. Deux configurations de bandes spectrales ont été utilisées l'une

correspondante à l'instrument Sentinel-2 et une autre correspondante à une configuration idéale pour l'étude des couverts végétaux. Plusieurs techniques d'inversion ont également été considérées, une technique d'optimisation itérative (SQP) et une autre utilisant les réseaux de neurones. En utilisant des mesures in situ du LAI ainsi que celle de deux expériences supplémentaires nous montrons que il est possible d'obtenir une précision de 10 %, similaire aux objectifs définis par le programme GMES/Kopernikus, pour la betterave rouge (8-9 %). Pour le maïs la précision est dégradée notablement (16-22%). La technique d'inversion ainsi que le choix des bandes spectrales n'ont qu'une influence moindre sur la précision dans la plupart des cas à l'exception des inversions utilisant la technique d'optimisation itérative. Ces résultats démontrent clairement la nécessité d'utiliser un modèle de transfert radiatif approprié pour chaque culture. Pour des cultures en rangées avec couverture incomplète du sol comme le maïs au premier stade du développement, l'utilisation du modèle SAILH+PROSPECT n'est pas appropriée.

* Received 15 December 2008. Accepted 03 May 2009

K. Richter¹ and G. D'Urso. Agriculture Faculty, University of Naples "Federico II", via Università 100, 80055 Portici (Na), Italy.

C. Atzberger. Joint Research Centre of the European Commission, JRC, Via Enrico Fermi 2749, 21027 Ispra (VA), Italy.

F. Vuolo. ARIESPACE srl, via Roma 47, 80056 Ercolano (NA), Italy.

P. Weihs. Institute for Meteorology Department of Water, Atmosphere, Environment, University of Natural Resources and Applied Life Sciences, Peter Jordan Str. 82, A-1190 Vienna, Austria.

¹Corresponding author (e-mail: katja.rich@gmail.com).

Introduction

In the last years a new generation of sensors was launched for various environmental applications (ESA, 2008). The additional sensors increase significantly the availability of high spectral, spatial and temporal resolution data. This new Earth Observation (E.O.) database offers on the one hand the opportunity to exploit the potential of remote sensing in an operational context, and on the other hand it provides the possibility to test the performance of existing and new methodologies for land surface characterization. This is of particular interest in the context of precision farming, where information of crop and soil characteristics must be obtained on a large scale, in a rapid and cost-effective way, with a stable and high accuracy.

Sentinel-2: future operational E.O. satellite

In the framework of Kopernikus (former GMES: Global Monitoring for Environment and Security), the European Space Agency (ESA) initiated the Sentinel-2 multi-spectral mission, aiming at replacing and improving the current generation of satellite sensors. GMES/Kopernikus is a joint initiative of the European Commission (EC) and ESA, designed to establish a European capacity for the provision and use of operational monitoring information for environment and security applications (ESA, 2007). Thus, GMES/Kopernikus Sentinel-2 mission intends to provide continuity to services relying on multi-spectral high-resolution optical observations over global terrestrial surfaces, such as the adequate quantification of geo-biophysical variables. Additionally, the mission aims at enhancing the quality of the current service, as required by the growing user demand. This implies advancements in E.O. products, such as improved land cover/change classification, atmospheric correction, cloud/snow separation and the quantitative assessment of the structural and biochemical vegetation status. Spectral sampling of Sentinel-2 satellite is based on sensors used for vegetation monitoring in the last decades, such as SPOT and Landsat, but also includes channels originating from MODIS, MERIS, ALI and LDCM, to fulfill the new requirements. The future satellite Sentinel-2 is scheduled to be launched in the year 2012. With a spatial resolution of 10-60 m, Sentinel-2 is designed to address medium resolution applications. As outcome the mission will provide service data, comprising Level 1a, 1b, 1c, 2a and a catalogue of Level 2b/3 products. More information about the mission, services and the technical details of the sensor can be found in the GMES mission requirement document (ESA, 2007) or in the indicated web-pages (see reference section).

The Level 2b/3 product Leaf Area Index (LAI) will be included in the final catalogue together with a number of other products, such as land cover maps, fractional vegetation cover, fraction of absorbed photosynthetically active radiation, leaf water and leaf chlorophyll content. To ensure that the final product can meet the user requirements, the committee defined a goal accuracy of 10 % for the “maps with the green leaf area per unit soil area”, i.e. LAI (ESA, 2007). Until now, only few studies addressed this precision requirement over contrasting crops.

Leaf Area Index – a key variable in land biophysical processes

The biophysical surface parameter attracting most interest in studies dealing with E.O. data is the Leaf Area Index. LAI is defined as the total one-sided area of photosynthetic tissue per unit of ground area (Breda, 2003). Due to the role of green leaves in a wide range of biological and physical processes, LAI represents a key parameter, characterizing the structure and functioning of vegetation cover (Scurlock et al., 2001): LAI describes the surface for mass and energy exchanges between the Earth's surface and the atmosphere; it influences the within- as well as the below-canopy microclimate, determines and controls canopy water interception, radiation extinction, water and carbon gas exchange. Moreover, any change in LAI, for instance caused by weather extremes (such as drought, frost and storms) or management practices, may modify the productivity of the crops (Breda, 2003). Due to its role as interface between ecosystem and atmosphere and involvement in many processes, information about LAI is requested in various fields of application and research, such as hydrology, ecophysiology, farm and forest management, ecology and meteorology (Breda, 2003; Gower et al., 1999; Liang, 2004a; Myneni et al., 2002).

LAI estimation from E.O. data: empirical and physical based approaches

Since ground based LAI measurements are time-consuming, cost-intensive and spatially as well as temporally constricted, E.O. data have been recognized as an important resource for LAI retrieval. Several studies have been carried out on estimating surface parameters by using newly developed hyperspectral vegetation indices (VI) (Darvishzadeh et al., 2008b; Haboudane et al., 2004; Schlerf et al., 2005), the analysis of the red edge (Cho et al., 2008; Filella and Penuelas, 1994; Liu et al., 2004), or spectral unmixing approaches (e.g., Haboudane et al., 2004; Hu et al., 2004) as an alternative to the traditional empirical approaches (Myneni et al., 1995; Thenkabail et al.,

2002). However, despite the intense work, there is still a need for collecting in situ calibration data sets, implying high costs and a labor intensive measurement program to cover a wide range of species, canopy conditions and view/sun constellations.

For these reasons, many studies focused on the more complex approach of physically based parameter estimation by means of radiative transfer model inversion (e.g. Jacquemoud et al., 2000; Koetz et al., 2005; Schlerf and Atzberger, 2006; Weiss et al., 2000; Baret and Buis, 2008). These radiative transfer models (RTM) permit to use the full spectrum acquired by hyperspectral sensors (400-2500 nm), as contrasted to VIs that generally use only two / three spectral bands. In addition, RTMs can also consider the directional signature of multi-angle sensors. Nevertheless, some shortcomings of these models, such as the need of an extensive parameterization, as well as the high computational demand, have to be considered. Moreover, some RTMs may be too simplistic to cope with complex canopies such as row crops, which are often affected by foliage clumping (Dorigo et al., 2008; Yao et al., 2008). Furthermore, the ill-posed problem has to be taken into account when performing model inversion: different parameter combinations may produce almost identical spectra, resulting in significant uncertainties in the estimated vegetation characteristics (Atzberger, 2004; Combal et al., 2002).

Model inversion methods: advantages and constraints

To retrieve canopy biophysical variables from radiative transfer models three inversion methods are commonly used (Atzberger, 2004; Kimes et al., 2000): iterative optimization techniques (Atzberger, 1997; Goel, 1988; Jacquemoud et al., 1995), look-up tables (LUT) (Combal et al., 2002, 2003; Darvishzadeh et al., 2008a; Pragnère et al., 1999; Weiss et al., 2000) and neural networks (NN) (Atkinson and Tatnall, 1997; Bacour et al., 2006; Schlerf and Atzberger, 2006; Walthall et al., 2004). Recently, the new approach of Support Vector Machines regression (SVR) has been applied to estimate biophysical variables from E.O. imagery (e.g. Camps-Valls et al., 2006; Durbha et al., 2007). Iterative optimization techniques and LUT based RTM inversions are based on the minimization of a distance between simulated and measured reflectance. The NN and SVR, on the contrary, directly map the reflectance into parameter space (Baret & Buis, 2008).

As proved and outlined by several studies, LUT and NN were performing best in the inversion of the RTMs in terms of accuracy and speed (e.g. Baret and Buis, 2008; Pragnère et al., 1999; Weiss et al., 2000). The constraints of the iterative optimization algorithms are a relatively high computational load, the requirement of

an initial guess and the risk of converging to a local minimum, which may not be necessarily close to the actual solution (Kimes et al., 2000; Liang, 2004b; Qiu et al., 1998). As for the LUTs, neural nets rely on a large database of pre-calculated (synthetic) canopy reflectance spectra first simulated using the RTM in direct mode. Alternatively, actual data (ground or remotely sensed) or a mix of actual and synthetic data can be used to feed the NN learning database or the LUT. The NN are then trained to learn the relation between canopy reflectance spectra (inputs) and canopy biophysical variables (outputs). To represent the relation between input and output variables, NN use connected layers composed of neurons. Weights and biases have to be learned (using the outputs of the forward RTM simulations) to transform spectral signatures into biophysical variables. Provided that there are enough neurons in the hidden layer, NN can represent any non-linear relationship between in- and outputs (Demuth and Beale, 2003). The major advantage of NN is their speed during application. Also, storage requirements are very low. Major drawbacks relate to the often time-consuming training phase and the unpredictable behavior of NNs when measured and/or RTM signatures are biased. As the NNs are extremely powerful in learning even complex relationships, care must also be taken to prevent overfitting and overspecialization.

The conceptually simple LUT procedure may partly overcome the limitations of the iterative optimization algorithms and the neural nets. Since the full parameter space is searched for the optimum solution, problems related to the initial guesses of iterative approaches are avoided. Further, by optimizing (minimizing) the number of cases, calculation time can be diminished. Moreover, in case that the spectral characteristics of the targets are not well represented by the modeled spectra, the LUT method shows less unexpected behavior than the NN (Darvishzadeh et al., 2008a; Schlerf and Atzberger, 2006). With LUT it is also relatively easy to associate different weights to the various spectral channels and to include prior knowledge about the retrieved canopy characteristics in the inversion process (Baret and Buis, 2008). Care has to be taken in the sampling of parameter spaces and the decision of the LUT size to avoid sub-optimal solutions. Concerning the LUT dimension, Weiss et al. (2000) investigated the effect of the size of the LUT for the accuracy of canopy variable estimation. The realization of a RTM inversion with tables ranging from 25 000 to 280 000 cases resulted in an 'optimal' size of 100 000 cases, regarded by the authors as a good compromise between computer resources requirements and the accuracy of the estimates. Only few studies addressed the issue of inversion approach over several crop types at the same time.

Objective of the study

The main objective of the present work is the experimental assessment of the future Sentinel-2 band setting for RTM-based LAI retrieval for early/mid season sugar beet and maize with a maximum value of LAI up to 4 - 5 for maize and up to 5 - 6 for sugar beet. We evaluated if the retrieval accuracy of 10 %, specified by the GMES user committee, can be reached for these two particular crops, using the widely used SAILH+PROSPECT canopy reflectance model, originally developed for homogeneous canopies, and employing LUT for RTM inversion. To verify that the retrieval errors are neither due to inappropriately selected spectral inputs nor to the chosen inversion approach, the RTM was alternatively inverted with a different spectral sampling and two other inversion algorithms: neural networks and iterative optimization. This allows refining the application range of the RTM used in this study.

Material and methods

Campaign and study area

The present research was mainly done in the context of the ESA AgriSAR 2006 campaign (Hajsek et al., 2007), designed and performed on the consolidated long-term test site DEMMIN (Durable Environmental Multidisciplinary Monitoring Information Network: http://www.caf.dlr.de/caf/anwendungen/umwelt/dauertestfeld_demmin). The DEMMIN test site is an agricultural flat area, located approx. 150 km north of Berlin in Mecklenburg-Western Pomerania, Germany (Figure 1). The DEMMIN site comprises four large-area farms with a size of 25 000 ha, managed by a farming association ("IG-Demmin"). The main crops of the region are winter wheat, sugar beet, winter barley, winter rape and maize, grown on very large parcels (in average 80 ha). The AgriSAR study was focused on the Goermin farm, situated in the north-eastern part of the test site, with the main geographical coordinates N ~ 54°00' and E ~ 13°16'.

The principal work, carried out by the AgriSAR teams, included intense airborne and ground data acquisitions on various crop types in the period between April 18th and August 2nd in 2006. A considerable amount of imagery was generated from different radar frequencies and polarizations (X-, C- and L-Band), as well as from thermal and hyperspectral optical sensors. Together with the simultaneously collected ground data, this database provides a valuable resource for the examination and validation of bio-/geo-physical parameter retrievals (Hajsek et al., 2007).

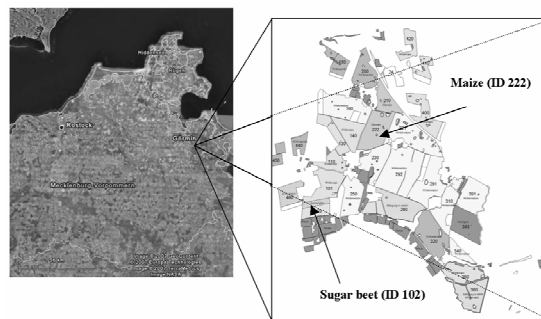


Figure 1. Study test site: DEMMIN area, Goermin farm with the two fields mainly used for this study: one sugar beet field (ID 102) with a size of 17.5 ha and a maize field (ID 222) of 101.8 ha. Further details of the two test fields can be found in Table 2.

Hyperspectral image acquisition

Hyperspectral images were acquired with the Compact Airborne Spectrographic Imager (CASI 1500, ITRES Research Ltd., Calgary, Canada) on July 5th 2006. The area of interest was scanned around 10:00 UTC, corresponding to a solar zenith angle of ~ 35°. The sensor (fly altitude 3100 meters above sea level (m.s.l.)) acquired hyperspectral data at 1.5 m spatial resolution in 288 bands located in the visible (VIS) to near infrared (NIR) range, i.e. from 370 to 1050 nm, with a bandwidth (FWHMs) of 2.2 nm and a field of view (FOV) equal to 23.6°. Spectral calibration and atmospheric correction of the imagery were carried out by the Laboratory for Earth Observation, Department of Earth Physics and Thermodynamics of the University of Valencia, by using an optimized version of the MODTRAN4 code. The procedure, described in Guanter et al. (2007) for two other field experiments, was also applied in the context of the AgriSAR field campaign.

CASI provides a nearly-continuum spectrum over the entire spectral range, with very fine observation channels, reproducing any small absorption feature due to surface or atmospheric components (Guanter et al., 2007). For these reasons CASI offers a good opportunity to test the potential of the future multi-spectral satellite Sentinel-2. Special features of the Sentinel-2 sensor include a 290 km wide coverage, 10-60 m spatial resolution and 13 spectral channels ranging from visible to shortwave infrared, as listed in Table 1. Quality enhancement is foreseen in comparison to current E.O. missions, such as a shorter revisit time, larger coverage area, improved image quality and spectral information.

The specific sensitivity function of Sentinel-2 wavebands (provided by ESA, personal

communication) was applied to configure the CASI measurements according to the future Sentinel-2 satellite. To mimic the planned spatial resolution of Sentinel-2 (4 channels with 10 m and 4 with 20 m, see Table 1), the high spatial resolution CASI data (1.5 m) were degraded to a coarser resolution of 20 m for the whole imagery.

Table 1. Spectral sampling of the proposed Sentinel-2 sensor: central wavebands, spectral widths, spatial resolution and purpose (from ESA GMES mission document, 2007). In grey the 8 bands used for the simulations.

Central waveb.	Spectral width	Spatial res. (m)	Purpose
λ (nm)	$\Delta\lambda$ (nm)		
443	20	60	Atmospheric correction (aerosol scattering)
490	65	10	Sensitive to vegetation senescing, carotenoid, browning and soil background; atmospheric correction (aerosol scattering)
560	35	10	Green peak, sensitive to total chlorophyll in vegetation.
665	30	10	Max. chlorophyll absorption.
705	15	20	Position of red edge; consolidation of atmospheric corrections / fluorescence baseline.
740	15	20	Position of red edge, atmospheric correction, retrieval of aerosol load.
775	20	20	LAI, edge of the NIR plateau
842	115	10	LAI
865	20	20	NIR plateau, sensitive to total Chlorophyll, biomass, LAI and protein; water vapor absorption reference; retrieval of aerosol load and type.
940	20	60	Water vapor absorption, atmospheric correction.
1375	20	60	Detection of thin cirrus for atmospheric correction.
1610	90	20	Sensitive to lignin, starch and forest above ground biomass. Snow/ice/cloud separation.
2190	180	20	Assessment of Mediterranean vegetation conditions. Distinction of clay soils for the monitoring of soil erosion. Distinction between live biomass, dead biomass and soil, e.g. for burn scars mapping.

In situ LAI measurements

Leaf area index measurements were carried out on two fields: one sugar beet field (ID 102: 8 samples) and one maize field (ID 222: 16 samples) (Figure 1). In situ LAI measurements were taken at the day of the sensor overpass or the evening of the preceding day. The measurements were performed with the Plant Canopy Analyzer LAI-2000 instrument (LICOR Inc., Lincoln, NE, USA).

Information about the monitored crop fields, phenological stages and some biophysical characteristics of the plants monitored during AgriSAR campaign are summarized in Table 2 together with two additional data sets used for validation purposes. Detailed information about these supplementary data can be found in Richter et al. (2008a) and Richter and Timmermans (2009).

The measurement principle of the LAI-2000 instrument is based on non-destructive indirect gap fraction measurements. The gap fractions are assessed by measuring the light transmission through the canopy. This is done by comparing differential light measurements above and below the canopy at five zenith angles (with central angles of 7, 23, 38, 53 and 68°) (Jonckheere et al, 2004). A detailed description of the instrument can be found in Cutini et al. (1998) or in the instruments manual (LI-COR, 1992). One shortcoming of the widely used instrument is that it does not distinguish photosynthetically active leaf tissue from other plant elements such as stems, branches, flowers or senescent leaves. The measurement should therefore be considered as “Plant Area Index” (PAI) (Jonckheere et al., 2004). Moreover, the possible non-random positioning of canopy elements is neglected. Hence, without carrying out a correction of the clumping, the term “effective LAI” (L_e) is more adequate (Chen and Black, 1992). In fact, the instrument tends to underestimate LAI, especially in case of discontinuous and heterogeneous canopies with clumped foliage (Jonckheere et al., 2004). On the contrary, vertical elements in canopies (such as stems) increase/overestimate LAI. Hence, the measurement accuracy does not only depend on phenological stage, but also on crop type and structure.

Since no corrections were applied to account for these two aspects, the term ‘LAI’ should, in the context of this study, be understood as ‘effective plant area index’ (PAI_{eff}) (Chen et al., 1997, Darvishzadeh et al., 2008a; Soudani et al., 2006). On the other hand, the LAI measured by LAI-2000 (or other optical methods) is quite close to the leaf surface visible by a remote

Table 2. Description of the test fields of the AgriSAR campaign (corresponding to time of sensor overpass), mainly analyzed in the study, and from the other two campaigns, when data were available.

Crop	AgriSAR	AgriSAR	PLEIADeS	SPARC	SPARC
	Sugar beet	Maize	Maize	Sugar beet	Maize
ID	102	222	-	-	-
Field size (ha)	17.5	101.8	-	-	-
Cultivar	Ricarda ^(a)	Salagor ^(a)	no information	no information	no information
Sowing date	end of March 2006 ^(b)	beginning of May 2006 ^(b)	end of May 2007	end of March 2004	beginning of June 2004
Developmental stage (Eucarpia Scale, EC)	EC stage 33 ^(a)	EC stage 39 ^(a)	no information	no information	no information
Plant height (m)	~0.25 ^(b)	~ 1 ^(b)	0.35 – 3.2 ^(d)	0.45-0.6 ^(d)	1.6 – 2.5 ^(d)
Plants per m ²	10 ^(b)	15 ^(b)	no information	no information	no information
Crop coverage (%)	50 ^(b)	40 ^(b)	10-95 ^(d)	60-80 ^(d)	40-80 ^(d)
Mean LAI (mean, SD)	1.5 (0.5) ^(b)	1.7 (0.5) ^(b)	2.0 (1.2) ^(d)	4.9 (0.4) ^(d)	2.4 (0.6) ^(d)
Chlorophyll (mean, SD) (µg/cm ²)	40 (10) ^(b,c)	45 (10) ^(b,c)	not measured	49 (1) ^(d)	52 (1) ^(d)

^a Personal communication (Agrisar Team); ^b Gerighausen et al., 2007 (3 measurement points); ^c Minolta SPAD measurements, ^d campaigns measurements, more information in: Richter et al., 2008a; Richter and Timmermans, 2009.

sensor which is not necessarily the case for the real leaf area index (Stenberg et al., 2004). According to Soudani et al. (2006), a correction for the clumping effect is therefore not absolutely necessary.

Each of the 24 AgriSAR in situ measurements (8 in ID 102 and 16 in ID 222) was based on three consecutive series of 8 readings below the canopy (plus one reference reading above the canopy) covering an Elementary Surface Unit (ESU) of approximately 20 x 20 m geolocated by means of a GPS (accuracy roughly 5 m). The average value of LAI, resulting from the set of 24 readings (576 measurements in total), has been considered as representative for the respective ESU. The standard deviation around the mean has been kept as a measure of uncertainty. Field measured LAI values ranged between 1.0 and 2.0 for the sugar beet field (ID 102) and 0.9 and 2.3 for the maize field (ID 222). Measurements were always taken under uniform clear diffuse skies at low solar elevation (i.e., ~ 1 h before sunset). Samples of below and above -canopy radiation were performed by experienced operators in the opposite direction to the sun to prevent direct sunlight on the sensor. A view restrictor of 180° was mounted on the sensor and care was taken that the instrument remained horizontal.

To avoid biases in the measurements due to particular crop architectures (such as sugar beet or maize in early

growth stages), the measurements were carried out in a systematic and standardized way; that is the sensor was placed alternately in the middle of the row and between two rows. Moreover, below canopy readings have been taken close to the soil with appropriate distances to the leaves.

To consider a wider range of LAI values than available from the AgriSAR campaign, data from two other experiments were consulted (see also Table 2): the LAI data set of 21 measurements of maize from the PLEIADeS 2007 field campaign, Sardinia, Italy (Richter et al., 2008a) and the LAI data set of 8 measurements of maize and 6 of sugar beet from the SPARC 2004 campaign, Barrax, Spain (Richter and Timmermans, 2009). In both experiments, measurements of LAI were performed by using the same protocol as described above for the AgriSAR campaign. During PLEIADeS, hyperspectral field measurements with the ASD FieldSpec UV-VNIR field spectrometer (operating in the spectral range from 350 to 1050 nm) were acquired in correspondence of LAI measurements and the spectral signatures configured according to the Sentinel-2 spectral bands. During SPARC experiment, imagery of CHRIS/Proba satellite was acquired and as well configured using the specific sensitivity function of Sentinel-2 wavebands (using near zenith view angle). The experiments are described in detail in the mentioned references.

Model and inversion techniques

Radiative transfer model: PROSAILH

A physical based method of canopy reflectance modelling was selected for the study: the widespread SAILH model (Scattering from Arbitrarily Inclined Leaves, Verhoef, 1984, 1985). It has been later extended by Kuusk (1991) to take into account the hot spot effect. The SAILH model is based on the turbid medium assumption, and describes the canopy structure in a fairly simple way. Despite its simplicity, it produces realistic results of bidirectional reflectance spectra as reported by several studies for different crops including maize and sugar beet (e.g. Andrieu et al., 1997; Goel and Thompson, 1984; Jacquemoud et al., 1995, 2000; Koetz et al., 2005; Major et al., 1992). For the purpose of our study, the SAILH model has been combined with the PROSPECT leaf optical properties model (Jacquemoud and Baret, 1990) to 'PROSAILH' (e.g., Atzberger, 1997; Baret et al., 2007; Verhoef and Bach, 2003; Weiss et al., 2000) to account for variations in leaf structure and composition.

The SAILH model simulates canopy bi-directional reflectance as a function of three structural parameters (i.e., *LAI*, average leaf inclination angle (*ALA*) and hot spot parameter (*HotS*) - roughly defined as the ratio of the leaf size to canopy height; Verhoef and Bach, 2003), soil spectral reflectance, leaf reflectance and transmittance, fraction of diffuse irradiance (*skyl*) and the view and illumination geometry. Leaf reflectance and transmittance were simulated by the PROSPECT model as a function of four structural and biochemical leaf parameters: leaf chlorophyll content (C_{ab}), dry matter content (C_m), leaf water thickness (C_w) and a leaf mesophyll structural parameter (N).

The PROSAILH model has been preferred to other radiative transfer models, describing the canopy in a more complex way (for a review on these models see Dorigo et al., 2007), such as 3D hybrid radiative transfer models (e.g. Goel and Grier, 1988), Monte Carlo ray tracing models (Goel and Thompson, 2000) and others (Peddle et al., 2003, 2004). This decision is justified with the focus of potential usage of the method for operational applications. For operational applications, the execution speed of complex models is a limiting factor, especially when large quantities of data have to be processed on a regular (daily) basis. Moreover, the higher the complexity of the model the larger the requirement of knowledge concerning parameterization, construction of the merit function or use of prior information (Dorigo et al., 2007). On the other hand, the generality and robustness of the physical model approach favored the choice over VIs, which may also achieve accurate results and are easy to apply with low computer requirements.

Look-up table approach (LUT)

In the standard setting, the PROSAILH radiative transfer model was inverted by using a look-up table (LUT). Three principal steps have to be performed to realize this approach:

(1) Generation of an appropriate number of canopy parameter combinations:

A LUT size of 100 000 ('LUT1') cases of canopy parameter combinations was chosen according to the results of Weiss et al. (2000). Canopy parameter realizations, i.e. bounds and distributions, are depicted in Table 3. Parameter bounds were taken from measurement campaigns and/or other studies working with the same crops. They were chosen in order to describe the characteristics of both crop types used in the study, maize and sugar beet. Gaussian distributions have been generated for *LAI* and C_{ab} in order to put more emphasis on the parameter values being present in the actual growth stages of the crops (Gerighausen et al., 2007). On the contrary, *HotS*, α_{soil} , C_m , and N were sampled from a uniform distribution (Koetz et al., 2005) since no information from the campaign measurements was available.

The range of C_{ab} was set to 10 – 70 μm , as in D'Urso et al. (2004) for a range of crops including sugar beet and maize. Similar ranges were used in other studies, e.g. in Weiss et al. (2000) and Koetz et al. (2005) for maize.

LAI was allowed to vary between 0 and 6 with a mean of 2 close to the observed average *LAI* value of the two fields. The range of *ALA* was set quite large: 40°-70°, allowing the simulation of planophile (40°) to erectophile (70°) canopies. Similar large ranges have been used by Bacour et al. (2002), Combal et al. (2003) and Weiss et al. (2000), whereas other studies used either very small ranges (Koetz et al., 2005) or even fixed *ALA* to a single value (España et al., 1999).

The bounds of the *HotS* parameter have been set to a large range (0.05-1). This range has also been used by Combal et al. (2003) for maize and Combal et al. (2002) for sugar beet.

As the absorption of leaf water is not influencing the spectral range used in this study (< 1000 nm), C_w was fixed to an arbitrary value ($C_w = 0.02$ cm). Dry matter content C_m has been measured during a field campaign for maize (Huber et al., 2006). The parameter limits were set accordingly ($C_m = 0.004$ - 0.007 mg/cm²). The N -parameter was set to a range corresponding to values often used in the literature for maize and sugar beet ($N = 1.3$ - 1.7). Similar values have been found by PROSPECT inversion (González-Sanpedro et al., 2007; Haboudane et al., 2004; Jacquemoud et al., 1995).

The soil reflectance spectrum for running the PROSAILH model was extracted from the CASI

imagery (mean of several bare soil pixel). A simple multiplicative soil brightness factor (α_{soil}) was introduced, representing the overall soil brightness, which was assumed to vary with soil water content and surface roughness (Atzberger et al., 2003). The range (0.7 - 1.3) was defined according to Koetz et al. (2005) and other studies. Within the distributions defined in Table 3, a random sampling scheme was applied to all parameters.

For PLEIADeS and SPARC data, the canopy parameter realizations were set in the same way (Richter et al., 2008a; Richter and Timmermans, 2009).

(2) Simulation of Sentinel-2 spectral sampling
The model was applied in direct mode to simulate reflectance signatures corresponding to the proposed spectral sampling for the Sentinel-2 sensor. Table 1 gives some specifications of the sensor, with central wavebands, spectral width, spatial resolution and field of application for each channel. All wavebands interesting for LAI or vegetation studies were included in the simulation. Hence, the calculations comprised the VIS (490, 560, 665 nm), the red edge (705 and 740 nm) and the NIR (775, 842 and 865 nm) parts of the spectrum. The channels located at 443, 940 and 1375 nm, sensitive to aerosol scattering and water vapor absorption, were not considered, since their scope is to support the atmospheric correction of the imagery. The two wavebands located in the short wave infrared (1610 and 2190 nm) were as well out of interest for the study, because they will be used for cloud/ice separation and burn scars mapping, respectively.

The measurement configuration used for the model simulations presented the actual condition during the sensor overpass with a solar zenith angle of 35° and a view zenith angle of 0° according to the almost-nadir position of the acquisitions. The fraction of diffuse irradiance, $skyl$, was fixed to 0.1 across all wavebands, according to many similar studies (Bacour et al., 2002; Schlerf and Atzberger, 2006; Weiss et al., 2002). Hence, we neglected both the wavelength dependence of $skyl$, as well as the fact that the amount of diffuse sky light depends on atmospheric conditions and solar zenith angle. This simplification seems justified by the fact that $skyl$ has only a very small influence on canopy reflectance (Clevers and Verhoef, 1993).

To take into account sensor and model uncertainties, a Gaussian (white) noise was added to the simulated canopy reflectance spectra before going to step (3). The noise was assumed to be proportional to the reflectance (mean of zero and standard deviation of 0.04) (Bacour et al., 2006, Baret et al., 2007). The simulated reflectance spectra were resampled according to the Sentinel-2 sensitivity.

(3) Sorting of the LUT along with a simple cost function:

The cost function used in this study calculates the root mean square error (RMSE) between measured and simulated spectra found in the LUT. The solution is the average of the parameter combinations found within less than 10 % of the lowest RMSE value.

$$RMSE = \sqrt{\frac{1}{n_\lambda} \sum_{i=1}^{n_\lambda} (R_{meas}^i - R_{LUT}^i)^2} \quad (1)$$

where n_λ is the number of wavelengths used in the calculation, R_{meas}^i the measured image reflectance, and R_{LUT}^i the simulated reflectance of the spectrum in the LUT at wavelength i .

Usually, only little information is available about the crop status in an agricultural area. Thus, from an operational point of view, algorithms used for parameter (LAI) estimation from E.O. data have to fulfill the requirement to be universally valid. Consequently, a simple cost function, instead of a modified one, including a-priori information (e.g., Combal et al., 2003; Huber et al., 2006; Weiss et al., 2000) was applied to the algorithm. Note however, that in the construction of the LUT we applied a denser sampling around the most probable C_{ab} and LAI values (see Table 3), which can also be seen as a kind of prior information.

Alternative retrieval algorithms

To test the potential of the LUT approach and the suitability of the Sentinel-2 band configuration, two other retrieval algorithms (iterative optimization and neural nets) have been applied to the AgriSAR data set. In this way we verified that the findings of the standard approach (as described in 2.4.2) are not biased by the selected inversion approach. Furthermore, an alternative band composition has been tested (B2), regarded as ‘ideal’ for vegetation studies (Thenkabail et al., 2004). By comparing the Sentinel-2 band setting (B1) with B2 we confirm/reject the band setting of the future sensor. To make the different approaches as comparable as possible, the same Gaussian (white) noise was used for all algorithms.

Neural Networking (NN)

To invert PROSAILH using a neural network (NN), the synthetic database (LUT) of simulated canopy spectra and corresponding parameter sets was used (section 2.4.2.). The simulated database allows training the non-linear relationship between the spectral variables (as “measured” inputs) and the desired canopy biophysical

Table 3. Range of input variables (lower (LB) and upper (UB) bounds) for PROSAILH model inversion using SQP algorithm, as well as number of classes and distribution of input variables used to establish the synthetic canopy reflectance data base for use in the LUT and for the training of the NN.

Model Variables		Units	Min (LB)	Max (UB)	Distribution of variables
<i>Leaf parameters:</i>					
(PROSPECT)					
$N^{(1,2/10)}$	Leaf structure index	unitless	1.3	1.7	Uniform
$C_{ab}^{(3)}$	Leaf chlorophyll content	$[\mu\text{g}/\text{cm}^2]$	10	70	Gaussian (mean 40, SD 10)
$C_m^{(4)}$	Leaf dry matter content	$[\text{g}/\text{cm}^2]$	0.004	0.007	Uniform
<i>Canopy variables:</i>					
(SAILH)					
$LAI^{(5)}$	Leaf area index	$[\text{m}^2/\text{m}^2]$	0	6.0	Gaussian (Mean 2, SD 1)
$ALA^{(6)}$	Average leaf angle	$[\text{°}]$	40	70	Uniform
$HotS^{(7,8)}$	Hot spot parameter	$[\text{m}/\text{m}]$	0.05	1	Uniform
$\alpha_{soil}^{(9)}$	Soil brightness factor	unitless	0.7	1.3	Uniform
θ_s	sun zenith angle	$[\text{degree}]$		35	/
θ_v	view zenith angle	$[\text{degree}]$		0	/
ϕ	azimuth anlge between sun and sensor	$[\text{degree}]$		0	/

Similar variable ranges/values were used by the following studies : ¹ González-Sanpedro et al., 2007 ; ² Haboudane et al., 2004 ; ³ D’Urso et al, 2004 ; ⁴ Huber et al., 2006; ⁵Geringhausen et al., 2007; ⁶ Atzberger 2004; ^{7,8} Combal et al., 2002, 2003; ⁹ Koetz et al., 2005

variables (as “estimated” outputs). Once trained, the NN is applied to the CASI/Sentinel-2 spectra to map the canopy biophysical variables.

To prevent network overfitting and overspecialization (and hence lack of generalization) several measures were taken. First of all, a simple three layer feed-forward backpropagation network with a tan-sigmoidal transfer function in the hidden layer and a linear transfer function in the output layer was selected. After several trial and errors, the following (compact) network structure was chosen: 5 neurons in the hidden layer, 7 input neurons (8 for the B2 band setting) and 3 output neurons (to predict simultaneously LAI , the leaf chlorophyll content, C_{ab} , and the soil brightness factor, α_{soil}) were used. Both, the low number of hidden neurons and the simultaneous estimation of several biophysical variables prevent overfitting and overspecialization (Atzberger, 2004; Udelhoven et al., 2000).

To further improve network generalization, the early stopping technique (Demuth and Beale, 2003) was applied. For this purpose, the patterns generated with PROSAILH were divided into three subsets (60, 20 and 20 %). The first subset (60 % of the pattern) was used

for updating the weight and biases of the network (training data set). The error on the test data set (20 % of the pattern) was monitored during the training process. The training was stopped automatically when the error in the test data set started to rise while the error on the training data set continued decreasing; such a situation is an indication of network overfitting. The third subset (remaining 20 % of the synthetic spectra) was used after completion of the training to assess the accuracy of the RTM inversion on synthetic spectra.

To avoid sub-optimal network results, 51 networks were trained with randomly initialized weights/biases and with different synthetic training, test and validation data sets. As the networks gave very similar results on the synthetic validation data sets, it was decided to keep them all and to invert the image spectra with all networks. The final output was then simply the average of the 51 results. The standard deviation around the estimated average was kept as a measure of uncertainty.

Iterative optimization approach (SQN)

Traditionally, radiative transfer models have often been inverted using iterative optimization techniques. Thus, we included this inversion strategy as another benchmark for comparison with the results achieved by means of the standard LUT approach. For the iterative optimization, the Sequential Quadratic Programming (SQP) has been implemented by using the MATLAB function *fmincon*. This function solves a quadratic programming (QP) sub-problem iteratively. The method allows to mimic closely Newton's method for constrained optimization. An approximation is performed for each major iteration of the Hessian Lagrangian function using a quasi-Newton updating method. An overview of SQP can be found in the Matlab documentation (MathWorks, Inc., 1984-2007). The SQP requires an initial set of parameters to start off the optimization process. However, these initial parameter values may affect strongly the solution achieved by the algorithm (Jacquemoud et al., 1995). In order to mitigate this effect, five different initial sets for the parameters were randomly selected in the ranges shown in Table 3.

Table 4. Spectral sampling (named B2) used as alternative band set to the Sentinel-2 band configuration. Wavebands and their sensitivity to plant components are extracted from the work of Thenkabail et al. (2004). Note: Thenkabail et al. (2004) proposed 22 bands, but here only those matching the CASI spectral configuration (≤ 885 nm) could be used.

Central waveband Δ (nm)	Sensitivity to plant components
495	Sensitive to senescing, carotenoid, browning, and soil background
555	Green peak, sensitive to total chlorophyll
655	Absorption pre-maxima, sensitive to biomass and soil background
675	Absorption maxima, greatest soil –crop contrast in 350–2500 nm
705	Start of rapid change of slope, sensitive to vegetation stress and dynamics
735	End of rapid change of slope, sensitive to vegetation stress and dynamics
885	NIR pre-peak; sensitive to biomass, LAI, and protein

In contrast to the LUT and NN based inversion, no prior information concerning the parameter distribution (such as *LAI* and *C_{ab}*) was implemented in the algorithm. The optimization algorithm was only forced to remain within the parameter bounds. This hinders a detailed comparison of the three approaches which was nevertheless out of the scope of this study.

Larger Look-up Table and alternative ‘ideal’ spectral sampling

To verify that the standard LUT size of 100 000 parameters is appropriate, a LUT with a size of 200 000 cases of canopy parameter combinations (‘LUT2’) was constructed for comparison. Parameter bounds, distribution and sampling scheme applied were the same as for the LUT described in section 2.4.2.

Furthermore, another band set (‘B2’) was chosen according to the results of a work from Thenkabail et al. (2004). These wavebands were found to characterize and classify best vegetation and crops due to their sensitivity to chlorophyll, biomass, LAI, plant moisture and vegetation stress. The seven bands (out of 22 proposed by Thenkabail et al., 2004) located in the CASI spectra were averaged in a bandwidth of 10 nm. Table 4 gives an overview of the B2 band set and the sensitivities of the various bands in vegetation related studies.

Results

In this chapter we first present the quality of LAI estimation from all campaigns using the standard LUT approach (3.1.). RTM simulation accuracy is then presented in the following sub-section (3.2.). Next, the standard LUT results are compared to other model inversion approaches and to results obtained by the B2 band combination (3.3.) using the data set of the AgriSAR campaign. A general discussion on the applied method(s), their problems and applicability in an operational context of Sentinel-2 is given in the discussion (4.).

Performance of the LUT with the Sentinel –2 spectral sampling

Scatterplots between measured and estimated LAI values are shown in Figure 2a-e, including error bars of ± 1 standard deviation of measurements and retrievals. The performance of the LUT approach using the spectral bands of the future Sentinel-2 sensor can be regarded as satisfying in the case of sugar beet (Figure 2a: AgriSAR; Figure 2d: SPARC) but indicates some problems for maize (Figure 2b: AgriSAR; Figure 2c: PLEIADeS; Figure 2e: SPARC). For sugar beet, a root mean square error (RMSE) of 0.18 was achieved for AgriSAR and a RMSE of 0.6 for SPARC. (rel. RMSE: 8 % and 9.2 % respectively). However, for maize the estimation performance was significantly lower with RMSE of 0.43 for AgriSAR and RMSE of 0.4 for PLEIADeS and SPARC (rel. RMSE: 22 %, 16.7 and 16.3 %, respectively). Thus, the estimation quality for

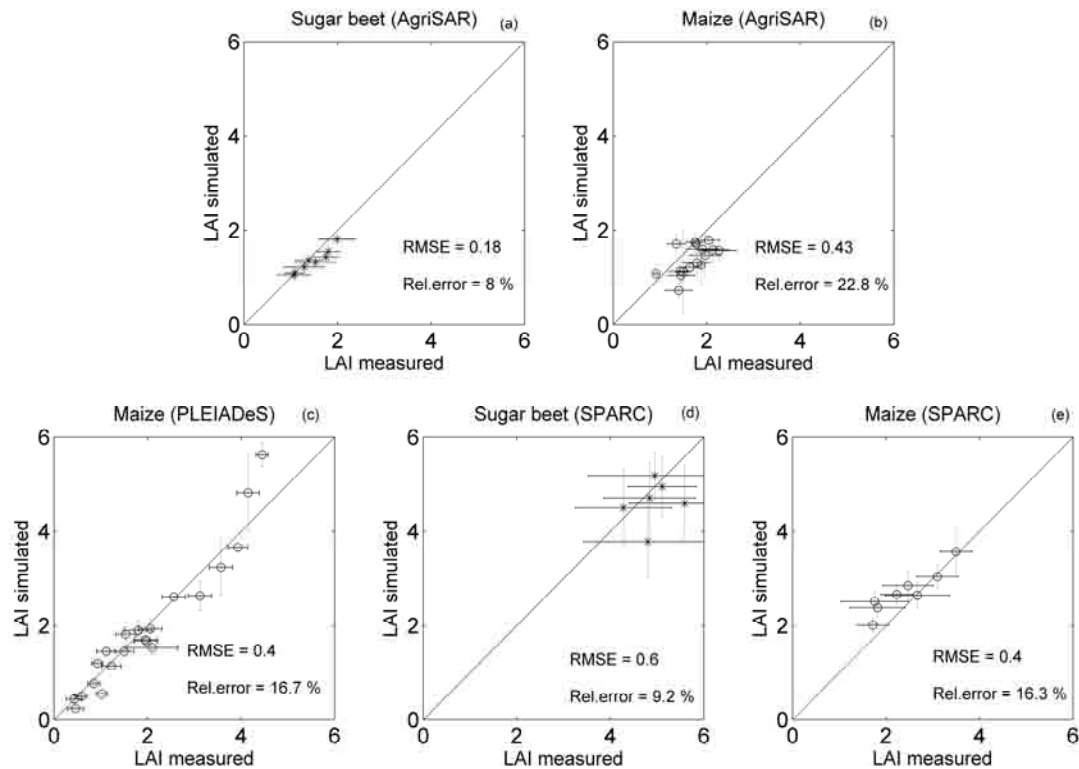


Figure 2. Measured and estimated LAI values for all campaigns (2a: AgriSAR sugar beet field (ID 102); 2b: AgriSAR maize field (ID 222); 2c: PLEIADeS maize; 2d: SPARC sugar beet; 2e: SPARC maize). The LAI estimates were obtained from LUT inversion approach and using the Sentinel-2 band configuration (B1). The standard deviations of measurements and simulations are indicated by error bars.

sugar beet is well within the 10 % requirements of the GMES mission. On the contrary, in the case of maize, the inversion falls short of expectations. Especially for the AgriSAR fields, a trend toward underestimation could be observed. The underestimation of LAI is small for sugar beet but pronounced for the maize field.

Spatial LAI of the two AgriSAR fields, obtained with the LUT inversion method, are illustrated in Figure 3ab. One easily recognizes distinct spatial structures, revealing the knowledge of the fields: The maps confirm a mean value of LAI around 1.5-2 for both crops, as monitored by the AgriSAR teams during this period (Gerighausen et al., 2007). Maize exhibited a slightly higher range (LAI: 0.5 - 3.0) than the sugar beet (LAI: 0.5 - 2.5). This within field growth variability reflects a typical pattern for crops in rainfed agriculture, being more sensitive to soil heterogeneity than irrigated crops (Richter et al., 2008b).

Match between measured spectra and RTM simulations

When inverting radiative transfer models an important aspect is to control its ability to recreate the measured spectra using the retrieved model parameters. After the LUT inversion process, the estimated parameters were used as input to run the model in the forward way. Then the RMSE between measured and re-simulated reflectance for all 8 wavebands was calculated pixelwise for the whole fields. The resulting maps of RMSE are depicted in Figure 3c for sugar beet and 3d for maize of the AgriSAR campaign. The results suggest a good overall performance of the model for sugar beet with generally acceptable matches between measured and simulated spectra (0.008-0.017). The higher RMSE values of maize (0.007-0.088) correspond to the lower LAI retrieval performance for this crop. It indicates a general mismatch between input spectra and PROSAILH simulated reflectances. Probably, the pronounced row structure (clumping) and the early growth stage of maize (with low coverage) requires a specific canopy reflectance model that takes this effects into account (e.g., Yao et al., 2008). As both fields were geographically close to each other and

Table 5. Root mean square error (RMSE), relative percentage error (%) and coefficient of determination (R^2) between measured and simulated LAI for two agricultural fields of the AgriSAR campaign: ID 102 (sugar beet) and ID 222 (maize). The results obtained with the standard LUT are shown in bold. Four alternative solutions are also presented: a larger LUT with 200 000 entries, SQP and NN with the Sentinel-2 band configuration and a LUT run with an alternative band setting B2 (Thenkabail et al., 2004).

		LUT1	LUT2	SQP	NN	LUT1
		100 000	200 000			100 000
		Sentinel-2	Sentinel-2	Sentinel-2	Sentinel-2	B2
ID102 sugar beet	RMSE	0.18	0.19	0.58	0.16	0.29
	% error	8.0	9.8	26.8	7.9	18.5
	R^2	0.92	0.90	0.19	0.88	0.70
ID222 maize	RMSE	0.43	0.40	0.62	0.94	0.34
	% error	22.8	21.4	30.5	52.8	18.7
	R^2	0.35	0.36	0.13	0.35	0.36

sampled within the same image, artifacts related to the atmospheric and radiometric pre-processing can be excluded.

Comparison with alternative methods

The standard LUT approach (size 100 000) has been compared with two alternative inversion approaches and a different band setting for the AgriSAR data set. Results are summarized in Table 5 giving RMSE, R^2 and % error for all inversion methods and the alternative (B2) band set. From Table 5 it can be seen that an increased LUT size (200 000) did not change the estimation accuracies compared to the standard approach. This confirms the findings of Weiss et al. (2000) who pointed out that 100 000 LUT entries are appropriate.

Larger differences were observed if SQP or NN were used for RTM inversion. SQP gave significantly lower accuracies for both fields with increased RMSE and lower R^2 . The neural nets performed well for sugar beet but resulted in strongly biased LAI values in the case of maize. Compared to the standard LUT approach, the R^2 remained more or less unchanged indicating that the spatial structure of the estimates was preserved. In summary, the results clearly show that the observed errors of the standard LUT are not the results of an inappropriately chosen inversion approach. Likewise, the alternative band setting (B2) had also only insignificant effects when compared to the standard LUT approach; for one field (sugar beet) the accuracies

decreased slightly, whereas for the other field (maize) somewhat better results have been obtained. From this finding it can be concluded that the Sentinel-2 band setting is well suited for vegetation related studies.

Retrieval accuracy of the neural net

The neural nets learned easily the relation between spectral inputs and the (three) output variables. For the synthetic validation data set, the RMSE for the three outputs and the 51 duplicate nets were $0.4 \text{ m}^2/\text{m}^2$ (LAI), $5.5 \mu\text{g}/\text{cm}^2$ (C_{ab}) and 0.12 (α_{soil}) with a slope close to one and intercept of zero (not shown). As the validation data set did not enter in the network calibration, the low RMSE indicate very good network learning.

Generally, the error of the synthetic training, test and validation data sets decreased very fast. The error curve was steep during the first 20 iterations before reaching a more or less horizontal level (not shown). On average, the early stopping criteria automatically stopped training after less than 50 iterations.

For the two AgriSAR fields, the NN explained between 35 % (maize) and 89 % (sugar beet) of the total variance in the field measured LAI. However, a strong offset in the retrieved LAI of maize (ID 222) can be noted, resulting in high RMSE for this field compared to the standard LUT approach. We suppose that the offset results from a combination of RTM shortcomings (i.e., the row structure of the maize is not taken into account) and biased in situ measurements (i.e., the stems reduce the measured gap fractions).

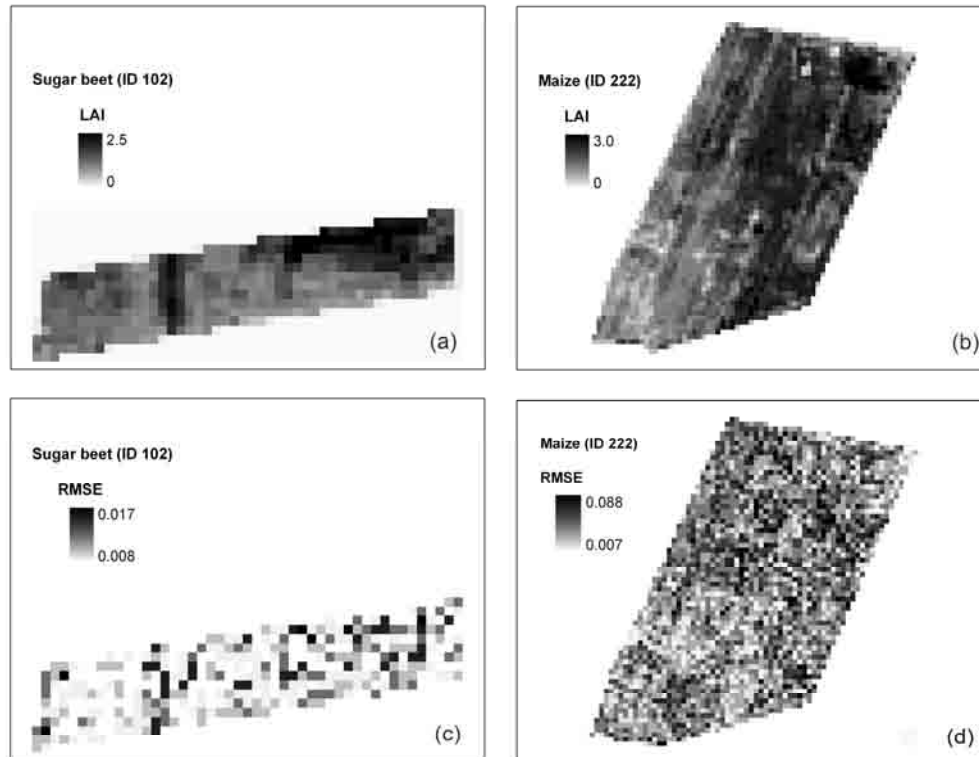


Figure 3. Sentinel-2 derived LAI maps (a-b) from the AgriSAR campaign and maps of the RMSE between measured and simulated spectra (c-d). The results were obtained using the standard LUT approach (100 000 cases of parameter combinations) with the proposed band configuration of the upcoming Sentinel-2 satellite. The RMSE (c-d) have been calculated across the 8 Sentinel bands with canopy parameters found by the LUT approach.

Retrieval accuracy using the iterative optimization approach

Despite the use of the same radiative transfer model, an identical cost function and range of input variables, the differences in accuracy between the SQP inversion, compared to the LUT and NN approaches, are pronounced (Table 5). The failure of the SQP inversion may be explained by the drawback of iterative optimization methods to converge into local minima (Qiu et al., 1998). To partially overcome this problem, five different initial parameter sets were considered to start off the optimization. According to the criterion applied for the LUT, 10% was added to the smallest RMSE (between simulated and measured reflectance) in order to average all solutions being in this range. However, the difference between the smallest RMSE and the other four cases resulted mostly in errors greater than 10 %, indicating the importance of the initial parameter set. Thus, only the result with the smallest RMSE was selected as single solution. No attempts were made to run further initializations as the iterative optimization is computationally intensive in particular if large data sets have to be inverted.

Discussion

The estimation accuracies achieved with the LUT algorithm can be seen as fair. For sugar beet, the GMES/ Kopernikus requirements were barely met (precision: 8 - 9 %). On the other hand, with only 16 - 22 % accuracy, the LAI estimated for maize was beyond the GMES/ Kopernikus goal. The results confirm the findings of several studies for similar crops, using the same and also other retrieval methods, for example:

(1) Sugar beet: Combal et al. (2002): RMSE = 0.5-1.4; D'Urso et al. (2004): RMSE = 0.49; Jacquemoud et al. (1995): RMSE = 0.79;

(2) Maize: Haboudane et al. (2004): RMSE = 0.46-1.21; Koetz et al. (2005): RMSE = 0.69-0.79; Koetz et al. (2007): RMSE = 0.73; Vuolo et al. (2006): RMSE = 0.41 - 0.76; Walthall et al. (2004): RMSE = 0.41-1.27; Wu et al. (2007): RMSE = 0.63.

In particular for small LAI values of maize, our results reveal a significant underestimation of the estimated LAI. The canopy characteristics of both crops deviate strongly from the turbid medium assumption of the PROSAILH model (Andrieu et al., 1997): maize and

sugar beet are typically row-planted and affected by leaf clumping (i.e. leaves are grouped together rather than distributed uniformly). The chosen PROSAILH model, however, does not account for the leaf clumping induced by the row structure of maize. Lopez-Lozano et al. (2007) compared canopy gap fractions of heterogeneous maize canopies with turbid, homogeneous canopies using simulations from a 3-dimensional RTM. The results showed that gap fractions of a heterogeneous canopy observed from nadir were generally higher than those of a homogeneous canopy. Consequently, inversion of the nadir measured remote sensing signal of row planted maize canopies leads to an underestimation of LAI values using turbid medium RTM. Similar findings were also described by Koetz et al. (2007). For maize it has also to be considered that the in situ measurements using the LAI-2000 instrument are probably too high as vertical elements like stems significantly reduce the measured gap fractions of the LAI-2000 instrument, albeit without influencing to the same extent the measured canopy reflectance.

A possible explanation of the better results achieved for sugar beet may also be related to the different crop growth stages during the image acquisition. In the AgriSAR campaign, the maize plants reached only a height of ca. 1 m (maximum usually up to 4 m) and a coverage of ~ 40 %; whereas the sugar beet showed in this later growth stage already a more homogeneous coverage (~ 50 %). During the SPARC campaign, sugar beet plants covered almost completely the ground (i.e. ~ 80 %). Consequently, the influence of the soil background (which is further enhanced by the row structure of these crops) is probably stronger for maize fields compared to the sugar beet. The RTM falsely interprets the strong soil signal as a low(er) coverage leading to a too low LAI. Also for PLEIADeS maize, the lower LAI values ($LAI < 4$) were slightly underestimated. This cannot be confirmed for SPARC data, but here all LAI values were higher than 2.

In a future study it has to be tested if a simple mixture model, such as the one proposed by Baret et al. (2007) at landscape level or GEOSAIL proposed by Huemmrich (2001), is capable of reducing this effect. These considerations are also supported by Yao et al. (2008), who proposed the use of a row structure model for the early growth stage (before elongation) of maize canopies, and a homogeneous one for later growth stages (after elongation).

In the present study we used a unique parameter set for both crop types as the objective was to select for every parameter the most realistic bounds and distributions without introducing too detailed prior information that usually is not available without a simultaneous field campaign. However, the differences in the resulting retrieval accuracy suggest that the use of a well adapted

parameter input set for every single crop species may be necessary to increase the estimation quality. That means, a priori information, such as from on-site measurements, knowledge of the type of canopy architecture and of the distribution of canopy biophysical variables (Combal et al., 2003) should be specified according to the crop type monitored. However, the establishment of crop and phenology specific LUTs can be a time-consuming task, which is sub-optimum in view of an operational monitoring process, where fast and universally valid (and accurate) algorithms are required. Our results also highlight the limitations of too simplistic RTMs which fail if the basic assumptions are not met by the crop under investigation. In an operational context, this also implies that a detailed crop map is available in order to choose the most appropriate RTM.

By comparing the standard LUT approach with two contrasting inversion approaches it was possible to verify that the sometimes inaccurate estimations are not due to an inappropriate inversion algorithm. The chosen LUT approach resulted more accurate and more robust than the iterative optimization approach and the neural net. The latter was accurate for the sugar beet field but gave strongly biased results in the case of maize. The insufficient accuracy of the NN to estimate the LAI of maize correctly highlights one of the major disadvantages of neural nets. In fact, NN often show relatively unpredictable behavior when fed with input spectra that are (too) different from what has been presented during the learning stage (e.g., Baret & Buis, 2008; Kimes et al., 1998; Schlerf and Atzberger, 2006). If the targets are not well represented by the modeled spectra, LUTs are indeed more robust compared to NN. Walthall et al. (2004) pointed out that the performance of the NN process may be improved if model input parameters were estimated from direct field measurements. This, however, would run counter to the stated objective of this analysis, which was to retrieve regional LAI estimates from satellite data without relying heavily on site-specific, ground calibration measurements. Another way to increase the robustness of the nets is to train them with higher noise levels as the one used in this research (e.g., Udelhoven et al., 2000). In the present study, however, such possible improvements have not been evaluated.

Unreliable results have been obtained for both crops with the SQP inversion. This finding, however, probably only holds for this study, as the SQP inversion was seriously penalized with respect to the LUT approach (and to some extent also the NN inversion) as it did not take advantage of the available prior information regarding LAI and C_{ab} (Table 3). This prior information has been taken into account for the LUT construction. The same LUT has also been used to train the NN. It would have been possible to include the prior information also in the SQP inversion (using a

modified cost function), but this was out of the scope of the present study.

The efficiency of LUT inversion approaches in operational contexts for LAI estimation was confirmed by other studies, even for more complex models (e.g. Myneni et al., 2002; Peddle et al., 2003, 2004). In the work from Peddle et al. (2003), a 5-scale geometric-optical reflectance model was applied for different forest classes, based on the Li and Strahler Geometric Optical Mutual Shadowing (GOMS) model in 'multiple forward mode' (MFM-5-Scale). Such modeling can provide a higher quality of canopy simulation, since radiative transfer properties are described more realistic than one-dimensional models such as SAILH, for heterogeneous canopies. Ground-measured LAI data were successfully retrieved with LUT based MFM-5-Scale inversion. However, for the reflectance and transmittance the model incorporates either spectral measurements or the leaf model LIBERTY. In a study of Moorthy et al (2003), LIBERTY was found to be more critical for the use in inversion procedures than PROSPECT, amongst others due to the need of detailed a priori knowledge. The PROSPECT model instead showed satisfying agreement with measured spectra, even for needles when implementing an empirically determined geometric form factor.

Conclusions

Leaf Area Index over the German DEMMIN test site was estimated for maize (16 ESU, corresponding to 348 individual observations) and sugar beet (8 ESU, corresponding to 192 observations) based on the proposed bands of the future earth observation satellite Sentinel-2 configuration from CASI imagery and by using a LUT inversion approach. The approach was additionally tested with two data sets of maize and sugar beet from two other campaigns leading to a range of LAI from 0.4 to 5.6. The LUT was constructed using the well established SAILH+PROSPECT radiative transfer model for homogeneous canopies. The physically-based approach was chosen since it does not require detailed in situ calibration data sets, constituting a major advantage of physical over empirical models.

In view of applications for vegetation monitoring, the findings of the study should be considered as preliminary as only two different crops were analyzed for the estimation of only one canopy variable (LAI). Moreover, additional measurements of other canopy characteristics (such as chlorophyll concentration, leaf dry matter content etc.) were missing and hence we cannot validate whether or not the PROSAILH - modeled reflectance agreed with CASI measured

reflectance for the choice of the right input parameter setting.

The expected GMES/ Kopernikus goal accuracy of $\leq 10\%$ could be achieved for sugar beet ($\sim 8 - 9\%$), but not for maize ($\sim 16 - 22\%$). Neither the implementation of alternative estimation approaches (including two model inversion techniques: neural nets and iterative optimization), nor the implementation of another waveband combination, an 'optimal sampling' (from Thenkabail et al., 2004), could achieve significant improvements, highlighting limitations of the selected radiative transfer model.

Our results confirm that the 1-dimensional SAILH+PROSPECT model is sufficient for homogeneous structured canopies, whereas for heterogeneous row crops, such as maize, a higher complexity of modeling is required. Such kind of 3-dimensional radiative transfer modeling is for instance implemented in the MODIS-15 operative algorithm for broadleaf crops (Myneni et al., 2002). However, the MODIS-15 approach requires information of canopy architectural types, derived from classification of vegetation in different biomes and multi-angular observations, which are not always available from high spatial resolution sensors needed for smaller field-scale management purposes. Moreover, classification of biomes can fail and a backup algorithm is applied using a simple empirical relationship between LAI and the normalized difference vegetation index (NDVI).

The PROSAILH model can be a reasonable compromise between such simple empirical VI-based methods and very complex RTMs for the retrieval of LAI in most crop systems when using spectral observations of limited spectral dimension and with one viewing angle only. The model is for instance applied in the CYCLOPES algorithm for globe wide biophysical products from VEGETATION (Baret et al., 2007).

The possibility of coupling canopy reflectance models, such as SAILH, with the leaf model PROSPECT, successfully validated e.g. by Newnham and Burt (2001) or Moorthy et al. (2003), can be seen as a promising instrument for a range of applications regarding crop status information. Hence, empirical based inclusion of leaf reflectance and transmittance, creating uncertainties and requiring calibration for each vegetation type, can be avoided.

Concerning the inversion approach, the simple and widely used LUT technique confirmed to be the most stable, accurate and fast approach for the estimation of LAI in this study.

Conclusively, the coupled PROSPECT+SAILH model with an implemented LUT algorithm can be a suitable tool to support the elaboration of Sentinel-2 satellite data to ensure the delivering of quality products.

However, when accuracies of 10 % are required even for row crops, more complex RTMs should be applied.

Acknowledgement

The authors thank L. Guanter and colleagues from the Laboratory for Earth Observation, Department of Earth Physics and Thermodynamics, University of Valencia, for radiometric and spectral calibrations and atmospheric correction of CASI imagery.

This work is carried out in the framework of PLEIADeS project (Participatory multi-Level EO-assisted tools for Irrigation water management and Agricultural Decision-Support; Contract 037095 financed by U.E.- VI F.P.).

References

- Andrieu, B., Baret, F., Jacquemoud, S., Malthus, T. and Steven, M. 1997. Evaluation of an improved version of SAIL model for simulating bidirectional reflectance of sugar beet canopies. *Remote Sensing of Environment*, Vol. 60, No. 3, pp. 247-257.
- Atkinson, P. M. and Tatnall, A. R. L. 1997. Neural networks in remote sensing. *International Journal of Remote Sensing*, Vol. 18, No. 4, pp. 699–709.
- Atzberger, C. 1997. Estimates of winter wheat production through remote sensing and crop growth modeling. *VWF Verlag fuer Wissenschaft und Forschung*, Berlin. 261 pp.
- Atzberger, C. 2004. Object-based retrieval of biophysical canopy variables using artificial neural nets and radiative transfer models. *Remote Sensing of Environment* Vol. 93, pp. 53-67.
- Atzberger, C., Jarmer, T., Schlerf, M., Koetz, B., Werner, W. 2003. Retrieval of wheat bio-physical attributes from hyperspectral data and SAILH+PROSPECT radiative transfer model. *Proceedings of 3rd EARSeL Workshop on Imaging Spectroscopy*, 13-16 May 2003, Herrsching, Germany.
- Bacour, C., Jacquemoud, S., Tourbier, Y., Dechambre, M. and Frangi, J.-P. 2002. Design and analysis of numerical experiments to compare four canopy reflectance models. *Remote Sensing of Environment*, Vol. 79, pp. 72–83.
- Bacour, C., Baret, F., Béal, D., Weiss, M., Pavageau, K. 2006. Neural network estimation of LAI, fAPAR, fCover and LAIxCab, from top of canopy MERIS reflectance data: Principles and validation. *Remote Sensing of Environment*, Vol. 105, No. 4, pp. 313-325.
- Baret, F. and Buis, S. 2008. Estimating canopy characteristics from remote sensing observations. Review of methods and associated problems. In *S. Liang (ed.), Advances in Land Remote Sensing: System, Modeling, Inversion and Application*. Springer Netherlands, DOI: 10.1007/978-1-4020-6450-0_7, pp. 172-301.
- Baret, F., Hagolle, O., Geiger, B., Bicheron, P., Miras, B., Huc, M., Berthelot, B., Nino, F., Weiss, M., Samain, O., Roujean, J.L., Leroy, M. 2007. LAI, fAPAR and fCover CYCLOPES global products derived from VEGETATION. Part 1: Principles of the algorithm. *Remote Sensing of Environment*, Vol. 110, No. 3, pp.275- 286.
- Breda, N.J.J. 2003. Ground-based measurements of leaf area index: a review of methods, instruments and current controversies. *Journal of Experimental Botany*, Vol. 54, No. 392, pp. 2403-2417.
- Camps-Valls, G., Bruzzone, L., Rojo-Álvarez, J.L., Melgani, F. 2006. Robust Support Vector Regression for Biophysical Variable Estimation From Remotely Sensed Images. *IEEE Geoscience and Remote Sensing Letters*, Vol. 3, No. 3, pp. 339-343.
- Chen, J.M., Black, T.A. 1992. Defining leaf area index for non-flat leaves. *Plant, Cell and Environment*, Vol. 15, pp. 421–429.
- Chen, J. M., Rich, P. M., Gower, S. T., Norman, J. M. and Plummer, S. 1997. Leaf area index of boreal forests: Theory, techniques and measurements. *Journal of Geophysical Research*, Vol. 102, No. D24, pp. 29429– 29444.
- Cho, M., Skidmore, A., Atzberger, C. 2008. Towards red-edge positions less sensitive to canopy biophysical parameters for leaf chlorophyll estimations using properties optique spectrales des feuilles (PROSPECT) and scattering by arbitrarily inclined leaves (SAILH) simulated data. *International Journal of Remote Sensing* Vol. 29, No. 7-8, pp. 2241-2255.
- Clevers, J.G.P.W. and Verhoef, W. 1993. LAI estimation by means of the WdVI: a sensitivity analysis with a combined PROSPECT-SAIL model. *Remote Sensing Reviews*, Vol. 7, No. 1, pp. 43-64.
- Combal, B., Baret, F. and Weiss, M. 2002. Improving canopy variables estimation from remote sensing data by exploiting ancillary information. Case study on sugar beet canopies. *Agronomie*, Vol. 22, No. 2, pp. 205–215.
- Combal, B., Baret, F., Weiss, M., Trubuil, A., Macé, D., Pragnère, A. 2003. Retrieval of canopy biophysical variables from bidirectional reflectance using prior information to solve the ill-posed inverse problem. *Remote Sensing of Environment*, Vol. 84, pp. 1–15.
- Cutini, A., Matteucci, G. and Mugnozza, G. S. 1998. Estimation of leaf area index with the Li-Cor LAI 2000 in deciduous forests. *Forest Ecology and Management*, Vol. 105, pp. 55–65.
- Darvishzadeh, R., Skidmore, A., Schlerf, M., Atzberger, C. 2008a. Inversion of a radiative transfer model for estimating vegetation LAI and chlorophyll in a heterogeneous grassland. *Remote Sensing of Environment*, Vol. 112, pp. 2592-2604.
- Darvishzadeh, R., Atzberger, C., van Wieren, S. and Skidmore, A. 2008b. Estimation of vegetation LAI from hyperspectral reflectance data: effects of soil type and plant architecture. *International Journal of Applied Earth Observation and Geoinformation*, Vol. 10, No. 3, pp. 358-373.
- Demuth, H. and Beale, M. 2003. Manual of Neural Network Tool Box - For Use with MATLAB, *MATLAB User's Guide*, Version 4, the Math Works Inc.
- Dorigo, W.A., Zurita-Milla, R., de Wit, A.J.W., Brazile, J., Singh, R. and Schaepman, M.E. 2007. A review on reflective remote sensing and data assimilation techniques for enhanced agroecosystem modelling. *International Journal of Applied Earth Observation and Geoinformation*, Vol. 9, No. 2, pp. 165-193.
- Durbha, S. S., King, R. L., and Younan, N. H. 2007. Support vector machines regression for retrieval of leaf area index from multi-angle imaging spectroradiometer. *Remote Sensing of Environment*, Vol. 107, No. 1–2, pp. 348–361.
- D'Urso G., Dini L., Vuolo F., Guanter L. 2004. Retrieval of vegetation biophysical parameters by inverting hyperspectral, multiangular CHRIS/PROBA Data from SPARC 2003. *Proceedings of the 2nd CHRIS/Proba Workshop*, ESA/ESRIN, 28-30 April 2004, Frascati, Italy.
- España, M., Baret, L., Aries, F., Chelle, F., Andrieu, B. and Prévot, L. 1999. Modeling maize canopy 3D architecture application to reflectance simulation. *Ecological Modelling*, Vol. 122, pp. 25–43.
- EUCARPIA, the European Association for Research on Plant Breeding. URL: <http://www.eucarpia.org/index.html> (Accessed March 4, 2009)
- European Space Agency (ESA) 2007. GMES Sentinel-2 Mission Requirements Document, issue 2 revision 0- 30/01/2007, EOP-SM/1163/MR-dr, 31 p., European Space Agency (ESA), 2007.
URLs:
http://www.esa.int/esaLP/ASERBVNW9SC_index_0.html
http://www.esa.int/esaLP/SEMZHMODU8E_LPgmes_2.html
http://www.esa.int/esaEO/SEMHS74XQEF_environment_0.html

- (Accessed March 4, 2009)
- European Space Agency (ESA) 2008. The Earth Observation Handbook, Climate Change Special Edition 2008. URL: <http://www.eohandbook.com/eohb2008/earthobservation.htm> (Accessed March 4, 2009)
- Filella, I. and Penuelas, J. 1994. The red edge position and shape as indicators of plant chlorophyll content, biomass and hydric status. *International Journal of Remote Sensing*, Vol. 15, No. 7, pp.1459-1470.
- Gerighausen, H., Borg, E., Wloczyk, C., Fichtelmann, B., Günther, A., Vajen, H.H., Rosenberger, M., Schulz, M., Engler, H-G. 2007. DEMMIN – a test site for the validation of Remote Sensing data products. General description and application during AgriSAR 2006. *Proceedings of the AGRISAR and EAGLE campaigns final workshop*, 15-16 October, 2007. ESA/ESTEC, Noordwijk, The Netherlands. 9 p.
- Goel, N. S. 1988. Models of vegetation canopy reflectance, their use in estimation of biophysical parameters from reflectance data. *Remote Sensing Reviews*, Vol. 4, pp. 1–212.
- Goel, N.S. and Grier, T. 1988. Estimation of canopy parameters for inhomogeneous vegetation canopies from reflectance data: III. Trim: A model for radiative transfer in heterogeneous three-dimensional canopies. *Remote Sensing of Environment*, Vol. 25, No. 3, pp. 255–293.
- Goel, N. S. and Thompson, R. L. 1984. Inversion of vegetation canopy reflectance models for estimating agronomic variables: 4. Total inversion of the sail model. *Remote Sensing of Environment*, Vol. 15, No. 3, pp. 237–253.
- Goel, N.S. and Thompson, R.L. 2000. A snapshot of canopy reflectance models and a universal model for the radiation regime. *Remote Sensing Reviews*, Vol. 18, pp. 197–225.
- González-Sanpedro, M. C., Le Toan, T., Moreno, J., Kergoat, L., Rubio, E. 2007. Seasonal variations of leaf area index of agricultural fields retrieved from Landsat data. *Remote Sensing of Environment*, Vol. 112, No. 3, pp. 810–824.
- Gower, S.T., Kucharik, C.J., Norman, J.M. 1999. Direct and indirect estimation of leaf area index, f_{APAR} , and net primary production of terrestrial ecosystems. *Remote Sensing of Environment*, Vol. 70, No.1, pp. 29-51.
- Guanter, L., Estellés, V., Moreno, J. 2007. Spectral calibration and atmospheric correction of ultra-fine spectral and spatial resolution remote sensing data. Application to CASI-1500 data. *Remote Sensing of Environment*, Vol. 109, pp. 54–65.
- Haboudane, D., Miller, J.R., Pattey, E., Zarco-Tejada, P.J., Strachan, I.B. 2004. Hyperspectral vegetation indices and novel algorithms for predicting green LAI of crop canopies: Modeling and validation in the context of precision agriculture. *Remote Sensing of Environment*, Vol. 90, pp. 337-352.
- Hajsek, I., Bianchi, R., Davidson, M., D'Urso, G., Gomez-Sanches, A., Hausold, A., Horn, R., Howse, J., Low, A.J., Lopez-Sanchez, J.J., Ludwig, R., et al. 2007. AgriSAR 2006: airborne SAR and optics campaigns for an improved monitoring of agricultural processes and practices. *Proceedings of the AGRISAR and EAGLE campaigns final workshop*, 15-16 October, 2007. ESA/ESTEC, Noordwijk, The Netherlands. 8 p.
- Hu, B., Miller, J.R., Chen, J.M. and Hollinger, A.B. 2004. Retrieval of the canopy leaf area index in the BOREAS flux tower sites using linear spectral mixture analysis. *Remote Sensing of Environment*, Vol. 89, pp. 176–188.
- Huber K., Dorigo W. A., Bauer T., Eitzinger J., Haumann J., Kaiser G., Linke R., Postl W., Rischbeck P., Schneider W., Suppan F., Weihs P. 2006. Changes In Spectral Reflectance Of Crop Canopies Due To Drought Stress. *Proceedings of Earth observation for vegetation monitoring and water management, American American Institute of Physics*. 10-11 November 2005, Napoli. G. D'Urso, M.A. Osann Jochum, J. Moreno. (Eds), pp. 258-265.
- Huemmrich, K. F. 2001. The GeoSail model: a simple addition to the SAIL model to describe discontinuous canopy reflectance. *Remote Sensing of Environment*, Vol. 75, No. 3, pp. 423-431.
- Itres Research Ltd, 2006. URL: http://www.itres.com/CASI_1500 (Accessed March 4, 2009).
- Jacquemoud, S. and Baret, F. 1990. PROSPECT: A model of leaf optical properties spectra. *Remote Sensing of Environment*, Vol. 34, pp. 75-91.
- Jacquemoud, S., Baret, F., Andrieu, B., Danson, F. M. and Jaggard, K. 1995. Extraction of Vegetation Biophysical Parameters by Inversion of the PROSPECT + SAIL Models on Sugar Beet Canopy Reflectance Data. Application to TM and AVIRIS Sensors. *Remote Sensing of Environment*, Vol. 52, pp. 163-172.
- Jacquemoud, S., Bacour, C., Poilve, H. and Frangi, J.P. 2000. Comparison of four radiative transfer models to simulate plant canopies reflectance: Direct and inverse mode. *Remote Sensing of Environment*, Vol. 74, pp. 417–481.
- Jonckheere, I., Fleck, S., Nackaerts, K., Muys, B., Coppin, P., Weiss, M. and Baret, F. 2004. Review of methods for in-situ leaf area index determination. Part I. Theories, sensors and hemispherical photography. *Agricultural and Forest Meteorology*, Vol. 121, pp. 19–35.
- Kimes, D.S., Nelson, R.F., Manry, M.T. and Fung, A.K. 1998. Attributes of neural networks for extracting continuous vegetation variables from optical and radar measurements. *International Journal of Remote Sensing*, Vol. 19, No. 14, pp. 2639-2662.
- Kimes, D., Knjazikhin, Y., Privette, J. L., Abuelgasim, A. and Gao, F. 2000. Inversion methods for physically-based models. *Remote Sensing Reviews*, Vol. 18, pp. 381-440.
- Koetz, B., Baret, F., Poilvè, H., Hill, J. 2005. Use of coupled canopy structure dynamic and radiative transfer models to estimate biophysical canopy characteristics. *Remote Sensing of Environment*, Vol. 95, pp. 115–124.
- Koetz, B., Kneubühler, M., Huber, S., Schopfer, J. and Baret, F. 2007. LAI Estimation Based on Multi-Temporal CHRIS/PROBA Data and Radiative Transfer Modelling. *Proceedings of ENVISAT Symposium*, Montreux (CH), 23-27 April 2007, ESA Publications Division, Noordwijk (NL), SP-636, CD-ROM.
- Kuusk, A., 1991. The hot-spot effect in plant canopy reflectance. *Photon – vegetation interactions. Applications in Optical Remote Sensing and Plant Ecology*. R.B. Myneni and J. Ross (Ed.), Springer-Verlag, New York, pp. 139–159.
- LI-COR 1992. LAI-2000 Plant Canopy Analyzer Instruction Manual Lincoln, NE, USA: LICOR Inc.
- Liang, N.S. 2004a. *Quantitative remote sensing of land surfaces*. John Wiley and Sons, New York.
- Liang, N.S., 2004b. Estimation of Land Surface Biophysical Variables. *Qualitative Remote Sensing of Land Surfaces*. Kong, G.A. (Ed.), New York: Wiley Series in Remote Sensing. John Wiley and Sons, pp. 246–309.
- Lopez-Lozano, R., Baret, F., Chelle, M., Rochdi, N., and Espana, M. 2007. Sensitivity of gap fraction to maize architectural characteristics based on 4D model simulations. *Agricultural and Forest Meteorology*, Vol. 143, No. 3-4, pp. 217-229.
- Liu, J., Miller, J.R., Haboudane, D., Pattey, E. 2004. Exploring the relationship between red edge parameters and crop variables for precision agriculture. In *IGARSS'04, Proceedings of the International Geoscience and Remote Sensing Symposium*, 20-24 September 2004, Anchorage, Alaska, Vol. 2, pp. 1276-1279.
- Major, D. J., Schaalje, G. B., Wiegand, C. and Blad, B. L. 1992. Accuracy and sensitivity analyses of sail model-predicted reflectance of maize. *Remote Sensing of Environment*, Vol. 41, No. 1, pp. 61–70.
- Moorthy, I., Miller, J.R., Zarco-Tejada, P.J., Noland, T.L. 2003. Needle chlorophyll content estimation: a comparative study of PROSPECT and LIBERTY. In *IGARSS'03, Proceedings of the IEEE International Geoscience and Remote Sensing Symposium*, 21 – 25 July 2003, Toulouse, France, Vol. 3, pp. 1676-1678.
- Myneni, R.B., Maggion, S., Iaquinio, J., Privette, J.L., Gobron, N., Pinty, B. 1995. Optical remote-sensing of vegetation — modeling, caveats and algorithms. *Remote Sensing of Environment*, Vol. 51, pp. 169–188.

- Myneni, R.B., Hoffman, S., Knyazikhin, Y., Privette, J.L., Glassy, J., Tian, Y., Wang, Y., Song, X., Zhang, Y., Smith, G. R., Lotsch, A., Friedl, M., Morisette, J. T., Votava, P., Nemani, R. R. and Running, S. W. 2002. Global products of vegetation leaf area and fraction absorbed PAR from year one of MODIS data. *Remote Sensing of Environment*, Vol. 83, No. 1-2, pp. 214-231.
- Newnham, G.J. and Burt, T. 2001. Validation of a leaf reflectance and transmittance model for three agricultural crop species. In *IGARSS'01, Proceeding of the International Geoscience and Remote Sensing Symposium*, 9–13 July 2001, Sydney, Australia, Vol. 7, pp. 2976-2978.
- Peddle, D.R., Johnson, R.L., Cihlar, J., Leblanc, S.G., Chen, J.M. and Hall, F.G. 2003. Physically-Based Inversion Modeling for Unsupervised Cluster Labeling, Independent Forest Classification and LAI Estimation using MFM-5-Scale. *Canadian Journal of Remote Sensing*, Vol. 33, No. 3, pp. 214-225.
- Peddle, D.R., Johnson, R.L., Cihlar, J., Latifovic, R. 2004. Large area forest classification and biophysical parameter estimation using the 5-Scale canopy reflectance model in Multiple-Forward-Mode. *Remote Sensing of Environment*, Vol. 89, No. 2, pp.252-263.
- Pragnère, A., Baret, F., Weiss, M., Myneni, R., Knyazikhin, Y., Wang, L.B. 1999. Comparison of three radiative transfer model inversion techniques to estimate canopy biophysical variables from remote sensing data. In *IGARSS'99, Proceeding of the International Geoscience and Remote Sensing Symposium*, 28 June – 2 July 1999, Hamburg, Germany, Vol. 2, pp. 1093-1095.
- Qiu, J., Gao, W., Lesht, B.M. 1998. Inverting optical reflectance to estimate surface properties of vegetation canopies. *International Journal of Remote Sensing*, Vol. 19, No. 4, pp. 641–656.
- Richter, K. and Timmermans, W., 2009. Physically based retrieval of crop characteristics for improved water use estimates. *Hydrology and Earth System Sciences*, Vol. 13, pp. 663-674.
- Richter, K., Vuolo, F., D'Urso, G. 2008a. Leaf area index and surface albedo estimation: comparative analysis from vegetation indexes to radiative transfer models. In *IGARSS'08, Proceeding of the International Geoscience and Remote Sensing Symposium*, 6-11 July 2008, Boston (MA), Vol. 3, pp. 736-739.
- Richter, K., Rischbeck, M.P., Eitzinger, J., Schneider, W., Suppan, F., Weihs, P. 2008b. Plant growth monitoring and potential drought risk assessment by means of Earth Observation data. *International Journal of Remote Sensing*, Vol. 29, No. 17-18, pp. 4943-4960.
- Schlerf, M. and Atzberger, C. 2006. Inversion of a forest reflectance model to estimate structural canopy variables from hyperspectral remote sensing. *Remote Sensing of Environment*, Vol. 100, No. 3, pp. 281-294.
- Schlerf, M., Atzberger, C. and Hill, J. 2005. Remote sensing of forest biophysical variables using HyMap imaging spectrometer data. *Remote Sensing of Environment*, Vol. 95, No. 2, pp. 177-194.
- Scurlock, J. M. O., Asner, G. P. and Gower, S. T. 2001. Worldwide Historical Estimates of Leaf Area Index, 1932- 2000. *Oak Ridge National Laboratory, ORNL/TM-2001/268*.
- Soudani, K., Francois, C., le Maire, G., Le Dantec, V., Dufrene, E. 2006. Comparative analysis of IKONOS, SPOT, and ETM+ data for leaf area index estimation in temperate coniferous and deciduous forest stands. *Remote Sensing of Environment*, Vol. 102, No. 1, pp. 161-175.
- Stenberg, P., Rautiainen, M., Manninen, T., Voipio, P. and Smolander, H. 2004. Reduced simple ratio better than NDVI for estimating LAI in Finnish pine and spruce stands. *Silva Fennica*, Vol. 38, No. 1, pp. 3–14.
- Thenkabail, P.S., Smith, R.B., De-Pauw, E. 2002. Hyperspectral vegetation indices and their relationships with agricultural crop characteristics. *Remote Sensing of Environment*, Vol. 71, pp. 158–182.
- Thenkabail, P.S., Enclona, E.A., Ashton, M.S., Van Der Meer, B. 2004. Accuracy assessments of hyperspectral waveband performance for vegetation analysis applications. *Remote Sensing of Environment*, Vol. 91, pp. 354– 376.
- Udelhoven, T., Atzberger, C. and Hill, J. 2000. Retrieving Structural and Biochemical Forest Characteristics Using Artificial Neural Networks and Physically Based Reflectance Models. *Proceedings of the 20th EARSeL Symposium*, Dresden, 14-16 June, Dresden, Buchroithner (ed.), pp. 205-211.
- Verhoef, W. 1984. Light scattering by leaf layers with application to canopy reflectance modeling: the SAIL Model. *Remote Sensing of Environment*, Vol. 16, pp. 125-141.
- Verhoef, W. 1985. Earth observation modeling based on layer scattering matrices. *Remote Sensing of Environment*, Vol. 17, pp. 165–178.
- Verhoef, W., Bach, H. 2003. Simulation of hyperspectral and directional radiance images using coupled biophysical and atmospheric radiative transfer models. *Remote Sensing of Environment*, Vol. 87, pp. 23–41.
- Vuolo, F., D'Urso, L. Dini, G. 2006. Cost-effectiveness of vegetation biophysical parameters retrieval from remote sensing data. In: *SPIE's conference proceedings: Remote Sensing for Agriculture, Ecosystems, and Hydrology VIII*. M. Owe, G. D'Urso, C. M. Neale, Ben T. Gouweleeuw (Eds), Stockholm, Sweden, September 2006, Vol. 6359, pp. 63590N.
- Walshall, C., Dulaney, W., Anderson, M., Norman, J., Fang, H. and Liang, S. 2004. A comparison of empirical and neural network approaches for estimating corn and soybean leaf area index from Landsat ETM+ imagery. *Remote Sensing of Environment*, Vol. 92, No. 4, pp. 465-474.
- Weiss, M., Baret, F., Myneni, R.B., Pragnère, A. and Knyazikhin, Y. 2000. Investigation of a model inversion technique to estimate canopy biophysical variables from spectral and directional reflectance data. *Agronomie*, Vol. 20, pp. 3-22.
- Weiss, M., Baret, F., Leroy, M., Hauteceur, O., Bacour, C., Prévot, L., Bruguier, N. 2002. Validation of neural net techniques to estimate canopy biophysical variables from remote sensing data. *Agronomie*, Vol. 22, No. 6, pp. 547-553.
- Wu, J., Wang, D., Bauer, M.E. 2007. Assessing broadband vegetation indices and QuickBird data in estimating leaf area index of corn and potato canopies. *Field Crops Research*, Vol. 102, No. 1, pp. 33-42.
- Yao, Y., Liu, Q., Liu, Q., Li, X. 2008. LAI retrieval and uncertainty evaluations for typical row-planted crops at different growth stages. *Remote Sensing of Environment*, Vol. 112, No. 1, pp. 94-106.

4.2 Publikation II

Physically based retrieval of crop characteristics
for improved water use estimates.

Katja Richter and Wim Timmermans

Hydrology and Earth System Sciences 13: 663-674, 2009.

Physically based retrieval of crop characteristics for improved water use estimates

K. Richter¹ and W. J. Timmermans²

¹Department of Agricultural Engineering, University of Naples “Federico II”, via Università 100, 80055 Portici (Na), Italy

²International Institute for Geo-information Sciences and Earth Observation, Dept. of Water Resources, P. O. Box 6, 7500 AA Enschede, The Netherlands

Received: 28 January 2009 – Published in Hydrol. Earth Syst. Sci. Discuss.: 6 March 2009

Revised: 20 May 2009 – Accepted: 21 May 2009 – Published: 27 May 2009

Abstract. The increasing scarcity of water from local to global scales requires the efficient monitoring of this valuable resource, especially in the context of a sustainable management in irrigated agriculture. In this study, a two-source energy balance model (TSEB) was applied to the Barrax test site. The inputs of leaf area index (LAI) and fractional vegetation cover (fCover) were estimated from CHRIS imagery by using the traditional scaled NDVI and a look-up table (LUT) inversion approach. The LUT was constructed by using the well established SAILH + PROSPECT radiative transfer model. Simulated fluxes were compared with tower measurements and vegetation characteristics were evaluated with in situ LAI and fCover measurements of a range of crops from the SPARC campaign 2004. Results showed a better retrieval performance for the LUT approach for canopy parameters, affecting flux predictions that were related to land use.

last years that describe this interaction between land surface and atmosphere. Those models, known as soil-vegetation-atmosphere transfer schemes (SVAT), vary widely in their complexity and dimensionality (Timmermans et al., 2007).

The conjunction of currently optical, thermal and microwave Earth Observation (E. O.) data with SVAT schemes allows the spatial estimation of surface flux partitioning from land-surface temperature and dynamic vegetation variables (Anderson et al., 2007; Bindlish et al., 2001; Schmugge et al., 1998). For homogeneous canopies and land surfaces, a single-source modelling approach can be sufficient. However, vegetated surfaces are usually under heterogeneous conditions, which are better described by two-source models, treating the land surface as a composite of soil and vegetation components with separate fluxes and temperatures (Anderson et al., 2007; Timmermans et al., 2007). The Two-Source Energy Balance model (TSEB) for instance, first described in Norman et al. (1995) and updated by Kustas and Norman (1999) and Kustas et al. (2004), uses directional radiometric surface temperature for estimating component heat fluxes from soil and vegetation, i.e. instantaneous fluxes of net radiation (R_N), soil (G), sensible (H) and latent heat (LE). Several studies validated TSEB successfully against flux tower measurements or other modelling schemes (e.g. Anderson et al., 2007; Schmugge et al., 1998; Timmermans et al., 2007) and research is ongoing to improve model performance (Kustas and Norman, 1999; Li et al., 2005). Innumerable publications focused on improving accuracy of temperature and roughness characteristics, but despite the importance of vegetation characteristics, still either rather simple empirical models are used, or vegetation parameters are derived from visual observations, some samples or indirectly from measurements of biomass or plant species type (Zhan et al., 1996). However, analyses by Zhan et al. (1996) and

1 Introduction

Given the increasing scarcity of water at local, regional and global scales, an efficient monitoring of this valuable resource becomes more and more essential, especially in the context of a sustainable management in irrigated agriculture and other water-related disciplines, such as hydrological modelling, numerical weather forecasting or climate change prediction (Anderson et al., 2007). Partitioning of available energy between sensible and latent heat is hereby of prime interest and various models have been developed in the



Correspondence to: K. Richter
(katja.rich@gmail.com)

more recently by Timmermans et al. (2007) revealed that TSEB, as well as other existing models, shows a considerable sensitivity to small variations of fractional vegetation cover (fCover) and/or leaf area index (LAI) on soil and canopy temperature estimation, in particular for high cover conditions. These findings emphasize the importance of accurate values of these parameters, usually determined from optical E. O. data. Although not model specific, the common approach applied within the TSEB model to estimate LAI and fCover is by means of rather simple empirical formulations utilizing either the Normalized Difference Vegetation Index (NDVI) (Schmugge et al., 1998) or a scaled NDVI (Choudhury et al., 1994; French et al., 2003; Kustas and Norman, 1999). Such empirical approaches are based on relationships between the parameter (e.g. LAI) and Vegetation Indices (VIs). Many studies showed that the application of VIs can give appropriate results, especially when using newly developed hyperspectral VIs (e.g. Haboudane et al., 2004). However, a spectral signature is the integration of several factors and can not be explained by just one parameter. Moreover, these empirical models are often crop-, site- and sensor-specific (Atzberger, 2004; Vuolo et al., 2008). Therefore, many efforts have been undertaken in the last decades to develop and improve canopy reflectance models based on radiative transfer equations. In these radiative transfer models (RTM), the complexity of the spectral signal is taken into account by a function of canopy geometry (e.g. LAI, leaf angle distribution), optical leaf and soil properties, illumination and viewing geometry. Inversion of such models then offers the possibility of extracting these biophysical parameters.

The objective of the present study is to test whether a physically based retrieval of LAI and fCover can support more accurate estimations of fluxes in two-source energy balance modelling.

2 Material and methods

In this section first a description of the models used for the estimation of vegetation characteristics and energy fluxes is given. Then the campaign with ground and E. O. data acquisitions is described.

2.1 Estimation of vegetation characteristics

2.1.1 Empirical model

Traditionally, the estimation of surface parameters for energy balance modelling is based on empirical methods. Several empirical models have been developed to estimate the biophysical parameters. Though not characteristic for the TSEB model, recent versions (French et al., 2003; Li et al., 2005) employ the approach as proposed by Choudhury et al. (1994). This so-called scaled NDVI – approach deter-

mines fCover for nadir viewing angles (fCover(θ_o), $\theta_o=0$) as follows:

$$fCover(0) = 1 - \left(\frac{NDVI_{max} - NDVI}{NDVI_{max} - NDVI_{min}} \right)^p \quad (1)$$

Hereby, the end-member NDVI values, $NDVI_{max}$ and $NDVI_{min}$, characterize a surface fully covered and completely uncovered by vegetation, respectively. The parameter p is defined as $p=\Lambda/\kappa$, describing the ratio of a leaf angle distribution term, Λ (set to 0.5 for randomly oriented leaves, Campbell and Norman, 1998), to canopy extinction, κ (set to 0.55, approximating typical extinction for many canopies at a solar zenith angle of 25 degrees, following Campbell and Norman, 1998), leading to a p value of 0.9.

The NDVI end-members were obtained by combining an NDVI histogram analysis (Timmermans et al., 2007) with local field observations resulting in $NDVI_{max}=0.85$ and $NDVI_{min}=0.10$.

Leaf area index (LAI), is then calculated from fCover (Choudhury, 1987):

$$LAI = \frac{\ln(1 - fCover(0))}{\Lambda} \quad (2)$$

2.1.2 Radiative transfer model

As an alternative to the empirical approach, a physically based model of canopy reflectance was applied: the combined SAILH (Kuusk, 1991; Verhoef, 1984, 1985) and PROSPECT (Jacquemoud and Baret, 1990) models (called “PROSAILH”), widely used for canopy reflectance modelling and applications, amongst others by Atzberger (2004), Baret et al. (2007), Darvishzadeh et al. (2008), Richter et al. (2009) or Weiss et al. (2000).

SAILH is a one-dimensional turbid medium radiative transfer model, later modified to take into account the hot spot effect (Kuusk, 1991). It simulates the bidirectional top-of-canopy (TOC) reflectance as a function of three structure parameters, defined by LAI (m^2/m^2); average leaf inclination angle, ALA (deg), assuming an ellipsoidal distribution, and hot spot size parameter, Hot (m/m). Further it requires the soil spectral reflectance, fraction of diffuse incoming solar radiation ($skyl$), and the view and illumination geometry (i.e. sun zenith angle, θ_s (deg); sensor viewing angle, θ_o (deg) and azimuth angle between sun and sensor, ϕ (deg)). Leaf hemispherical reflectance and transmittance are simulated by the PROSPECT model as a function of four structural and biochemical parameters: leaf chlorophyll a+b concentration, C_{ab} ($\mu g/cm^2$); dry matter content, C_m (mg/cm^2); leaf water thickness, C_w (cm) and a leaf mesophyll structural parameter, N (unitless). To account for the changes in soil reflectance (induced by soil water content and roughness), a wavelength independent scaling factor “ α_{soil} ” is introduced, i.e. multiplied with the soil spectrum.

Table 1. Ranges of the input variables for PROSAILH to generate the LUT database.

Model Variables		Units	Min (LB)	Max (UB)
Leaf parameters: (PROSPECT)				
N^a	Leaf structure index	unitless	1.3	1.7
C_{ab}^b	Leaf chlorophyll content	$[\mu\text{g}/\text{cm}^2]$	20	70
C_m^b	Leaf dry matter content	$[\text{g}/\text{cm}^2]$	0.004	0.01
Canopy variables: (SAILH)				
LAI	Leaf area index	$[\text{m}^2/\text{m}^2]$	0	6.0
ALA ^c	Average leaf angle	$[\text{°}]$	40	60
HotS ^d	Hot spot parameter	$[\text{m}/\text{m}]$	0.01	1
α_{soil}^e	Soil reflectance factor	unitless	0.6	1.4

^a not measurable, therefore range set in order to comprise values often used in literature (e.g. by Weiss et al., 2000);

^b (somewhat extended) range of measurements (SPARC report 2004);

^c ALA – mean of MTA (measured with LAI-2000 instrument) \pm standard deviation, sd (mean: 50, sd: 11) (SPARC report 2004);

^d similar to range often used in literature (e.g. Baret et al., 2007; Vuolo et al., 2008);

^e distribution of the factor observed over a number of bare soil pixels from the CHRIS imagery.

When calculating reflectance, the SAILH model estimates the gap fraction, which is a key variable driving light interception by the canopy. Gap fraction is defined as the probability of a ray of light passing through the canopy without encountering foliage or other plant elements, and is consequently the complement of fCover. The gap fraction, calculated by SAILH corresponds therefore to $1 - \text{fCover}$.

In order to estimate LAI and/or the other parameters, the PROSAILH model must be inverted. In this study a fast look-up table (LUT) approach (e.g. Darvishzadeh et al., 2008; Richter et al., 2009; Weiss et al., 2000) has been chosen, offering a good alternative to other inversion procedures such as artificial neural networks (NN) (Atzberger, 2004) or numerical optimization methods (Vuolo et al., 2008), amongst others for the following reasons: first, the LUT technique permits a global search and avoids therefore the trapping into local minima as occurs with the optimisation methods (Darvishzadeh et al., 2008). Second, it shows less unexpected behaviour than NN when the spectral signal of the surface is not well simulated by the model (for a discussion of different inversion methods see Atzberger, 2004; Darvishzadeh et al., 2008; or Richter et al., 2009).

PROSAILH was selected since it presents a good compromise between physical complexity and computation time requirements and has been therefore preferred over (perhaps more accurate) models with complex parameterization schemes.

2.1.3 RTM models setup

The LUT is established in advance of the model inversion process. For this purpose PROSAILH is run to simulate bidirectional canopy reflectance and fCover for a number of

100 000 parameter combinations. This size was regarded by Weiss et al. (2000) as a good compromise between computer resources requirements and the accuracy of the estimates. The LUT was established by randomly sampling all parameters within their bounds. In this way, all combinations of parameters were covered, but no adaptations to possible sensitivities of the parameters were implemented.

The range of canopy characteristics was described by taking partly into account a priori information from the campaigns measurements. The usage of on-site measurement information is one possibility to regulate the ill-posed inverse problem, which is pronounced between LAI and ALA, and therefore to improve the parameter (LAI) retrievals (Atzberger, 2004; Combal et al., 2003) (Sect. 2.3.3, SPARC report, 2004). The information about all parameter ranges can be found in Table 1.

Distributions of all parameters were uniform, so that no emphasis was placed on higher or larger values. Illumination and view conditions were set according to the conditions during the overpass: $\theta_s = 21^\circ$, $\theta_o = 8.4^\circ$ and $\phi = 138^\circ$. The parameter *skyl* was set to 0.1 across all wavebands, according to similar studies (e.g. Richter et al., 2009).

As the absorption of leaf water is not influencing the spectral range used in this study ($< 0.9 \mu\text{m}$), C_w was fixed to an arbitrary value ($C_w = 0.02 \text{ cm}$).

Only a limited number of bands is necessary to describe and differentiate the influence of canopy and soil parameters on the spectrum (Weiss et al., 2000). Consequently, in order to minimize redundancy of spectral data and to speed up the calculation process of the LUT, a spectral sampling of only 8 bands has been selected. It is based on the future ESA satellite Sentinel-2, developed in the

framework of Global Monitoring for Environment and Security (GMES/Kopernikus, ESA, 2007) to replace and improve the old generation of satellite sensors. Sentinel-2 is scheduled to be launched in the year 2012 and as outcome the mission will provide service data, comprising products such as LAI and fCover. The multi spectral data, used for the simulations in the study, involve the following CHRIS wavebands: 492, 563, 664, 706, 738, 773, 844 and 862 nm (corresponding to Sentinel-2: 490, 560, 665, 705, 740, 775, 842 and 865 nm, ESA 2007). In this way all spectral bands of Sentinel-2 with the purpose to retrieve LAI and other vegetation characteristics (i.e. 8 out of 13 bands) are included. This spectral sampling has been tested for its suitability for LAI estimation by Richter et al. (2009).

In the final step the solution within the LUT is selected by applying a simple cost function calculating the root mean square error (RMSE) between simulated and measured spectra (e.g. Darvishzadeh et al., 2008), as follows:

$$\text{RMSE} = \sqrt{\frac{\sum_{i=1}^n R_{\text{meas}(\lambda)} - R_{\text{lut}(\lambda)}^2}{n}} \quad (3)$$

where R_{meas} corresponds to the measured reflectance at wavelength λ , and R_{lut} stands for the simulated reflectance calculated with the PROSAILH model. The number of bands is indicated with n .

The resulting parameter combination was built as the average of all parameter combinations found within less than 20% of the lowest RMSE value (e.g. Richter et al., 2009).

2.2 TSEB model

The land surface model used here to derive latent and sensible heat fluxes is originally designed to use input data primarily from remote sensing platforms. Its main characteristic is that it discriminates between a soil and vegetation component, aiming at a more physical description of heterogeneous surfaces when dealing with radiative and aerodynamic properties. Required remote sensing input consists of spatial information on surface temperature as well as vegetation density, being fCover and LAI. The version implemented here basically follows what is described as the “series resistance network” in Appendix A of Norman et al. (1995). In the current version a physically based algorithm is implemented for estimating the net radiation, which is described in detail in Kustas and Norman (1999). As such, the model implemented is described in detail in Norman et al. (1995) and Kustas and Norman (1999); reason to only sketch its main characteristics and highlight those parts that are affected by fCover and LAI.

First of all, fCover is used to estimate canopy and soil temperatures (T_C and T_S , respectively) from observed radiometric surface temperature, T_R , with a simple non-linear mixing model, described by:

$$T_R^n = \text{fCover} T_C^n + (1 - \text{fCover}) T_S^n. \quad (4)$$

where n is the power in the Stefan-Boltzmann equation that reasonably approximates the appropriate integral of the Planck blackbody emission function for the wavelength of the sensor.

A first estimate of the latent heat flux from the canopy, LE_C , is obtained by applying the Priestley and Taylor approach on the canopy component of the net radiation, $R_{N,C}$, which works reasonably well under unstressed vegetation conditions. The canopy sensible heat flux, H_C , is then determined by evaluating the canopy energy budget. By using a linearized form of Eq. (4), following the procedure outlined in the Appendix A of Norman et al. (1995), the within-canopy air temperature, T_{AC} , is derived, which also yields the canopy temperature, T_C . Substitution in Eq. (4) yields T_S , providing the possibility of obtaining the soil sensible heat flux, H_S . The soil heat flux, G , is determined as a time-dependant ratio of the soil net radiation, $R_{N,S}$, after which the soil latent heat flux, LE_S , is determined by evaluating the soil energy budget. In case LE_S is negative, then the soil is likely to be dry and LE_S is set to zero. Under these circumstances, H_S is derived from the soil energy budget, and an adjusted T_S is obtained. Equation (4) provides a new estimate for T_C which is then used to calculate an updated H_C .

The algorithm used for estimating the net radiation divergence requires incident solar radiation observations and formulations for the transmission of direct and diffuse shortwave radiation and for the transmission of longwave radiation through the canopy (Campbell and Norman, 1998). The canopy component of net radiation, $R_{N,C}$, is given by:

$$R_{N,C} = (1 - \tau_{LW}) \times (R_{LW,\text{sky}} + R_{LW,S} - 2R_{LW,C}) + (1 - \tau_{SW}) \times (1 - \rho_C) \times R_{SW} \quad (5)$$

and the soil net radiation component, $R_{N,S}$, by:

$$R_{N,S} = \tau_{LW} \times R_{LW,\text{sky}} + (1 - \tau_{LW}) \times R_{LW,C} - R_{LW,S} + \tau_{SW} \times (1 - \rho_S) \times R_{SW} \quad (6)$$

where τ represents transmissivity through the canopy and subscripts *SW* and *LW* stand for shortwave and longwave, respectively. Subscripts *sky*, *S* and *C* represent the sky, soil and canopy components, whereas ρ is the reflectance, or shortwave albedo. Since the reflection and absorption of radiation in the visible and near-infrared wavelengths are rather different for vegetation and soils, the visible and near-infrared albedos of the soil and canopy were evaluated differently before combining to give an overall shortwave albedo. The equations for estimating the transmission and reflection of direct and diffuse shortwave radiation are provided in Campbell and Norman (1998). We suffice here with the observation that their spatial variation is solely determined by LAI. The longwave transmissivity finally is approximated by a single exponential function depending on an extinction coefficient and LAI.

The parameterization of the resistances used in the series resistance network was taken from Norman et al. (1995). Aerodynamic properties such as canopy height, displacement height, aerodynamic roughness, leaf width, as well as limited micrometeorological observations are required as input parameters and are assigned a priori. They are described in the following section.

2.3 Experimental setup and observations

2.3.1 Site description

The analyses are based on data of the interdisciplinary ESA SPARC 2004 Campaign. (Moreno et al., 2004; SPARC report 2004). The objective of the campaign was to advance the understanding of land – atmosphere exchanges of water and energy in space and time over heterogeneous land surfaces.

In this context, satellite and ground data were collected in Barrax ($30^{\circ}3' N$, $2^{\circ}6' W$), an agricultural test area situated in the Castilla-La Mancha region in southern Spain. Figure 1 shows an overview of the location and the area of interest.

The Barrax site, a flat area at 700 m above sea level, is characterized by a large variety of uniform land use units of different crops and dry bare soils, leading to a wide range of LAI from 0 up to 6.5.

The Castilla-La Mancha region receives an annual precipitation of only 400 mm and is therefore one of the driest regions in Europe. One third of the land is irrigated (35%), comprising amongst others alfalfa, maize, potatoes, sunflower, onion, garlic, sugar beet and vineyard. The other two thirds (65%) are rainfed cultivations, such as winter/spring cereals and bare soils/fallow land.

2.3.2 E. O. data acquisition

Optical data

Hyperspectral and multiangular E. O. data from Compact High Resolution Imaging Spectrometer (CHRIS) instrument, located on the Project for On-Board Autonomy (PROBA) platform, were acquired on 16 July 2004 around 11:25 UTC. Since the system PROBA/CHRIS has multiangular capabilities, five consecutive images from five different view angles have been obtained during the overpass, with a minimum satellite zenith angle of 8.4° . Since it was not the scope of the current study to analyze the contribution of directional information to the parameter estimates (Vuolo et al., 2008), only the imagery with the viewing angle closest to nadir has been considered.

The sensor covers the visible/near-infrared region (from 400 nm to 1050 nm) with a spectral sampling interval ranging between 1.25 nm (at 400 nm) and 11 nm (at 1000 nm). CHRIS data were acquired in Mode-1, having a spatial resolution of 34 m and 62 spectral bands.



Fig. 1. Location of the study area: Barrax Site, La-Mancha, Spain.

Radiometric calibration and atmospheric and geometric correction of CHRIS imagery were carried out by the Department of Thermodynamics of the University of Valencia.

Thermal imagery

The thermal remote sensing data from SPARC 2004 used in this study consisted of ASTER imagery, acquired on 18 July 2004 to obtain surface temperature. ASTER has 5 thermal infrared bands with a 90 m spatial resolution.

After atmospheric correction, the land surface temperature was extracted using a split-window technique (Jimenez-Munoz and Sobrino, 2007) on channels 13 and 14 of the ASTER data. This method was preferred over the standard TES algorithm due to insufficient accuracy in land surface temperature retrieval that was noted over certain land cover types (Sobrino et al., 2007).

Despite ASTER's excellent capabilities for surface energy flux mapping here CHRIS/PROBA data were used due to their more advantageous spectral characteristics for mapping the vegetation characteristics, assuming these do not change significantly within 2 days time.

2.3.3 Ground observations

The ground-based data used here consisted of vegetation characteristics, meteorological observations as well as radiation and turbulent flux exchanges (Su et al., 2008), collected during the time of the satellite acquisitions.

Observations of vegetation surface parameters, such as vegetation height, LAI, mean tilt angle (MTA), fCover, leaf chlorophyll, water and dry matter content, were conducted

(Fernandez et al., 2005) at several locations for calibration and validation of remote sensing derived vegetation input to the flux model.

Non-destructive field measurements of LAI were performed with the Plant Canopy Analyzer LAI-2000 instrument (LICOR Inc., Lincoln, NE, USA), measuring simultaneously the MTA that corresponds to the ALA parameter in the PROSAILH model (Sect. 2.1.2).

To reduce the effect of multiple scattering on LAI-2000 measurements, the instrument was operated maximal two hours after sunrise or before sunset, under diffuse radiation conditions. In order to prevent interference caused by the operator's presence and the illumination condition, the sensor field of view was limited with a 180° view-cap. Measurements were azimuthally oriented opposite to the sun azimuth angle. Each single LAI value was the result of an average of 24 measurements taken randomly within an Elementary Sampling Unit (ESU) of approximately 15 × 15 m².

Since no corrections were applied to account for clumping or the influence of non-photosynthetic plant components (such as stems), the term “LAI” should here be understood as “effective plant area index” (PAI_{eff}) (Chen et al., 1997; Darvishzadeh et al., 2008). However, LAI measured by LAI-2000 (or other optical methods) is quite close to the leaf surface visible by a remote sensor which is not necessarily the case for the real LAI. Therefore, a correction for the clumping effect is not absolutely necessary (Stenberg et al., 2004).

A data set of 48 LAI measurements, located in/near the area of interest (maize: 8, garlic: 13, potatoes: 15, sugar beet: 6, sunflower: 6) have been selected for the validation.

Measurements of fCover, being of essential interest for this study, have been performed using hemispherical photography. According to the crop structure, different sampling strategies were applied. The photographs were processed using a specialized software package (CAN-EYE), developed at INRA-CSE Avignon. The procedure of the software is based on gap fraction estimation using classification techniques (detailed information about the measurements and data elaboration can be found in the SPARC 2004 report). The final fCover estimate for each ESU (20 × 20 m) was calculated as the average of twelve measurements. For the present study, a total number of 21 measurements have been used for validation (garlic: 4, potatoes: 4, sunflower: 4, onion: 4, sugar beet: 3, maize: 2).

Meteorological and radiation observations (incoming shortwave radiation, air temperature, relative humidity, air pressure and wind speed) that were needed as input to the TSEB model, were taken from a tower in the centre of the area.

Validation data concerning turbulent fluxes exchanges and radiation for the time of the ASTER overpass were made at several locations that were chosen such that typical land cover units were covered (described in detail in Su et al., 2008). They comprised a forest nursery, a wheat stubble field, vineyard (2 sites), a sunflower field and a corn field. At

all sites measurements of sensible heat flux, H , were made either by 1-D or 3-D sonic anemometers or by scintillometer (vineyard) and in one position also latent heat flux, LE , was measured (vineyard). However, due to the pivot irrigation system at the corn field, the sensor had to be located at the edge of the corn field adjacent to the vineyard, meaning that the measurement either represented the vineyard or the corn, depending on wind direction. Net radiation and soil heat flux were measured only at four sites; the vineyard, forest nursery, corn and a wheat stubble field. For a location map one is referred to Fig. 1 in Van der Kwast et al. (2009) where also a land cover map is provided, showing the main land cover units.

Aerodynamic properties were assigned to the different land cover units using averaged field observations of canopy height, h_c (Fernandez et al., 2005) in combination with the classical relations (Brutsaert, 1982) where surface roughness length for momentum transport, z_{0M} , is taken equal to $1/8 * h_c$ and the displacement height, d_0 , equal to $2/3 * h_c$. An exception was made for the roughness length of the corn fields, which were extremely dense, resulting in a much smoother surface. Therefore a roughness length value equal to that of the sunflower was assigned, which closely resembled estimates from turbulence measurements done over the maize (Timmermans et al., 2009). Moreover, the displacement heights of the wheat stubble and forest nursery land cover were chosen equal to zero, since these units were characterized by a very open and heterogeneous character.

3 Results and discussion

In this section we first present the quality and the differences in LAI and fCover estimations using the LUT inversion and the scaled NDVI approaches. Validation of the energy balance model output is then performed by means of the flux towers measurements. Differences in the flux components simulated with both canopy parameter retrieval methods are analyzed additionally in a spatial context. A general discussion on the applied method(s), their problems and applicability (in an operational context) concludes this section.

3.1 Vegetation characteristics versus observations

Retrieval performances of the LUT inversion and NDVI approaches were evaluated using LAI and fCover data from campaigns measurements (see Sect. 2.3.3). Crops not covered by the flux stations, such as sugar beet, garlic, potatoes and onion, were included in the analyses as well to test the general applicability of the models.

The comparison with the ground measured fCover data with both approaches (LUT inversion: “fCover_{LUT}”; NDVI approach: “fCover_{ndvi}”) resulted in a slightly higher accuracy of fCover_{LUT}, with Root Mean Squared Differences (RMSD) for fCover_{LUT} of 0.12 and for fCover_{ndvi} of 0.15. The

plots in Fig. 2a, b give a graphical impression of the estimation quality, indicating a tendency of overestimation of the NDVI approach, especially at the higher values. Since TSEB has a greater sensitivity to fCover, in determining the turbulent fluxes, especially at high vegetation cover conditions (Timmermans et al., 2007) this is considered an important drawback of the NDVI approach.

In case of LAI (LUT inversion: “LAI_{lut}”; NDVI approach: “LAI_{ndvi}”) the LUT inversion approach provided clearly a higher retrieval accuracy in comparison with the ground data (Fig. 2c, d), with RMSD of 0.79 (LAI_{lut}) versus RMSD of 1.44 (LAI_{ndvi}). Also here the empirical model has a trend to overestimate the parameter. Clearly noticeable is also the well-known problem of saturation at higher LAI values (“plateau-effect”), illustrated by the scatter plot in Fig. 2c.

The overestimation of fCover using the scaled NDVI approach can be caused by an inaccurate NDVI_{min} value, i.e. the value for bare soil reflectance, which in reality varies and is probably different (higher) when calculating the mean over all bare soil pixels in the scene (Montandon and Small, 2008). Soils have a variable NDVI due to the fact that the relative variation of the spectral signal in the visible red waveband region is larger than in the near infrared. Increasing soil water leads consequently to an augmentation of NDVI, generating for example a difference of NDVI of 10% between a wet and a dry soil background for a LAI of 1 (Bach and Verhoef, 2003). Differences of land cover and irrigation practise which influence the soil background will therefore also have an effect on fCover estimation accuracy.

The PROSAILH model overcomes this problem by taking into account the soil reflectance variation by means of the α_{soil} -factor.

However, the model tends to slightly underestimate high LAI values for crops with strong leaf clumping, as it was the case for potatoes in the present growth stage. This behaviour results from the nonlinearity of the LAI-reflectance relationship, leading to saturation effects (Baret et al., 2007). On the other hand, even the measurements could cause an overestimation of LAI, since the LAI-2000 can not separate between photosynthetic and non-photosynthetic plant components. This may occur whenever the built-in assumption of randomly distributed plant elements holds true. Thus, non-green elements (such as stems or senescent leaves) reduce the measured gap fractions.

A detailed interpretation of the retrieval performances for the specific crop types is not given, since the objective is to evaluate the overall applicability of the RTM model for canopy parameter estimations. Considering that the PROSAILH model simplifies the canopy as a turbid medium, of which none of the crops really corresponds to, the retrieval performance can be regarded as satisfying. The implementation of some a priori information from the field measurements can support accurate retrievals.

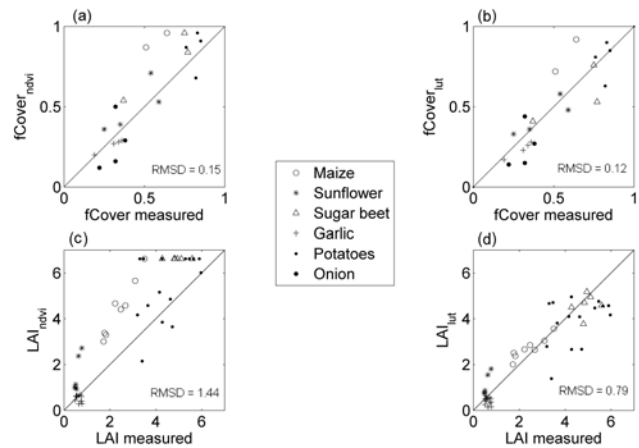


Fig. 2. Estimated versus measured fCover (a, b) and LAI values (c, d) using the scaled NDVI approach (a, c) and a LUT inversion approach based on PROSAILH model (b, d), for different crops monitored during the SPARC 2004 campaign.

3.2 Water and heat fluxes

Validation of the TSEB model output was performed in comparison with tower-based flux observations for the day of ASTER overpass. Model flux components were extracted from the image pixels in the vicinity of the flux towers, following a simple analytical footprint model, which is a reformulated version of Gash (1986). Details of the footprint model can be found in Timmermans et al. (2009).

The models are run on an area of almost 6×6 km comprising 64×64 pixels around the Barrax vineyard which was the centre point of attention during the SPARC 2004 campaign (see also Fig. 1).

For all components, both TSEB runs (RTM inversion: “TSEB_{lut}” and scaled NDVI: “TSEB_{ndvi}”) yielded comparable results versus observations and RMSD were in all cases lower than 50 W/m^2 , which is considered acceptable. Net radiation yielded a RMSD of 46 W/m^2 versus observations for both approaches and gave almost identical results in all 4 sites (Fig. 3a). Also for the soil heat flux (Fig. 3b) and the sensible heat flux (Fig. 3c) output negligible differences between the NDVI and LUT approaches were seen. RMSD with observations for G were 36 and 38 W/m^2 for the NDVI and LUT approaches, whereas for H these were 43 and 42 W/m^2 , respectively.

Although RMSD for G and H were almost equal for both TSEB_{ndvi} and TSEB_{lut}, TSEB_{lut} appears to perform better at the lower values of G and H . With the exception of the G observation at the cut wheat site, all other sites showed similar performances for both G and H . TSEB_{lut} performing better at low values of G and H may indicate that the model performs better at sites that are characterized by high fCover, such as it is the case for the sunflower and maize fields. Therefore the model performance is discussed in a spatial context in the next section.

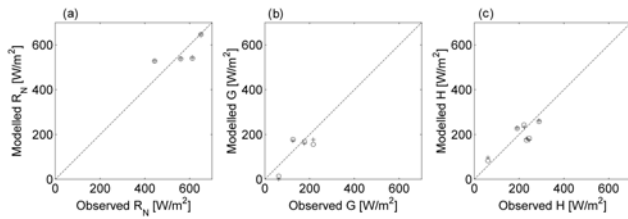


Fig. 3. Modelled versus observed fluxes of R_N (a), G (b) and H (c), using the two approaches of canopy parameter estimations. Cross symbols represent the output from the scaled NDVI approach and the circles from LUT inversion.

3.3 Spatial differences of flux modelling

Differences between the two modelling approaches are shown in Fig. 4. Spatially distributed output for R_N , G , H and LE from TSEB_{ndvi} are subtracted from output of TSEB_{lut} (TSEB_{lut} – TSEB_{ndvi}).

The maps reflect what was noticed from observations at the flux tower sites; R_N differences are negligible whereas G estimates for TSEB_{lut} are higher than for TSEB_{ndvi} at high fCover, while H (and to a lesser extent LE) shows lower fluxes for TSEB_{lut} in these areas, especially in the maize fields. The net radiation estimation seems rather insensitive to variations in LAI and fCover. This is understandable since LAI and fCover are only indirect inputs to the net radiation estimation, which is mainly driven by incoming solar radiation, and their effects basically act on the soil and canopy components. For example an increase in LAI will decrease the shortwave transmission which will increase the canopy net radiation but at the same time decrease the soil net radiation, see also Eqs. (4) and (5). As a result the net effect on the total net radiation is negligible. In order to consider the variations in the other energy balance components, that seem to originate from crop characteristics, the flux estimates will be analyzed in terms of land cover classes.

On the basis of a land cover map (Van der Kwast et al., 2009), simulated fluxes were extracted for all land uses. However, here we will focus on the five different land use classes covered by the stations (forest nursery, vineyard, sunflower, corn and wheat stubble), which enables us to assess the model accuracy to a certain extent. Since R_N estimates are rather similar for both approaches we will focus on the remaining flux components from now on.

Figure 5 shows the spatial differences between TSEB_{lut} and TSEB_{ndvi} calculated flux components, for every of the five land use classes and Fig. 6 the estimated fCover and LAI values for the respective classes.

Even though the estimation of H and G was almost identical for both model versions at the flux site at the forest nursery, the physical approach shows a trend of higher H and lower G fluxes when examining the entire class. Higher H values theoretically might indicate more realistic results from

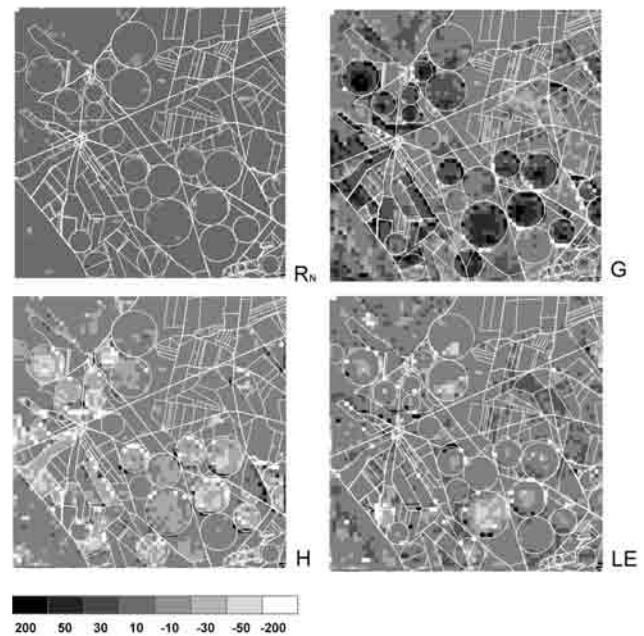


Fig. 4. Differences between TSEB output R_N , G , H and LE (W/m^2), subtracting empirical approach of surface parameter estimations from the physical (TSEB_{lut} – TSEB_{ndvi}), Barrax test site, 18 July 2004.

TSEB_{lut}, although uncertain as to how high, since this land use class is characterized by rather small green vegetation cover, low LAI values, but at the same time has rather large amounts of senescent grass cover. This would imply relatively high H and relatively low G . To a certain extent this is also reflected in the higher estimates of fCover by the LUT approach. However, unfortunately there are no observations of fCover and LAI made over the forest nursery.

The vineyard case shows almost no differences between the two approaches, but the small number of pixels ($n=5$) does not allow to draw significant conclusions.

Due to their planophile leaf orientation, sunflowers in early growth stages exhibit – with still relatively low LAI values (≤ 2.7) – already high fCover (here up to 0.76). For this crop class the physical approach yielded also more realistic estimates of fCover (RMSD=0.07 for fCover_{lut} and RMSD=0.11 for fCover_{ndvi}). Since TSEB is sensitive to fCover with respect to H , the fluxes were probably modelled more accurate by TSEB_{lut} (as is shown for H). No measurements of G and R_N were available from this station, but the trend of higher G from TSEB_{lut} confirms the conclusion of lower fCover and LAI (visible in Fig. 6) being more realistic.

The land use class maize must be regarded as a special case. During the time of ASTER overpass, the dominating wind direction was west, causing the flux observation in this site to reflect the vineyard instead of the maize. This is confirmed by a high value for H , equal to $233 W/m^2$, which appears far too high for an irrigated maize field with an fCover

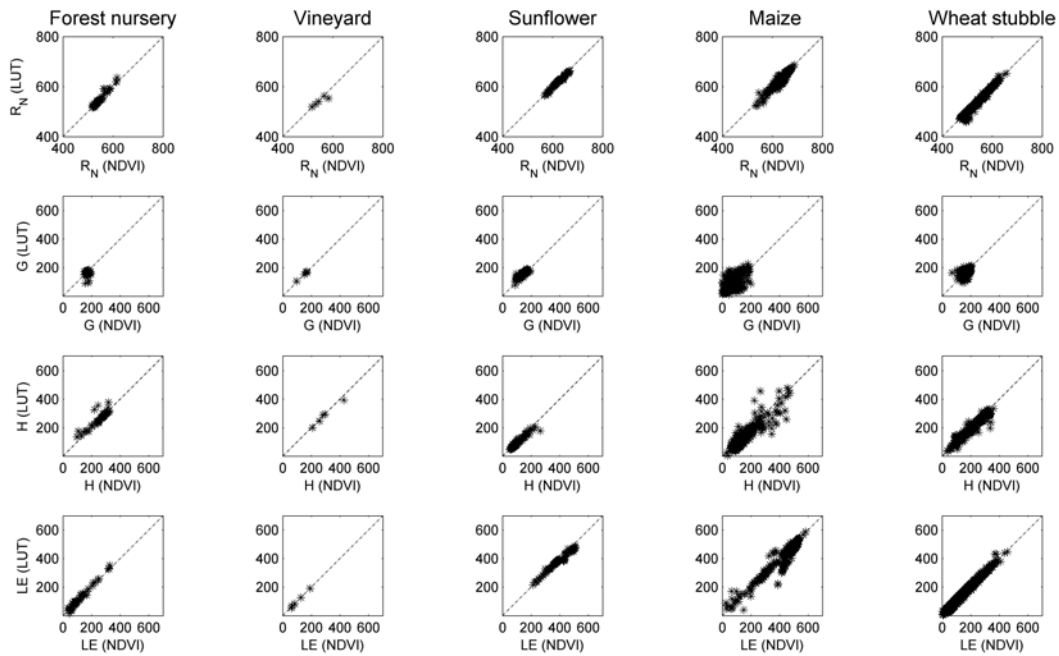


Fig. 5. Simulated fluxes of R_N , G , H and LE and by $TSEB_{ndvi}$ versus $TSEB_{lut}$ for different land use classes.

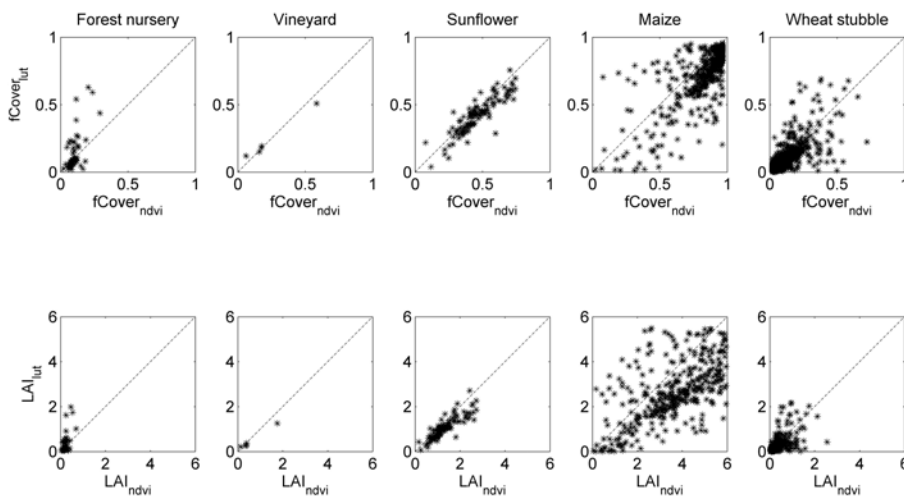


Fig. 6. Estimated values of $fCover$ and LAI from scaled $NDVI$ versus estimated by LUT inversion for the land use classes.

of 0.9 and LAI up to 6. The estimation of LAI for maize was performed more accurate by the physical model (RMSD of 0.4 from LAI_{lut} against RMSD of 2.1 from LAI_{ndvi}), as well as for $fCover$, even though only two measurements were available (RMSD=0.24 for $fCover_{lut}$ and RMSD=0.34 for $fCover_{ndvi}$).

The overestimation of LAI , and to a lesser extent $fCover$, by the $TSEB_{ndvi}$ approach results in an underestimation of G for this land use, also illustrated by the observation at this site, Fig. 3b. This effect is clearly visible for all maize-fields in Fig. 4b.

$TSEB_{lut}$ estimates of H for this land cover generally were lower than those from $TSEB_{ndvi}$, where differences over the maize field next to the vineyard reached values up to 50 W/m^2 , with $TSEB_{lut}$ values around 75 W/m^2 . These values resemble observations made over the maize during days preceding the ASTER overpass, when wind direction was coming from the maize (Timmermans et al., 2009). Therefore we feel that the H fluxes are simulated more realistically by using the RTM based values of LAI and $fCover$ as input. Differences for LE estimates were variable within this land cover class, with a tendency of $TSEB_{lut}$ yielding lower

estimates. The differences seem to vary from field to field, which may originate from the irrigation scheme. The different estimation results of the two approaches may be caused by variations in soil reflectance due to (superficial) soil moisture differences, which are taken into account only by the physical model. This may also be an explanation for the fact that regarding the comparison of fluxes between $TSEB_{lut}$ and $TSEB_{ndvi}$, maize exhibits the most pronounced differences of all land use classes, since some fields were fully irrigated and some neglected. The tendency of overestimating fCover with the NDVI approach seems to influence especially the LE for a certain group of pixels, mainly over irrigated maize, resulting in differences ranging from 30 to 35 W/m^2 .

In the last land use class, a wheat field shortly harvested, $TSEB_{lut}$ resulted in a slightly better estimate of H , whereas G was better estimated by $TSEB_{ndvi}$ at the flux observation site. When looking at the entire land cover class however, no distinct differences are seen for either one of the fluxes. Both G and H exhibit some scatter around the 1:1 line, which is also seen in the LE flux but at a lesser extent. Although no measurements of LAI and fCover were made over this land use, it is characterized by rather low fCover (<0.1) and LAI (≤ 2). When looking at the scatter plots of Fig. 6 it is noticed that in the lower regions of LAI and fCover no clear distinction can be made between the NDVI and LUT approach, which is reflected in the scatter of the fluxes around the 1:1 line in Fig. 5 for this class.

Summarizing, R_N shows for all land use classes the smallest variations between the two approaches. G and H , and to a somewhat lesser extent LE , exhibit more pronounced differences, mainly over areas with high vegetation cover and high LAI. The LAI mainly influences the estimation of G , since an increase in LAI invokes a decrease in radiation received at the soil, whereas fCover mainly influences the turbulent fluxes through its effect on the component temperatures. This is of importance since the TSEB model is sensitive to fCover, when estimating turbulent fluxes, in particular at the high end as stated by Timmermans et al. (2007). This could be of interest for a wider range of crops or vegetation, because even for other crops with high fCover – not included in the measurements of flux towers – the physical approach yielded a slightly higher retrieval accuracy (see also Fig. 2) with sugar beet: $RMSD(fCover_{lut})=0.14$ vs. $RMSD(fCover_{ndvi})=0.16$ and potatoes: $RMSD(fCover_{lut})=0.10$ vs. $RMSD(fCover_{ndvi})=0.11$. Even though flux observations were only available for a limited number of land covers, it is argued that the improved estimation of both LAI and fCover in general leads to slightly better flux estimates. However, further research is needed to demonstrate this effect also under a wider range of canopy characteristics.

Spatial differences between the $TSEB_{lut}$ and the $TSEB_{ndvi}$ model results were clearly related to land cover, with noticeable differences up to 50 W/m^2 for H and 35 W/m^2 for LE over irrigated crops and up to 20 W/m^2 for both the turbulent fluxes over dry areas. Although this may seem rather

small, an instantaneous error of 35 W/m^2 could translate into 1.2 mm error in water use, which has considerable consequences for irrigation management.

4 Conclusions

In this study, the TSEB model was applied to the Barrax test site and evaluated with ground measurements from the SPARC campaign 2004. The inputs of leaf area index and fractional vegetation cover were estimated from CHRIS imagery by using the traditional scaled NDVI and a LUT inversion approach, based on the proposed bands of future ESA Sentinel-2 satellite. The LUT was constructed using the well established SAILH+PROSPECT radiative transfer model. The validation by means of a range of crops over the SPARC Barrax test site resulted in a better retrieval performance for the LUT approach. Differences in flux predictions in comparison with a limited number of station measurements were rather small. However, a differentiation between land use classes indicated a higher estimation quality of the physical approach, especially over areas that were characterized by higher LAI and higher fCover.

In view of operational applications, a physically based approach has several advantages over empirical methods. Differences in soil background due to soil moisture variations are taken into account by the RTM model and thus canopy parameters, such as LAI and fCover can be estimated more accurately. Moreover, the RTM based inversion does not (necessarily) require detailed in situ calibration data sets. This constitutes a major general advantage of physical over empirical models, rendering them more robust and generally applicable. The application of physically based models for estimating vegetation parameter as input for energy balance models is therefore recommended.

Acknowledgements. This work has been partly funded through ESA 18307/04/NL/FF. We would like to thank Juan-Carlos Jimenez-Muñoz from the Global Change Unit of the University of Valencia for radiometric and atmospheric correction of the thermal ASTER data and Luis Guanter from Geo-ForschungsZentrum (GFZ) Potsdam, and his former Department of Thermodynamics of the University of Valencia, for preprocessing of CHRIS/Proba data.

Edited by: J. Wen

References

- Anderson, M. C., Norman, J. M., Mecikalski, J. R., Otkin, J. A., and Kustas, W. P.: A climatological study of evapotranspiration and moisture stress across the continental U.S. based on thermal remote sensing. I. Model formulation, *J. Geophys. Res.*, 112, D11112, doi:10.1029/2006JD007506, 2007.
- Atzberger, C.: Object-based retrieval of biophysical canopy variables using artificial neural nets and radiative transfer models, *Remote Sens. Environ.*, 93, 53–67, 2004.

- Bach, H. and Verhoef, W.: Sensitivity studies on the effect of surface soil moisture on canopy reflectance using the radiative transfer model GeoSAIL, in proceedings of IGARSS 2003, 1679–1681, 2003.
- Baret, F., Hagolle, O., Geiger, B., Bicheron, P., Miras, B., Huc, M., Berthelot, B., Nino, F., Weiss, M., Samain, O., Roujean, J. L., and Leroy, M.: LAI, fAPAR and fCover CYCLOPES global products derived from VEGETATION. Part 1: Principles of the algorithm, *Remote Sens. Environ.*, 110, 275–286, 2007.
- Bindlish, R., Kustas, W. P., French, A. N., Diak, G. R., and Mecikalski, J. R.: Influence of near-surface soil moisture on regional scale heat fluxes: model results using microwave remote sensing data from SGP97, *IEEE T. Geosci. Remote*, 39, 1719–1728, 2001.
- Brutsaert W.: Evaporation into the atmosphere. Reidel, Dordrecht, The Netherlands, 299 pp., 1982.
- Campbell, G. S. and Norman, J. M.: An introduction to Environmental Biophysics, Springer, New York ISBN 0-387-94937-2, 286 pp., 1998.
- Chen, J. M., Rich, P. M., Gower, S. T., Norman, J. M., and Plummer, S.: Leaf area index of boreal forests: Theory, techniques and measurements, *J. Geophys. Res.-Atmos.*, 102, 429–443, 1997.
- Choudhury, B. J., Ahmed, N. U., Idso, S. B., Reginato, R. J., and Daughtry, C. S. T.: Relations between evaporation coefficients and vegetation indices studied by model simulations, *Remote Sens. Environ.*, 50, 1–17, 1994.
- Choudhury, B. J.: Relationships between vegetation indices, radiation absorption, and net photosynthesis evaluated by a sensitivity analysis, *Remote Sens. Environ.*, 22, 209–233, 1987.
- Combal, B., Baret, F., Weiss, M., Trubuil, A., Mace, D., Pragnère, A., Myneni, R., Y. Knyazikhin, Y., and Wang, L.: Retrieval of canopy biophysical variables from bidirectional reflectance using prior information to solve the ill-posed inverse problem, *Remote Sens. Environ.*, 84, 1–15, 2003.
- Darvishzadeh, R., Skidmore, A., Schlerf, M., and Atzberger, C.: Inversion of a radiative transfer model for estimating vegetation LAI and chlorophyll in a heterogeneous grassland, *Remote Sens. Environ.*, 112, 2592–2604, 2008.
- European Space Agency (ESA): GMES Sentinel-2 Mission Requirements Document, issue 2 revision 0-30/01/2007, EOP-SM/1163/MR-dr, p. 31, 2007.
- Fernandez, G., Moreno, J., Gandia, S., Martinez, B., Vuolo, F., and Morales, F.: Statistical variability of field measurements of biophysical parameters in SPARC-2003 and SPARC-2004 data campaigns, in: Proceedings of the SPARC Final Workshop WPP-250, Enschede, The Netherlands, 4–5 July 2005, 2005.
- French, A. N., Schmugge, T. J., Kustas, W. P., Brubaker, K. L., and Prueger, J.: Surface energy fluxes over El Reno, Oklahoma, using high-resolution remotely sensed data, *Water Resour. Res.*, 39 (6), 1164, 2003.
- Gash, J. H. C.: A note on estimating the effect of a limited fetch on micrometeorological evaporation measurements, *Bound.-Lay. Meteorol.*, 35, 409–413, 1986.
- Haboudane, D., Miller, J. R., Pattey, E., Zarco-Tejada, P. J., and Strachan, I. B.: Hyperspectral vegetation indices and novel algorithms for predicting green LAI of crop canopies: Modeling and validation in the context of precision agriculture, *Remote Sens. Environ.*, 90, 337–352, 2004.
- Jacquemoud, S. and Baret, F.: PROSPECT: A model of leaf optical properties spectra, *Remote Sens. Environ.*, 34, 75–91, 1990.
- Jimenez-Munoz, J. C. and Sobrino, J. A.: Feasibility of retrieving land-surface temperature from ASTER TIR bands using two-channel algorithms: a case study of agricultural areas, *IEEE T. Geosci. Remote*, 4, 60–64, 2007.
- Kustas, W. P. and Norman, J. M.: Evaluation of soil and vegetation heat flux predictions using a simple two-source model with radiometric temperatures for partial canopy cover, *Agr. Forest Meteorol.*, 94, 13–29, 1999.
- Kustas, W. P., Norman, J. M., Schmugge, T. J., and Anderson, M. C.: Mapping surface energy fluxes with radiometric temperature, in: Thermal remote sensing in land surface processes, edited by: Quattrochi, D. A. and Luvall, J. C., Boca Raton, Florida, CRC Press, 205–253, 2004.
- Kuusik, A.: The hot-spot effect in plant canopy reflectance, in: R.B. Myneni and J. Ross (Ed.), Photon –vegetation interactions, Springer-Verlag, New York, 139–159, 1991.
- Li, F., Kustas, W. P., Prueger, J. H., Neale, C. M. U., and Jackson, T. J.: Utility of remote sensing based two-source energy balance model under low and high vegetation cover conditions, *J. Hydrometeorol.*, 6, 878–891, 2005.
- Montandon, L. M. and Small, E. E.: The impact of soil reflectance on the quantification of the green vegetation fraction from NDVI, *Remote Sens. Environ.*, 112(4), 1835–1845, 2008.
- Moreno, J. and participants of the SPARC campaigns: The SPARC-Barrax Campaign (SPARC): Overview and first results from CHRIS data, in: Proceeding of the 2nd CHRIS/Proba Workshop Frascati, Italy, ESA/ESRIN, 28–30 April, 2004.
- Norman, J. M., Kustas, W. P., and Humes, K. S.: A two-source approach for estimating soil and vegetation energy fluxes in observations of directional radiometric surface temperature, *Agr. Forest Meteorol.*, 77, 263–293, 1995.
- Richter, K., Atzberger, C., Vuolo, F., Weihs, P., and D’Urso, G.: Experimental assessment of the Sentinel-2 band setting for RTM-based LAI retrieval of sugar beet and maize, *Can. J. Remote Sens.*, in press, 2009.
- Schmugge, T. J., Kustas, W. P., and Humes, K. S.: Monitoring land surface fluxes using ASTER observations, *IEEE T. Geosci. Remote*, 36, 1421–1430, 1998.
- Sobrino, J. A., Jimenez-Munoz, J. C., Balick L., Gillespie, A. R., Sabol, D. A., and Gustafson W. T.: Accuracy of ASTER level-2 thermal-infrared standard products of an agricultural area in Spain, *Remote Sens. Environ.*, 106, 146–153, 2007.
- SPARC data acquisition report, Contract no: 18307/04/NL/FF, University Valencia, 2004.
- Stenberg, P., Rautiainen, M., Manninen, T., Voipio, P., and Smolander, H.: Reduced simple ratio better than NDVI for estimating LAI in Finnish pine and spruce stands, *Silva Fenn.*, 38(1), 3–14, 2004.
- Su, Z., Timmermans, W. J., Gieske, A. S. M., Jia, L., Elbers, J. A., Olioso, A., Timmermans, J., Van der Velde, R., Jin, X., Van der Kwast, H., Sabol, D., Sobrino, J. A., Moreno, J., and Bianchi, R.: Quantification of land-atmosphere exchanges of water, energy and carbon dioxide in space and time over the heterogeneous Barrax site, *Int. J. Remote Sens.*, 29, 5215–5235, 2008.
- Timmermans, W. J., Kustas, W. P., Anderson, M. C., and French, A. N.: An intercomparison of the Surface Energy Balance Algorithm for Land (SEBAL) and the Two-Source Energy Balance (TSEB) modeling schemes, *Remote Sens. Environ.*, 108, 369–

- 384, 2007.
- Timmermans, W. J., Su, Z., and Olioso, A.: Footprint issues in scintillometry over heterogeneous landscapes, *Hydrol. Earth Syst. Sci. Discuss.*, 6, 2099–2127, 2009, <http://www.hydrol-earth-syst-sci-discuss.net/6/2099/2009/>.
- van der Kwast, J., Timmermans, W., Gieske, A., Su, Z., Olioso, A., Jia, L., Elbers, J., Karssenbergh, D., and de Jong, S.: Evaluation of the Surface Energy Balance System (SEBS) applied to ASTER imagery with flux-measurements at the SPARC 2004 site (Barrax, Spain), *Hydrol. Earth Syst. Sci. Discuss.*, 6, 1165–1196, 2009, <http://www.hydrol-earth-syst-sci-discuss.net/6/1165/2009/>.
- Verhoef, W.: Light scattering by leaf layers with application to canopy reflectance modeling: the SAIL Model, *Remote Sens. Environ.*, 16, 125–141, 1984.
- Verhoef, W.: Earth observation modeling based on layer scattering matrices, *Remote Sens. Environ.*, 17, 165–178, 1985.
- Vuolo, F., Dini, L., and D’Urso, G.: Retrieval of Leaf Area Index from CHRIS/PROBA data: an analysis of the directional and spectral information content, *Int. J. Remote Sens.*, 29(17), 5063–5072, 2008.
- Weiss, M., Baret, F., Myneni, R. B., Pragnère, A., and Knyazikhin, Y.: Investigation of a model inversion technique to estimate canopy biophysical variables from spectral and directional reflectance data, *Agronomie*, 20, 3–22, 2000.
- Zhan, X., Kustas, W. P., and Humes, K. S.: An intercomparison study on models of sensible heat flux over partial canopy surfaces with remotely sensed surface temperature, *Remote Sens. Environ.*, 58, 242–256, 1996.

4.3 Publikation III

Plant growth monitoring and potential drought risk assessment by means of Earth Observation data

Katja Richter, Pablo Rischbeck, Josef Eitzinger, Werner Schneider,
Franz Suppan, and Philipp Weihs

International Journal of Remote Sensing 29 (17-18): 4943 – 4960, 2008.

Plant growth monitoring and potential drought risk assessment by means of Earth observation data

K. RICHTER*†‡, P. RISCHBECK†‡, J. EITZINGER†, W. SCHNEIDER‡, F. SUPPAN‡ and P. WEIHS†

†Institute of Meteorology, University of Natural Resources and Applied Life Sciences, Vienna, Austria

‡Institute of Surveying, Remote Sensing and Land Information, University of Natural Resources and Applied Life Sciences, Vienna, Austria

(Received 15 November 2006; in final form 5 December 2007)

The potential of hyperspectral imagery for the determination of drought risk zones, responsible for heterogeneous plant growth due to different soil compositions, was assessed at the field scale. The research was carried out in the Marchfeld region, an agricultural, flat area east of Vienna, Austria, during June 2005 by means of an airborne imaging spectrometer (HyMap). The inversion of a radiative transfer model by using a look-up-table (LUT) approach was performed to retrieve canopy parameters, indicators of plant growth, such as leaf area index (LAI), chlorophyll content and a soil reflectance factor (ALFA). To quantify ALFA with respect to its relationship to soil surface water content, the soil reflectance was measured at different levels of known soil water conditions. Finally, a cluster analysis was performed using the parameters estimated from the model inversion to explain plant growth variability, quantified by means of measured yield. The results were compared with a simple Normalized Differenced Vegetation Index (NDVI) approach to evaluate the contribution of hyperspectral data to vegetation monitoring. Areas characterizing different levels of drought risk could be determined by both methods with a similar performance.

1. Introduction

The early detection of potential drought stress areas within crop fields is a vital issue because of the substantial importance of an efficient crop production and thus prevention of food shortages. Drought stress, which occurs when plant water demand exceeds the water supply, can be traced back to two main factors: (1) low availability of soil water, limiting the water supply to the roots, and (2) specific dry weather conditions, such as high temperature, high irradiance, low precipitation and low relative air humidity. This can take place on a seasonal or diurnal time-scale, depending on the geographical situation of the agricultural area and its specific climate and soil characteristics.

Water deficiency leads to changes in plant energy balance. As one of the first reactions, plants reduce stomatal conductance, which causes a decrease in assimilation rate. The reduction of transpiration through stomatal closure results in higher leaf temperatures. Furthermore, depending on the type of vegetation,

*Corresponding author. Email: katja.huber@boku.ac.at

changes in leaf form and inclination might occur. Most of these short-term reactions are reversible when the stress is alleviated, whereas longer-lasting water deficiencies lead to a change in the canopy structure (Casa 2003). The consequence is a reduction in leaf area development, expressed by the leaf area index (LAI), when plants are still in the vegetative phase. The LAI was first defined as the total one-sided area of photosynthetic tissue per unit of ground area (Watson 1947). Thus, the LAI is one of the quantities characterizing the status of crops and may be seen as one of the most important parameters indicating drought stress on a medium-term time-scale (Casa 2003, Casa and Jones 2005).

Several studies have reported an effect of drought stress on plant pigments (Ashraf *et al.* 1994, Ashraf and Iram 2005). In most crop species water deficiency leads to a reduction of chlorophyll content. Sarker *et al.* (1999), for instance, studied the effect of water stress on the biochemical constituents of wheat crops and found a higher chlorophyll *a* and *b* content and a higher *a*:*b* ratio of the fourth and flag leaves of irrigated compared with non-irrigated plants.

These biophysical parameters can be determined from *in situ* measurements (Ross 1981, Weiss *et al.* 2004) for many localized studies (i.e. at the scale of 1–10 ha). However, when repetitive measurements are needed over larger heterogeneous areas, in most cases field campaigns do not provide a feasible solution because ground-based measurements of the vegetative surface are time-consuming and cost-intensive as well as spatially and temporally constricted.

Remote sensing from space has shown its potentiality in the retrieval of biophysical parameters of vegetation, in particular LAI, because of its relevance in many land surface processes.

Besides the LAI, chlorophyll and the other canopy parameters, the soil system must be regarded as an important factor in the context of crop growth. Soil moisture availability plays an essential role in the process of mass and energy exchange between surface and atmosphere (Weidong *et al.* 2002), resulting in a need for data availability in application systems. Thus, as for vegetation parameters, the benefits of Earth observation (EO) data have also been exploited to study the soil system.

Different wavelength regions have been investigated in terms of soil moisture sensitivity, particularly by using remote sensing in the microwave region of the spectrum. The potential of active microwave sensors (ERS/SAR) has been studied, for instance, by Quesney *et al.* (2000). The authors indicated the difficulty in retrieving soil moisture by means of active sensors because of the effects of spatial and temporal fluctuations of soil roughness and the presence of dense vegetation cover, leading to attenuation and scattering.

However, passive remote sensing in the microwave region reveals a high potential to retrieve soil moisture information with high temporal sampling and on a regional scale (Wigneron *et al.* 2002). Observations at frequencies between 1 and 3 GHz (L-band) are useful for the detection of soil moisture because the energy emitted from deeper soil layers is less affected by absorption and reflection from vegetation. In this context SMOSREX (Surface Monitoring Of the Soil Reservoir EXperiment), the first long-term field experiment for the L-band, and also multispectral remote sensing of the surface, was initiated in January 2001 (Rosnay *et al.* 2006).

Finally, even the solar domain (400–2500 nm) has been exploited regarding its potential for soil moisture assessment (e.g. Dalal 1986, Leone and Sommer 2000, for review see Weidong *et al.* 2002). Several studies have analysed the change in spectral

reflectance in this wavelength region with varying soil surface moisture content (e.g. Bowers and Hanks 1965, Stoner and Baumgardner 1980, Neema *et al.* 1987, Weidong *et al.* 2002). All of these studies confirmed an overall decrease in reflectance with increasing soil moisture. However, when carrying out the experiment up to very high soil moisture content, the authors noted a reversal of this trend: the reflectance increased again. This phenomenon was called ‘cut-off thickness’, defined by the thickness of sand that transmits only 5% of incident light. However, under typical agriculture conditions the soil moisture is normally too low to reach this critical point.

Soil reflectance is mainly controlled by three components that determine brightness and colour:

- (1) the absorption and scattering properties of its constituents (water, air, minerals and organic matter);
- (2) physical structure (aggregation, surface roughness, soil texture); and
- (3) observation configuration (zenith and azimuth angles of the sun and the observer).

For a given location, such as a field, soil mineral components and organic matter as well as soil structure should reveal only small modifications within the course of a vegetation period. However, surface water content can change depending on the weather conditions and soil water storage capacity.

Weidong *et al.* (2002) proposed that a simple linear relationship could be used for a rough estimation of soil moisture from bare soil reflectance. The complexity of soil moisture estimation from spectral signals increases in the presence of vegetation cover. Depending on canopy type and site conditions, there is a development from a high soil influence on the spectra at the beginning of the season until the soil ceases to affect the signal when it is completely overshadowed by the vegetation (see Weidong *et al.* 2002). For a low LAI (up to 2–3) the soil still influences the reflectance spectra acquired by a sensor. In particular, the red and near-infrared wavelength regions exhibit a pronounced difference between vegetation and soil components (Atzberger *et al.* 2003). The challenge is to distinguish between these components and extract the respective information needed. Consequently the monitoring of vegetation by airborne or satellite remote sensing provides the only way to retrieve the LAI, chlorophyll, soil characteristics and other canopy properties on a large scale and in a rapid, accurate and cost-effective way. In particular, the recent availability of hyperspectral data, ranging from the visible to the mid-infrared, provides a promising source for applications in agriculture, for example in precision farming. Compared to broadband data, the higher spectral information content of these data may allow more accurate analyses of the canopy spectral response within a high spatial resolution.

The estimation of canopy structure (such as the LAI or leaf angle distribution) and biochemical parameters (such as chlorophyll or leaf water content) from remote sensing data is generally performed by two different approaches:

- (1) The classical and most simple methods are based on statistical–empirical relationships between the parameter and ‘vegetation indices’ (VIs) (Myneni *et al.* 1995, Thenkabail *et al.* 2002, Casa and Jones 2005). These regression models consist of different mathematical forms with empirical coefficients that vary depending on canopy structure (leaf angle distribution, leaf spatial distribution, row orientation and spacing), leaf and soil optical properties

and sun–target–sensor geometry (Huete 1987, Bacour *et al.* 2002). VIs may provide a satisfactory level of accuracy in the estimation of important vegetation biophysical parameters such as LAI. A limiting factor of this method is the need for reference measurements to calibrate the models for specific vegetation type, site and sensor characteristics (Curran and Williamson 1986).

- (2) The alternative to VIs is the estimation of biophysical parameters by means of physically based models of canopy reflectance. This may allow more accurate parameter retrieval than with VI for the following reasons. The physical approach allows a higher validity as there is no restriction by empirical relationships. The particular advantage of the physical approach is its ability to exploit the full spectrum obtained by hyperspectral sensors. However, there are also restrictions, such as the need for an extensive parameterization, which causes high computational demand. Furthermore, the ill-posed inverse problem has to be taken into account, as it may lead to significant uncertainties in parameter estimation because different parameter combinations may produce almost identical spectra (Baret and Guyot 1991, Myneni *et al.* 1995, Casa and Jones 2005).

Different methodologies have been proposed to alleviate the inverse problem, for example by constraining some of the parameters to fixed values or by the use of a priori knowledge, taking into account the temporal evolution of the crop cycle. Another possibility is the object-based retrieval of canopy parameters, considering the radiometric information of neighbouring pixels during model inversion (reviews in Kimes *et al.* 2000, Combal *et al.* 2002, Atzberger 2004).

The present work is part of a study in the framework of the project ‘crop drought stress monitoring by remote sensing’ (DROSMON) (Schneider *et al.* 2005). DROSMON aims to adapt and develop existing and new EO techniques for the detection of drought stress of crops. The objective of this study was to exploit the potential of hyperspectral imagery for analysing the degree of within-field variability of plant growth due to heterogeneous soil conditions. This should provide valuable information for mapping potential risks of crop drought stress. Physical methods of canopy reflectance modelling were used to estimate biophysical parameters (i.e. LAI, average leaf angle, leaf chlorophyll content and soil brightness). The estimation of these parameters, all sensitive to drought stress, was then used to classify a single field in terms of potential drought risk. A statistical cluster analysis was applied to group estimated parameters into similar zones. These clusters can provide a starting point for examining the reasons for yield variability (Reyniers 2003, Vrindts *et al.* 2005) due to soil conditions causing drought stress.

2. Experiment and methods

2.1 Study area and experimental data sampling

2.1.1 Experimental field area. In the Marchfeld, an agricultural area situated in the east of Vienna, Austria, wheat is grown as one of the principal crops. Under the regional climate conditions, which are considered as semi-arid, cereals are generally not irrigated. The dominant soil types of this area are chernozem and fluvisol, the latter being present at the test site of this study. The general soil conditions are characterized by a humus-rich A horizon and a sandy C horizon, followed by fluvial gravel from the former river bed of the Danube. The groundwater table is situated in

this gravel body at a depth of more than 6 m. Gravel inhibits capillary rise and thus no groundwater impact is present in the rooting zone of the crops. A particular attribute of these soils is the local presence of sand streams caused by former river meanders. Sand, characterized by lower water storage capacity, interferes with the plant growth. In dry periods, as was the case in the weeks before the data acquisition, this negative effect can be increased. For this study a *Triticum durum* wheat field was selected (location shown in figure 1), representing this situation.

2.1.2 Field data acquisition. At the beginning of the campaign 20 soil profiles were dug, spread equally over the field. They revealed the presence of sandy streams at different depths within the field. A spatial map of sand depth distribution was attained by means of the Kriging interpolation technique, demonstrated in figure 2. The minimal depth of sand appearance under the surface is 30 cm due to the even ploughing of the field at a depth of about 30 cm before seeding. Therefore, sandy bands were not visible on the surface.

Agriculture practices, such as fertilization treatments and seedbed preparation, were carried out uniformly within the field. Weather and environmental conditions can be considered as unchanged within the extension of the field (~13 ha). Consequently, for this case study, the soil can be regarded as the only factor that could significantly lead to differences in plant growth.

The yield (in dt ha⁻¹) was measured destructively at the end of the growing season (end of July 2005) accompanied by differential Global Positioning System (GPS) techniques to locate harvest samplings in a 2-m resolution. For one HyMap pixel four measured yield points were averaged and thus made directly comparable to the results of image processing. Due to missing simultaneous and area-wide *in situ* measurements of biophysical parameters, these data were used for indirect validation.

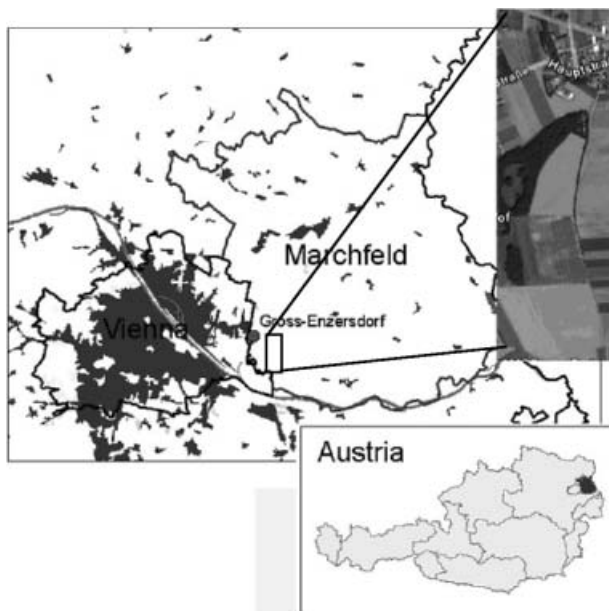


Figure 1. Location of the study area, Marchfeld, Austria.

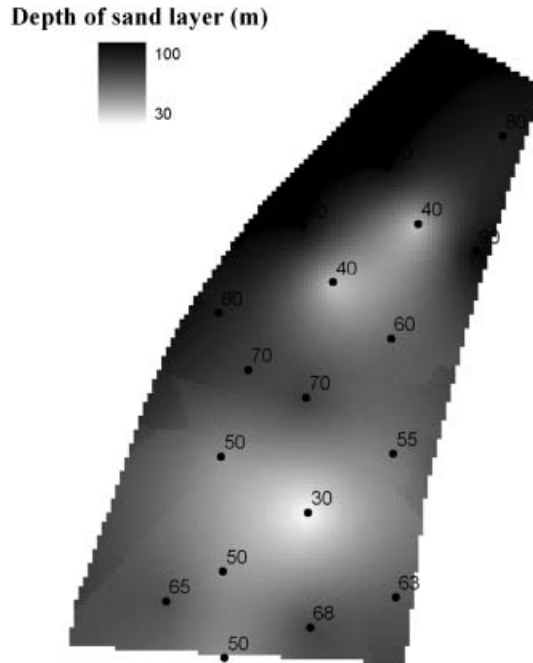


Figure 2. Sand depth distribution within the field, Kriging interpolation of soil profiles.

2.1.3 Hyperspectral airborne and ground data. The test site was monitored on 21 June 2005 by means of the airborne imaging spectrometer HyMap. HyMap data have a high spatial and spectral resolution (3.9 m, 126 bands, ranging from ~400 to 2500 nm). The availability of ground-based spectra, carried out with an Analytical Spectral Devices (ASD) field spectroradiometer, enabled atmospheric correction of the HyMap image to be performed by means of the empirical line (EL) approach (see Roberts *et al.* 1985, Conel *et al.* 1987). This method is based on a linear correlation between the radiance measured by the sensor and the reflectance simultaneously measured in the field (Smith and Milton 1999). Nine targets of the scene were linearly correlated against the corresponding field spectra. In the visible (434–722 nm) and mid-infrared (1313–2485 nm) parts of the spectrum, radiance from the HyMap sensor and reflectance from FieldSpec were well correlated ($R^2=0.96$ and 0.98 , respectively). However, in the near-infrared part of the spectrum (737–1299 nm), the correlation performed less well ($R^2=0.5$).

2.2 Data processing

In this study the turbid medium SAILH (Scattering by Arbitrarily Inclined Leaves, with Hotspot effect) model (Verhoef 1984, Kuusk 1985) was used in combination with the leaf model PROSPECT (Jacquemoud and Baret 1990, Baret and Fourty 1997). This is a widely used approach and many authors (e.g. Jacquemoud *et al.* 2000) have reported its reliable performance for a variety of crops, in particular for wheat.

2.2.1 Parameter estimation by model inversion. The SAILH model simulates canopy reflectance as a function of structure parameters (defined by the LAI, the average leaf inclination angle (ALA) and a hotspot parameter (HOT)), soil spectral

reflectance, leaf reflectance and transmittance, fraction of diffuse irradiance and the view and illumination geometry. Leaf reflectance and transmittance were simulated by the PROSPECT model as a function of four structural and biochemical parameters: leaf chlorophyll content (C_{ab}), dry matter content (C_m), leaf water thickness (C_w) and a leaf mesophyll structural parameter (N).

Parameter estimation was based on a look-up-table (LUT) inversion approach, which is considered as one of the simplest methods to invert a model (Weiss *et al.* 2000). The working process is split into three parts:

(1) *Generation of an appropriate number of canopy parameter combinations and space.* The LUT size could be reduced to a number of 12 960 combinations realized in the following structure: parameters followed Gaussian distribution for LAI (ten classes, ranging from 0.1 to 6.0), ALA (four classes, ranging from 40° to 70°) and C_{ab} (six classes, ranging from 35 to $70 \mu\text{g}/\text{m}^2$). Because of the availability of a priori knowledge of the field properties and the presence of only one wheat cultivar, Gaussian distribution laws were chosen for these parameters. For the leaf parameters C_m and C_w , uniform distribution and only three classes were assumed (C_m : 0.004–0.007 g/cm^2 and C_w : 0.01–0.02 cm). The leaf structure parameter N was fixed to an average value of 1.55, as has been applied to many crops (see Haboudane *et al.* 2004). The HOT parameter is roughly defined as the ratio of the leaf size to canopy height (Verhoef and Bach 2003). In this study HOT was set to 0.2 according to the average of several measurements of canopy height (90 cm) and leaf size (18 cm) during the field campaign.

The soil reflectance spectrum was measured *in situ* with a field spectroradiometer and implemented in the model. A simple multiplicative soil brightness factor ‘ALFA’ was introduced (Atzberger *et al.* 2003), representing the overall brightness of the soil, which was assumed to vary according to the surface water content. Figure 3 demonstrates the measured soil spectrum with the ALFA factor ranging from 0.7 to 1.3, representing the range from wettest to driest soil conditions.

A first approach to quantify this relationship by means of a field experiment is described in section 2.2.2.

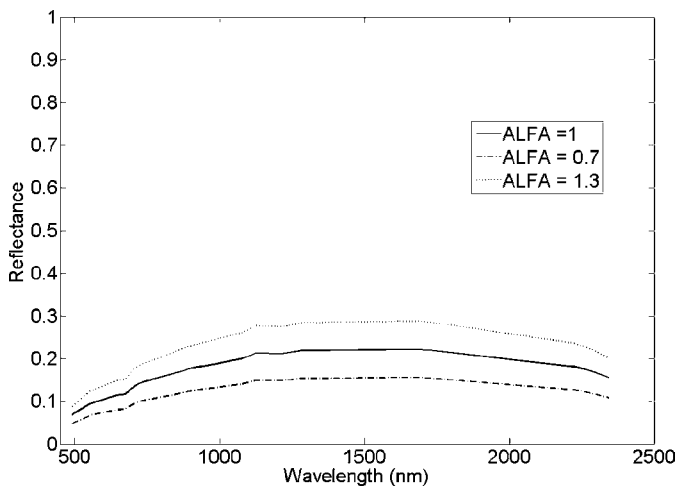


Figure 3. Average soil reflectance (21 selected bands) used as input for inversion of the PROSPECT+SAILH model, and its variance according to the ALFA soil factor.

(2) *Running the radiative transfer model to simulate the corresponding reflectance table.* For the simulation in direct mode, 21 out of the 126 HyMap bands were chosen according to the results of Thenkabail *et al.* (2004). A selection of 'optimal' spectral bands was considered because the number of spectral bands is not simply equal to the dimensionality of the information content because of band correlation and data redundancy (Vuolo *et al.* 2005).

The chosen wavebands were found to best characterize and classify vegetation and crops due to their sensitivity to chlorophyll, soil background, biomass, LAI, plant moisture and vegetation stress (Thenkabail *et al.* 2004). They cover the ultra-violet (492.7 nm), the visible (554.3, 646.2 and 676.5 nm), the red edge (707.3, 722.4 and 737.5 nm), the near-infrared (874, 888.5, 911.1, 990.2, 1082.9, 1127.7, 1214.5, 1243.1 and 1285.4 nm), the early mid-infrared (1675.7 and 1725.4 nm) and the far mid-infrared (2225.7, 2293.7 and 2343.1 nm) parts of the spectrum. The measurement configuration used for the model simulations presented the actual conditions during the sensor overpass with a solar zenith angle of 25° and a view zenith angle of 2° according to the almost-nadir position of the plane with respect to the field.

(3) *Sorting of the LUT along with a simple cost function.* This function calculates the root mean square error (RMSE) between modelled spectra found in the LUT and measured reflectance. The solution is the average of the parameters corresponding to the 10% lowest RMSE values between measured and simulated spectra.

The procedure was applied to all 8599 pixels situated in the wheat field.

2.2.2 Quantification of the ALFA soil factor. The inhomogeneous plant growth in the test field can be traced back mainly to sand streams causing dryer soil conditions (see section 2.1.1 for more details). As stated in section 2.2.1., the ALFA factor, introduced into the SAILH model, represents the overall brightness of the soil, which is assumed to vary according to the surface water content.

The following approach was carried out to quantify the relationship between the ALFA factor and the soil surface water content (θ) by means of a spectral measurement experiment. A soil sample with a size of approximately 14.5 dm³ (54 × 30 × 9 cm) was taken from the wheat field, keeping the original bulk density and texture. The soil was dried in a laboratory until the water content was equal to zero. Five spectral reflectance measurements were achieved in the course of one day with the ASD Pro FR portable field spectroradiometer. The instrument acquires spectral reflectance in the range of 350–2500 nm with a spectral resolution of 1.4 nm in the shorter and 2.0 in the longer wavelength region. The sensor (with a 25° field of view) was set up nadir looking to the soil probe at a distance of ~20 cm. This configuration was chosen to minimize the influence of surface roughness leading to shadowing.

After each measurement a known quantity of water was added. Before performing the next measurement a period of 2–3 h was required to ensure even distribution of the water in the soil probe. Additionally, the soil was covered during this time to avoid evaporation. Simultaneously with every spectral measurement, the current soil water content was again determined by weighing the soil. The experiment was carried out under clear sky conditions and the soil sample was always adjusted perpendicularly to the sun.

2.3 Cluster analysis

As simultaneous and area-wide reference measurements of LAI, chlorophyll, leaf angle and soil water content were missing, direct validation of the inversion results

was not possible. Thus, the yield measurements, suggesting also the occurrence of drought stress of the crops during the growing period, provided the only alternative to validate the retrieved data set.

Cluster analysis is used in statistical studies to arrange a set of parameters into relatively homogeneous subgroups or clusters (see Leilah and Al-Khateeb 2005). It seeks to identify a set of groups that minimize within-group variation and maximize between-group variation. The procedure starts with each case of a variable in a separate cluster and then combines the clusters sequentially, reducing the number of clusters at each step until a defined number remains.

In this context the technique was applied to determine whether it was possible to sort the estimated parameters (LAI, ALA, ALFA and C_{ab}) into a number of groups in which the members had a strong degree of association to each other, but a weak association to another group. The following assumption was established: high ALA, LAI, C_{ab} and low ALFA values should characterize higher yield zones, whereas lower ALA, LAI, C_{ab} , but higher ALFA, values should correspond to lower yield areas.

Hierarchical cluster analysis was carried out using Ward's method and the squared Euclidian distance as the interval measure. Several numbers of clusters (ranging from two to seven) were built and analysed in terms of the above-mentioned assumption.

All statistical analyses were performed using the SPSS software package (SPSS Inc., 2001).

3. Results

3.1 Parameter estimation from model inversion

Figure 4 depicts the resulting distribution of the estimated canopy parameters and figure 5 shows the corresponding spatial maps of the wheat field.

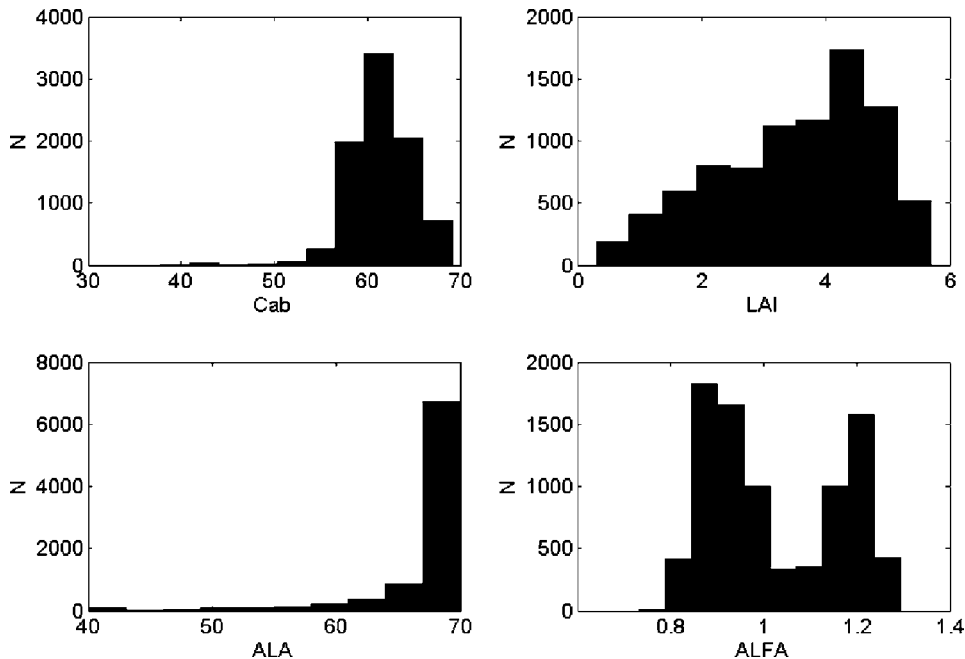


Figure 4. Distribution of wheat canopy parameters (LAI, ALA, ALFA and C_{ab}), estimated by model inversion from HyMap acquisition data (Marchfeld, 21 June 2005).

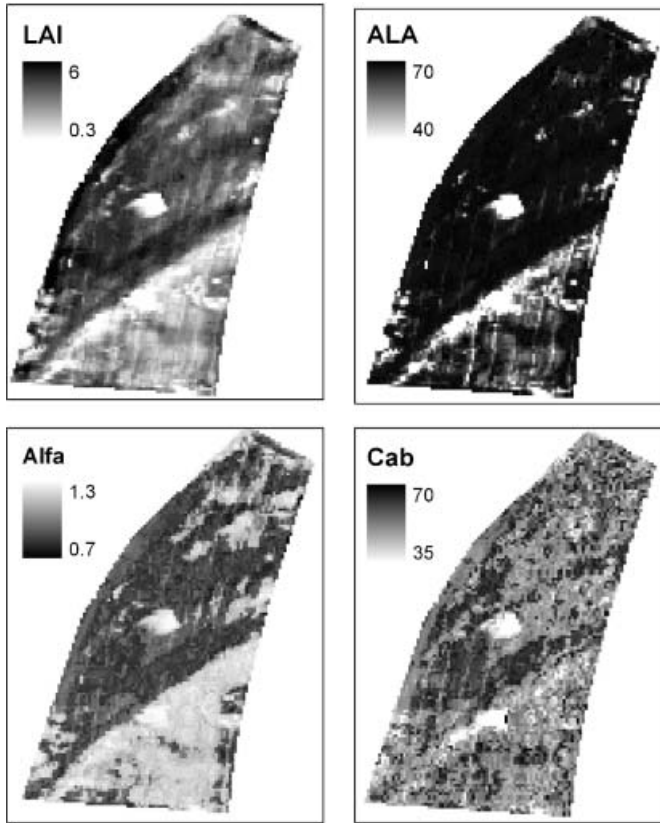


Figure 5. Maps of canopy parameters (LAI, ALA, ALFA and C_{ab}) of wheat, estimated by model inversion from HyMap acquisition data (Marchfeld, 21 June 2005).

As simultaneous and area-wide reference measurements of LAI, chlorophyll content and average leaf angle were missing, direct validation of the inversion results was not possible. Instead, the coefficient of determination (R^2) between the measured yield and LAI was calculated and the performance compared with the well-known Normalized Differenced Vegetation Index (NDVI) calculated from the wheat reflectance by using the relationship between red and near-infrared wavebands: $NDVI = (NIR - RED) / (NIR + RED)$. Figure 6 shows the results. Both coefficients reveal similar significant but moderate results (LAI and yield: $R^2 = 0.355$;

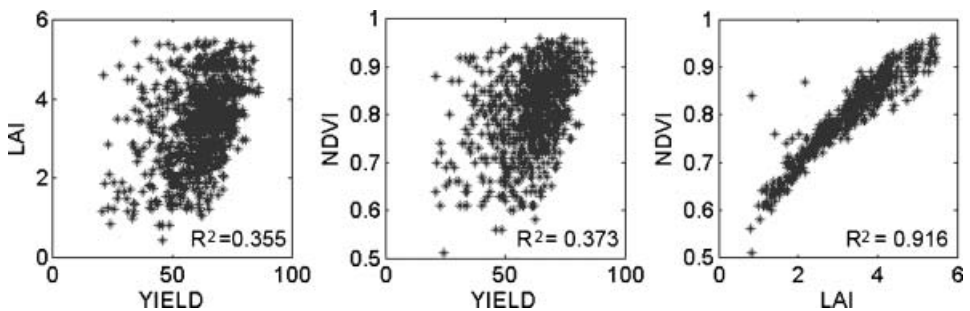


Figure 6. Correlation between measured yield and estimated LAI and NDVI.

NDVI and yield: $R^2=0.373$), whereas the coefficient of correlation between LAI and NDVI reaches a high significant level ($R^2=0.916$).

Concerning the performance of ALFA parameter estimation, only an approximate comparison with the interpolated soil depth map (figure 2) could be used for the validation. The comparison partly revealed a concordance between high ALFA values and lower depth of sand streams, especially in the lower middle part of the field, whereas lower ALFA values correspond to deeper sand occurrence in the northern and western parts of the field. Nevertheless, spatial soil moisture measurements and accurate texture analysis are necessary for a reliable validation of this parameter.

3.2 Soil experiment

Figure 7 shows the resulting reflectance curves (using the 21 bands mentioned in section 2.2.1) with the corresponding percentage volumetric water content. The maximal amount of water content measurements did not reach the cut-off thickness (see section 1.2).

Various empirical relationships were tested to estimate the soil surface water content from the reflectance values. For low water content levels (up to about $\theta=2.5$) a linear relationship can be used to estimate the soil water content. However, for higher water content levels the relationship shows a nonlinear behaviour. Regarding soil reflectance for single wavebands plotted against soil water content, the curve is comparable to an exponential function.

Thus, the reflectance data were transformed and the best fit was achieved by using an exponential function of the form:

$$f(x) = a_1 \exp[b_1 x^{-1}] \quad (1)$$

where x is the wavelength specific reflectance value.

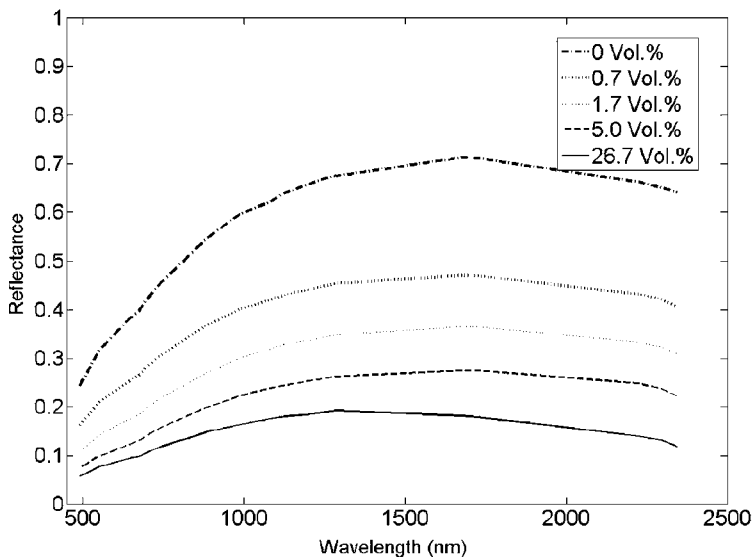


Figure 7. Results of the soil experiment, reflectance curves (21 selected bands) with corresponding soil water content.

Table 1. Wavelength-specific coefficients for the exponential function (equation(1)) to determine volumetric soil water content (θ) from reflectance, and results for measured soil spectrum.

	a	b	R^2	RMSE	θ (soil reflectance)
B3	0.03949	0.6051	0.99	0.4417	7.83
B6	0.04314	0.7173	0.99	0.3214	6.87
B11	0.07081	0.9662	0.99	0.3054	11.79
B18	0.1737	0.8973	0.99	0.5466	10.25
B20	0.3463	0.5704	0.99	0.9298	10.31

Five wavelength regions, representing the visible 646.2 nm ('B3'), red edge 722.4 nm ('B6'), near-infrared 990.2 nm ('B11'), early mid-infrared 1725.4 nm ('B18') and far mid-infrared 2293.7 nm ('B20') were selected and coefficients calculated (see table 1). Figure 8 shows an example of the fitted functions for wavebands B6 and B18. By means of this function, the soil surface water content could be calculated for the measured soil spectra (figure 3), introduced in the model inversion procedure. Calculating the mean of the five resulting water content values (presented in table 1), resulted in 9.41 vol% (standard deviation 2.01).

3.3 Cluster analysis

Applying different numbers of clusters (two up to seven) to the parameters C_{ab} , LAI, ALA and ALFA should ideally result in the establishment of four clusters (see figure 9(a)). This decision was taken by analysing the statistics of the parameters and the yield in every cluster. Table 2 shows results for the 'optimal' cluster composition. From cluster 1 to cluster 4 there is an increase of the mean value of C_{ab} (from 48.9 to 64.7 $\mu\text{g m}^{-2}$), LAI (from 0.6 to 4.1) and ALA (from 45.4° to 69.1°) but a decrease of mean ALFA from 1.26 to 0.98. The application of the function for the retrieval of soil water content from reflectance would result in $\theta=10.33$ (SD=2.17) for ALFA 0.98 and $\theta=3.74$ (SD=1.17) for ALFA 1.26. Yield means are increasing from cluster 1 (42.5 dt ha⁻¹) to cluster 4 (68.4 dt ha⁻¹), confirming the assumptions.

The establishment of four clusters leads to the greatest possible distinction of the grouped parameters. By increasing the number of clusters (up to seven), this tendency could no longer be observed, probably because of the increasing relative errors from parameter estimation when aggregating the data into smaller clusters.

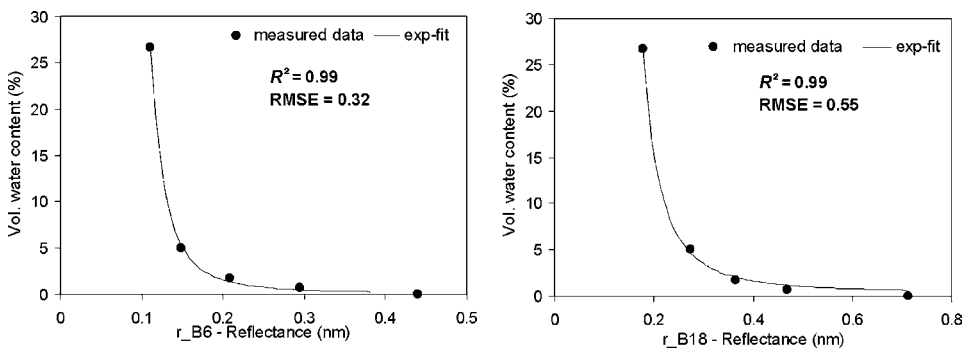


Figure 8. Exponential fit between measured reflectance data and volumetric water content for two wavelengths: 722.4 nm (B6) and 1725.4 nm (B18).

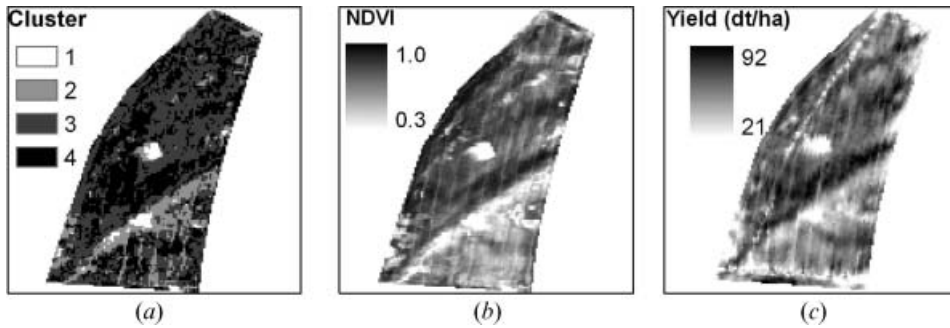


Figure 9. Resulting four clusters for the wheat field (a), established by means of cluster analysis, four classes of NDVI map (b) and ground measured yield (dt h^{-1}) (c) by GPS in July 2005.

In addition, when comparing the resulting maps of estimated LAI, ALA, ALFA and C_{ab} (see figure 5), yield and cluster (see figure 9(c)), the general structure of the field is clearly visible in all: first, the large stream of high ALFA, low LAI, ALA, C_{ab} and yield that is stretching from the southwest to the east of the field, and second, the notable spot in the middle of the field. In these parts the humus-rich A horizon of the soil reached a depth of only 30–40 cm and therefore the area is mostly grouped to cluster 1, corresponding to the driest conditions. The underlying sand band was identified by four of the 20 soil profiles (figure 2). Instead, a section of high yield with high ALA, C_{ab} and LAI, but lower ALFA, was found in the northwest part of this sand band and in the north of the field. In this region the A horizon reached a thickness up to 80 or 90 cm and was grouped to higher clusters (3 to 4).

Table 2. Statistics of parameters and yield in the four clusters: number of cases (N), mean values (Mean) and standard deviation (SD). Clusters were generated by means of a cluster analysis, using estimated LAI, ALA, ALFA and C_{ab} parameters from model inversion.

Parameter	Cluster	N	Mean	SD
Chlorophyll $a+b$ (C_{ab}) ($\mu\text{g cm}^{-2}$)	1	167	48.93	5.23
	2	1135	58.49	2.25
	3	4177	60.12	1.43
	4	3120	64.69	1.42
Leaf area index (LAI)	1	167	0.64	0.23
	2	1135	1.60	0.58
	3	4177	3.65	0.98
	4	3120	4.12	0.87
Average leaf angle (ALA) ($^{\circ}$)	1	167	45.43	4.18
	2	1135	60.69	4.30
	3	4177	68.39	1.23
	4	3120	69.15	0.53
Soil factor ALFA	1	167	1.26	0.02
	2	1135	1.20	0.05
	3	4177	1.00	0.13
	4	3120	0.98	0.12
Measured yield (dt ha^{-1})	1	167	42.54	9.69
	2	1135	53.54	8.74
	3	4177	65.33	9.83
	4	3120	68.38	9.49

Table 3. Statistics of NDVI and yield in four classes, based on NDVI quartiles: number of cases (N), mean values (mean) and standard deviation (SD).

Class	N	Mean NDVI (SD)	Mean yield (SD)
1	2195	0.64 (0.08)	54.92 (9.76)
2	2226	0.78 (0.03)	63.66 (9.27)
3	2229	0.86 (0.02)	68.34 (8.88)
4	1949	0.92 (0.02)	71.6 (8.56)

In the last step, the results were compared with the NDVI map to evaluate the contribution of hyperspectral data for vegetation monitoring, in particular with regard to the aim of the present study, the drought risk zones assessment within a field. The classification of the NDVI into four parts (quartiles) revealed a similar result to the cluster establishment. Table 3 presents the resulting statistics (means and standard deviation) of yield and NDVI, indicating comparable behaviour of the yield distribution as in the clusters: from the first to the fourth class, there is an increasing trend of the values from both parameters (NDVI from 0.64 to 0.92 and yield from 54.9 to 71.6 dt ha⁻¹). In addition, the structure of the NDVI map (figure 9(b)) depicts a similar pattern to the cluster map.

4. Conclusions

Due to the typical soil conditions in the Marchfeld region (sandy streams from former river meanders), the soil can be seen as one of the most important factors inducing potential drought risk, with a decrease in plant growth and loss in crop yield (especially for non-irrigated conditions). An understanding of the current spatial distribution of the sandy streams can be useful for establishing differential field management strategies (Taylor *et al.* 2003, Vrindts *et al.* 2005), enabling farmers to effectively control each zone and adjust the application rate of irrigation and fertilization input, and consequently improve crop production efficiency.

In this study the monitoring of plant growth at the field scale has been used as an indicator of the sandy stream location. Thus, the heterogeneous plant growth due to different soil compositions has been characterized by means of a physical-based approach for canopy parameter estimation from EO data.

The experiment was carried out within a wheat crop field by using airborne data acquired from the hyperspectral and high spatial resolution HyMap sensor. At the time of airplane overpass, most of the soil was covered with plants (wheat crop in the anthesis stage). The data acquisition within the vegetation period may complicate the image analysis because of interference of soil and plant information on the spectral signal. Nevertheless, in this time period the presence of the sandy soil streams is assumed to be more visible than in winter, when crops are absent from the fields, for the following reason: every year, before seeding, the fields are ploughed evenly to a depth of approximately 30 cm, so that the influence of the sandy soil vanishes, at least on the surface.

As an indication of plant state variability, the canopy parameters LAI, ALA, ALFA and C_{ab} were estimated by model inversion and analysed by means of multiple cluster analysis. The study demonstrated that the estimated canopy parameters correlated moderately with yield measurements. They can be used to group the yields into zones ranging from lower to higher values within a field. Thus, it was possible to cluster the parameters in zones with different 'potential drought

levels'. The method could be applied to the prediction of potential drought risk areas within fields on a medium-term time-scale. Considering the amount of error and sources of uncertainty covering the measurements, radiometric calibration, modelling, inversion technique and limitations of the statistic method, the results can be considered as an acceptable compromise.

Nevertheless, this work also aimed at demonstrating processing and modelling techniques, to assess the strengths and limitations of vegetation parameter estimation from EO data, in particular from high spectral resolution sensors, such as HyMap. However, nowadays only data from multispectral broadband and high spatial resolution imagery from space (such as IKONOS, Quickbird or SPOT) are available for studies on a small scale. They represent the only cost-effective way to operatively gather information on the Earth's surface status even within the small scale of single fields. Therefore, the use of a simple empirical method, that is one based on a vegetation index and on a few spectral bands, has been considered here as an alternative approach to model inversion in an operational context for drought risk zone assessment. To this end, the NDVI was calculated and grouped into the same number of clusters. The results revealed no significant difference in the performance of the two approaches.

However, high spectral resolution imagery, like that from a HyMap sensor, may provide the potential to estimate biophysical parameters, such as chlorophyll or soil water content, in a more accurate way as broadband imagery, either by means of model inversion or by using the new generation of narrow band vegetation indices.

In conclusion, it should be emphasized that this study was based on only one wheat field that served as calibration and validation data set. Although there were other factors influencing yield performance, such as local weather conditions (especially after the image acquisition), they could not be taken into consideration. Thus, in further studies the method should be validated and tested with other fields (e.g. in the Marchfeld region), taking into account all aspects influencing plant growth. There might also be variability in yield patterns within several years, as it is even higher in non-irrigated areas. Therefore, to classify the field into zones reflecting stable behaviour, the method should be tested using image acquisition and yield in consecutive years. Furthermore, direct validation data sets are required to test the applied methods comprising *in situ* chlorophyll and LAI measurements as well as a repetition of the soil experiment by collecting different soil probes.

Acknowledgements

This research study received financial support from the Fonds zur Förderung der wissenschaftlichen Forschung (FWF, Austria; grant no. P17647-N04). We thank the DROSMON team for acquiring field data and performing the geometric correction of the HyMap data.

References

- ASHRAF, M.Y., AZMI, A.R., KHAN, A.H. and ALA, S.A., 1994, Effect of water stress on total phenols, peroxidase activity and chlorophyll content in wheat (*Triticum aestivum* L.). *Acta Physiologiae Plantarum*, **16**, pp. 185–191.
- ASHRAF, M. and IRAM, A., 2005, Drought stress induced changes in some organic substances in nodules and other plant parts of two potential legumes differing in salt tolerance. *Flora – Morphology, Distribution, Functional Ecology of Plants*, **200**, pp. 535–546.
- ATZBERGER, C., 2004, Object-based retrieval of biophysical canopy variables using neural nets and radiative transfer models. *Remote Sensing of Environment*, **93**, pp. 53–67.

- ATZBERGER, C., JARMER, T., SCHLERF, M., KÖTZ, B. and WERNER, W., 2003, Retrieval of wheat bio-physical attributes from hyperspectral data and SAILH+PROSPECT radiative transfer model. In *The Third EARSeL Workshop on Imaging Spectroscopy*, 13–16 May 2003, Herrsching, Germany, M. Habermeyer, A. Müller and S. Holzwarth (Eds), pp. 473–482.
- BACOUR, C., JACQUEMOUD, S., LEROY, M., HAUTECOEUR, O., WEISS, M., PRÉVOT, L., BRUGUEIR, N. and CHAUKI, H., 2002, Reliability of the estimation of vegetation characteristics by inversion of three canopy reflectance models on airborne POLDER data. *Agronomie*, **22**, pp. 555–565.
- BARET, F. and FOURTY, T., 1997, Estimation of leaf water content and specific leaf weight from reflectance and transmittance measurements. *Agronomie*, **17**, pp. 455–464.
- BARET, F. and GUYOT, G., 1991, Potentials and limits of vegetation indices for LAI and APAR assessment. *Remote Sensing of Environment*, **35**, pp. 161–173.
- BOWERS, S.A. and HANKS, R.J., 1965, Reflection of radiant energy from soils. *Soil Science*, **100**, pp. 130–138.
- CASA, R., 2003, Multiangular remote sensing of crop canopy structure for plant stress monitoring. PhD thesis, University of Dundee.
- CASA, R. and JONES, G.H., 2005, LAI retrieval from multiangular image classification and inversion of a ray tracing model. *Remote Sensing of Environment*, **98**, pp. 414–428.
- COMBAL, B., BARET, F., WEISS, M., TRUBUIL, A., MACÉ, D., PRAGNÈRE, A., MYNENIC, R., KNYAZIKHINC, Y. and WANG, L., 2002, Retrieval of canopy biophysical variables from bidirectional reflectance using prior information to solve the ill-posed inverse problem. *Remote Sensing of Environment*, **84**, pp. 1–15.
- CONEL, J.E., GREEN, R.O., VANE, G., BRUEGGE, C.J., ALLEY, R.E. and CURTISS, B.J., 1987, Airborne imaging spectrometer-2: radiometric spectral characteristics and comparison of ways to compensate for the atmosphere. *Proceedings of SPIE*, **834**, pp. 140–157.
- CURRAN, P.J. and WILLIAMSON, H.D., 1986, Sample size for ground and remotely sensed data. *Remote Sensing of Environment*, **20**, pp. 31–41.
- DALAL, H., 1986, Simultaneous determination of moisture, organic carbon, and total nitrogen by infrared reflectance spectrometry. *Soil Science Society of America*, **50**, pp. 120–123.
- HABOUDANE, D., MILLER, J.R., PATTEY, E., ZARCO-TEJADA, P.J. and STRACHAN, I.B., 2004, Hyperspectral vegetation indices and novel algorithms for predicting green LAI of crop canopies: modeling and validation in the context of precision agriculture. *Remote Sensing of Environment*, **90**, pp. 337–352.
- HUETE, A.R., 1987, Soil and sun angle interactions on partial canopy spectra. *International Journal of Remote Sensing*, **8**, pp. 1307–1317.
- JACQUEMOUD, S., BACOUR, C., POILVE, H. and FRANGI, J.P., 2000, Comparison of four radiative transfer models to simulate plant canopies reflectance: direct and inverse mode. *Remote Sensing of Environment*, **74**, pp. 417–481.
- JACQUEMOUD, S. and BARET, F., 1990, A model of leaf optical properties spectra. *Remote Sensing of Environment*, **34**, pp. 75–91.
- KIMES, D.S., KNYAZIKHIN, Y., PRIVETTE, J.L., ABUEL GASIM, A.A. and GAO, F., 2000, Inversion methods for physically-based models. *Remote Sensing of Environment*, **18**, pp. 381–439.
- KUUSK, A., 1985, The hot spot effect on a uniform vegetative cover. *Soviet Journal of Remote Sensing*, **3**, pp. 645–658.
- LEILAH, A.A. and AL-KHATEEB, S.A., 2005, Statistical analysis of wheat yield under drought conditions. *Journal of Arid Environments*, **61**, pp. 483–496.
- LEONE, A.P. and SOMMER, S., 2000, Multivariate analysis of laboratory spectra for the assessment of soil development and soil degradation in the Southern Apennines. *Remote Sensing of Environment*, **72**, pp. 346–359.

- MYNENI, R.B., MAGGION, S., IAQUINTO, J., PRIVETTE, J.L., GOBRON, N. and PINTY, B., 1995, Optical remote-sensing of vegetation – modeling, caveats and algorithms. *Remote Sensing of Environment*, **51**, pp. 169–188.
- NEEMA, D.L., SHAH, A. and PATEL, A.N., 1987, A statistical optical model for light reflection and penetration through sand. *International Journal of Remote Sensing*, **8**, pp. 1209–1217.
- QUESNEY, A., LE HEGARAT-MASCLE, S., TACONET, O., VIDAL-MADJAR, D., WIGNERON, J.P., LOUMAGNE, C. and NORMAND, M., 2000, Estimation of watershed soil moisture index from ERS/SAR data. *Remote Sensing of Environment*, **72**, pp. 290–303.
- REYNIERS, M., 2003, Precision farming techniques to support grain crop production. PhD thesis, Faculty of Applied BioSciences, Katholieke Universiteit Leuven, Belgium.
- ROBERTS, D.A., YAMAGUCHI, Y. and LYON, R.J.P., 1985, Calibration of airborne imaging spectrometer data to percent reflectance using field spectral measurements. In *Proceedings of the 19th International Symposium on Remote Sensing of Environment*, 21–25 October 1985, Ann Arbor, MI, USA, pp. 295–298.
- ROSNEY, P., CALVET, J., KERR, Y., WIGNERON, J., LEMAÎTRE, F., ESCORIHUELA, M., SABATER, J., SALEH, K., BARRIÉ, J., BOUHOURS, G., CORET, L., CHEREL, G., DEDIEU, G., DURBE, R., FRITZ, N.E.-D., FROISSARD, F., HOEDJES, J., KRUSZEWSKI, A., LAVENU, F., SUQUIA, D. and WALDTEUFEL, P., 2006, SMOSREX: a long term field campaign experiment for soil moisture and land surface processes remote sensing. *Remote Sensing of Environment*, **102**, pp. 377–389.
- ROSS, J., 1981, *The Radiation Regime and Architecture of Plant Stands* (The Hague: W. Junk).
- SARKER, A.M., RAHMAN, M.S. and PAUL, N.K., 1999, Effect of soil moisture on relative leaf water content, chlorophyll, proline and sugar accumulation in wheat. *Journal of Agronomy and Crop Science*, **183**, pp. 225–229.
- SCHNEIDER, W., EITZINGER, J., HAUMANN, J., HUBER, K., KAISER, G., LINKE, R., POSTL, W. and WEIHS, P., 2005, Crop drought stress monitoring by remote sensing. *Geophysical Research Abstracts*, **7**, pp. 04665. Available online at: <http://www.cosis.net/abstracts/EGUOS/04665/EGUOS-J-04665.pdf> (accessed 21 April 2008).
- SMITH, G. and MILTON, E., 1999, The use of the empirical line method to calibrate remotely sensed data to reflectance. *International Journal of Remote Sensing*, **20**, pp. 2653–2662.
- STONER, E.R. and BAUMGARDNER, M.F., 1980, *Physiochemical, Site and Bidirectional Reflectance Factor Characteristics of Uniformly Moist Soils*, Technical Report 111679 (West Lafayette, IN: LARS/Purdue University).
- TAYLOR, J.C., WOOD, G.A., EARL, R. and GODWIN, R.J., 2003, Soil factors and their influence on within-field crop variability. Part II: Spatial analysis and determination of management zones. *Biosystems Engineering*, **84**, pp. 441–453.
- THENKABAIL, P.S., ENCLONA, E.A., ASHTON, M.S. and VAN DER MEER, B., 2004, Accuracy assessments of hyperspectral waveband performance for vegetation analysis applications. *Remote Sensing of Environment*, **91**, pp. 354–376.
- THENKABAIL, P.S., SMITH, R.B. and DE PAUW, E., 2002, Hyperspectral vegetation indices and their relationships with agricultural crop characteristics. *Remote Sensing of Environment*, **71**, pp. 158–182.
- VERHOEF, W., 1984, Light scattering by leaf layers with application to canopy reflectance modeling: the SAIL model. *Remote Sensing of Environment*, **16**, pp. 125–141.
- VERHOEF, W. and BACH, H., 2003, Simulation of hyperspectral and directional radiance images using coupled biophysical and atmospheric radiative transfer models. *Remote Sensing of Environment*, **87**, pp. 23–41.
- VRINDTS, E., MOUAZEN, A.M., REYNIERS, M., MAERTENS, K., MALEKI, M.R., RAMON, H. and DE BAERDEMAEKER, J., 2005, Management zones based on correlation between soil compaction, yield and crop data. *Biosystems Engineering*, **92**, pp. 419–428.
- VUOLO, F., DINI, L. and D'URSO, G., 2005, Assessment of LAI retrieval accuracy by inverting a RT model and a simple empirical model with multiangular and hyperspectral CHRIS/Proba data from SPARC. In *Proceedings of the Third ESA CHIRS/Proba*

- Workshop*, 21–23 March, M. Barnsley (Ed.) (Frascati, Italy: ESRIN), pp. 21–23. Available online at: http://earth.esa.int/workshops/chros_proba_OS/papers/16_vuolo.pdf (accessed 21 April 2008)
- WATSON, D.J., 1947, Comparative physiological studies in the growth of field crops. I. Variation in net assimilation rate and leaf area between species and varieties, and within and between years. *Annals of Botany*, **11**, pp. 41–76.
- WEIDONG, L., BARET, F., XINGFA, G., QINGXI, T., LANFEN, T. and BING, Z., 2002, Relating soil surface moisture to reflectance. *Remote Sensing of Environment*, **81**, pp. 238–246.
- WEISS, M., BARET, F., MYNENI, R.B., PRAGNÈRE, A. and KNYAZIKHIN, Y., 2000, Investigation of a model inversion technique to estimate canopy biophysical variables from spectral and directional reflectance data. *Agronomie*, **20**, pp. 3–22.
- WEISS, M., BARET, F., SMITH, G.J., JONCKHEERE, I. and COPPIN, P., 2004, Review of methods for in situ leaf area index (LAI) determination. Part II. Estimation of LAI, errors and sampling. *Agricultural and Forest Meteorology*, **121**, pp. 37–53.
- WIGNERON, J.P., CHANZY, A., CALVET, J.C., OLIOSO, A. and KERR, Y., 2002, Modeling approaches to assimilating L band passive microwave observations over land surfaces. *Journal of Geophysical Research*, **107**, pp. 4219.

4.4 Publikation IV

Validation of forward and inverse modes of a homogeneous canopy reflectance model

Philipp Weihs, Franz Suppan, Katja Richter, Richard Petritsch, Hubert Hasenauer, and Werner Schneider

International Journal of Remote Sensing 29 (5): 1317 – 1338, 2008.

Validation of forward and inverse modes of a homogeneous canopy reflectance model

P. WEIHS*†, F. SUPPAN‡, K. RICHTER†, R. PETRITSCH§, H. HASENAUER§
and W. SCHNEIDER‡

†Institute for Meteorology, Department of Water, Atmosphere and Environment,
University of Applied Life Sciences and Natural Resources (BOKU), Peter Jordan
Strasse 82, Vienna A-1190, Austria

‡Institute of Surveying, Remote Sensing and Land Information, Department of
Landscape, Spatial and Infrastructure Sciences, University of Applied Life Sciences and
Natural Resources (BOKU), Peter Jordan Strasse 82, Vienna A-1190, Austria

§Institute for Forest Growth Research, Department of Forest and Soil Sciences,
University of Applied Life Sciences and Natural Resources (BOKU), Peter Jordan
Strasse 82, Vienna A-1190, Austria

The homogeneous canopy reflectance model ACRM was used to simulate forest reflectance and was compared with hyperspectral data of the topographically complex experimental forest Rosalia of the University of Applied Life Sciences and Natural Resources (BOKU) in Austria. Forward and inverse modes of the ACRM model were validated. Ground truth data were taken (1) from experiments performed at 17 pure beech plots and (2) from model simulations performed for 21 pure beech plots using an ecosystem model. The validations were performed separately for these two types of reference data. The ground reflectance obtained from the HyMap data was compared with simulations performed with ACRM. In addition to the correction of the data to remove the atmospheric effects, corrections had to be applied to remove the effects of the complex topography of the area of Rosalia. The simulated reflectance showed an offset to the HyMap retrieved reflectance between +4% and +6% in the visible (extending from 400 nm to 700 nm), +28% to +30% in the near infrared (NIR) (extending from 700 nm to 1400 nm) +53% to +77% in the middle-infrared (MIR) (extending from 1400 nm to 3000 nm) using the modelled and the experimental ground truth, respectively. The correlation coefficient varied between 0.35 and 0.45 in the visible, 0.6 and 0.76 in the NIR and between 0.37 and 0.64 in the MIR. This correlation may be improved, if within canopy fluctuations of chlorophyll and water content were available. The leaf area index (LAI) was retrieved using the ACRM model. The estimated LAI was in good agreement with the LAI ground measurements and systematically higher by 0.1 compared to the simulated LAI. The correlation was 0.49 and 0.82, respectively. Altogether, the ACRM model showed a large offset to the HyMap retrieved reflectance in the NIR and MIR wavelength ranges. A precision around 33% to 74% may be expected after correction of the offset. The LAI may be determined with a precision between 0.32 and 0.5. The ACRM model is a useful tool to predict LAI. Care should be taken for the forward modelling of forest canopy reflectance.

*Corresponding author. Email: weihs@mail.boku.ac.at

1. Introduction

Interpretation of satellite remote sensing data requires appropriate reflectance models to interpret observed features in terms of ground reflectance. Forest reflectance models (FRMs) have been developed to improve the interpretation of airborne and satellite measurements of wooded areas. The inversion of these models is used to obtain—with reasonable accuracy—leaf area index (LAI) (e.g. Weiss and Baret 1999, Chen *et al.* 2002, Myneni *et al.* 2002, Eklundh *et al.* 2003, Meroni *et al.* 2004, Rautiainen 2005b, Soudani *et al.* 2006) and other structural canopy variables (Peddle *et al.* 2004, Rautiainen *et al.* 2004, Schlerf and Atzberger 2006), soil reflectance (Kimes *et al.* 2002) and other biochemical parameters (Demarez and Gastellu-Etchegorry 2000, Zarco Tejada *et al.* 2004). A good overview of investigations performed is given by Schlerf *et al.* (2005). Most of the inversions were performed using vegetation indices and bivariate regression analyses. The correlation coefficient between ground truth and retrieved LAI lies between 0.3 and 0.94.

Forest reflectance models are usually subdivided into 3-dimensional Monte Carlo ray tracing models (e.g. Govaerts and Verstraete 1998) and hybrid models (e.g. Li *et al.* 1995) or in 1-dimensional (for most of the canopies applicable) turbid medium reflectance models (Verhoef 1984) and radiosity reflectance models (e.g. Qin and Gerstl 2000). These models were intercompared within the radiation transfer model intercomparison exercise (RAMI) intercomparison exercise (Pinty *et al.* 2001, 2004). The model intercomparisons confirmed a good agreement between the models for simple radiation transfer problems, but showed significant discrepancies for more complex problems.

With regard to validation using ground truth data, more investigations have been performed on the validation of inversion procedures than on the validation of forward model calculations. The validation of forward calculations was addressed by Kuusk and Nilson (2001) who not only found a systematic overestimation of the NIR and MIR reflectance by the model in conifer stands but also a considerable overestimation of the MIR reflectance for deciduous trees.

The new techniques of hyperspectral instruments have opened new possibilities, such as the validation of forest reflectance models over the whole spectrum with high spectral resolution. Investigations into the potential of hyperspectral data have been performed (e.g. Schlerf *et al.* 2005, Schlerf and Atzberger 2006). Schlerf and Atzberger (2006) used hyperspectral data to estimate LAI, crown coverage and stem density of Norway spruce by model inversion and vegetation indices. The obtained accuracy of the LAI map amounted to a root mean square error (rmse) of 0.59 with an R^2 equal to 0.73 using a forest reflectance model. A slightly better accuracy (rmse equal to 0.52–0.54 and R^2 equal to 0.77–0.79) was obtained using some vegetation indices also for Norway spruce. In addition, model input parameters influence the accuracy of calculations (Eriksson *et al.* 2006) and also of the inversion performance. Eriksson *et al.* (2006) showed the importance of understory vegetation on canopy reflectance. Variations in understory vegetation could lead to changes in retrieved LAI of up to 1.6 units.

According to the statements made above, there is still a need for validation and improvement of reflectance models using hyperspectral data, and still a need for validation of forward and inverse modes of forest reflectance models.

The purpose of the study is to evaluate how well a homogeneous canopy reflectance can model the reflectance of a forest area. This will be tested, first in forward mode and secondly in inverse mode, by using hyperspectral data (HyMap).

Three-dimensional models are physically more accurate, but they usually lack information concerning the exact 3-dimensional structures within the forest canopy. Homogeneous 1-dimensional models have an advantage, compared to 3-dimensional models, in user friendliness and in ease of determination of the model input parameters. Because of the shortage of ground truth data we chose the second type of models and used the directional multispectral homogeneous (turbid medium) model ACRM (Kuusk 2001).

2. Study area

The experimental forest of BOKU is situated 70 km south of Vienna in the Rosalia Mountains. The forest covers 1000 ha and is situated at elevations between 400 m and 900 m. The forest consists mainly of Norway spruce (*Picea abies*), common beech (*Fagus silvatica*), but also includes silver fir (*Abies alba*) and some Scots pine (*Pinus silvestris*). Forest inventory is routinely performed, based on systematic sampling with permanent plots. In addition, more extensive measurements are performed at several research plots. Since it is well known that modelling of coniferous tree reflectance has not been solved in a satisfying way until now (Rautiainen 2005a, Kuusk and Nilson 2001), we only concentrate on pure beech stands, which are the most common deciduous tree type at the experimental forest Rosalia. Figure 1 shows an example of the large difference between beech and spruce reflectances derived from HyMap measurements. This difference is still not explained by model simulations at the moment.

The limitation of our study to one tree type restricts the number of factors that may influence the canopy reflectance and therefore simplifies our analysis. Two types of 'ground truth' data were used within the scope of this investigation: (1) At 17 locations, LAI was determined by analysing hemispherical photographs. (2) At 21 other locations, LAI was obtained from an ecosystem model (see §3.2 and §3.3).

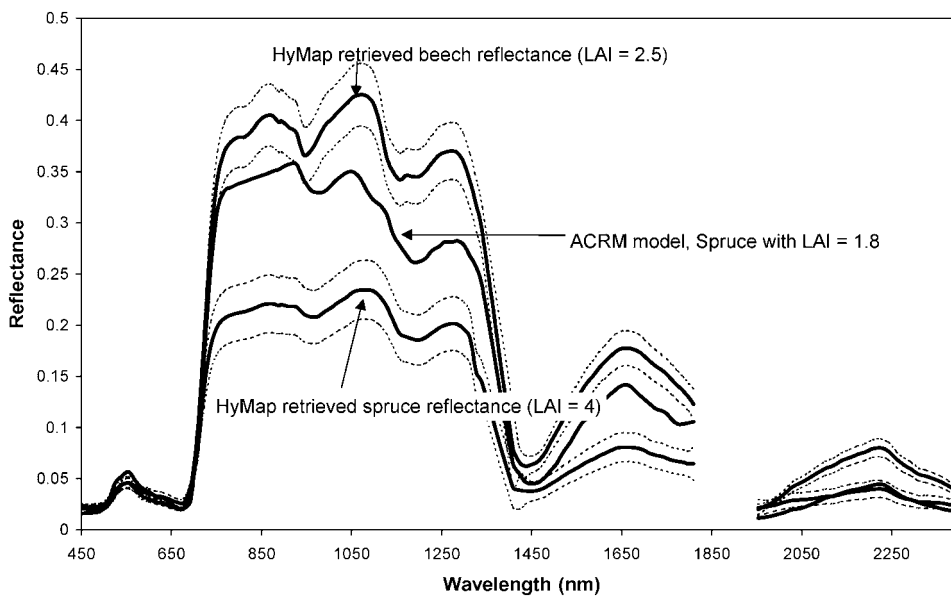


Figure 1. Comparison of HyMap measurements of pure beech stands and of pure spruce stands with an ACRM reflectance simulation for spruce.

The slope and aspect of the different plots were determined from a digital elevation model. Within one stand, inclination and orientation may vary respectively up to 17° and 56° due to the very complex topography. The average slope of the different plots ranges between 12° and 28°. More detailed information about the study site and the overflight is given in table 1.

3. Methodology

Following our aim, the validation of the ACRM model consisted of two steps: in a first step the forward mode of this model was compared to hyperspectral (HyMap) reflectance data taken during an overflight of Rosalia experimental forest. In a second step we tested the inversion procedure on LAI.

Before this comparison, HyMap data were first calibrated and then corrected for the atmospheric influence (see §3.3.2). For the determination of model input parameters, the observations in the field were used and some additional measurements were performed (see §3.4.).

3.1 Description of reflectance model ACRM

The model ACRM is a directional multispectral homogeneous (turbid medium) two layer canopy reflectance model. The input parameters include leaf area index (LAI), leaf angle inclination, leaf size, biochemical parameters of the leaves, and soil reflectance. The model performs the calculations in the wavelength range 400–2400 nm with a 1 nm resolution. The view angle and directional reflectance effects are taken into account. It works for any view and sun direction in forward and inverse modes. The values retrieved in inverse mode are obtained using a merit function, having its minimum value when the difference between measured and simulated data is minimized. The minimum value of the merit function is obtained in an optimization procedure (Kuusk 1991).

The canopy is divided into two horizontal layers. For each layer, the above mentioned parameters (LAI, leaf inclination, leaf size, biochemical parameters of the leaves) have to be defined. The lower layer is mainly used to define the understory vegetation parameters. The model consists of several sub-models, which can also be run independently. One sub-model includes parameters concerning the chemical properties of the leaves. It provides input parameters to the sub model PROSPECT (Jacquemoud and Baret 1990), which uses this information to simulate the reflectance of a single leaf.

Table 1. Overview of the study site.

Elevation of Rosalia Mountains	400–900 m above sea level
Flight altitude	1910 m above ground
Start latitude and longitude of flight	47.675° N; 16.3° E
End latitude and longitude of flight	47.833° N; 16.23° E
FOV HyMap	61.3°
Range of view angles for the studied plots	0.36–0.59° (3 × 3 pixels to 5 × 5 pixels)
Size of a pixel	Approx. 4 × 4 m
Forest stand types	Pure beech
Crown closure	50–100%
Tree density	150–2000 trees ha ⁻¹
Tree height	3–30 m
Stand age	10–155 years

The spectral reflectance of the soil is described using the four soil parameters of the Price function (Walthall *et al.* 1985, Price 1990). The Price function was, however, only used for the validation of the inverse mode. For the forward calculations (§4.1) the measured soil reflectance was used instead.

3.2 Description of the ecosystem model

The ecosystem model (EM) is based on the Biome-BGC 4.1.1 model (Thornton *et al.* 2002), which was originally developed by the Numerical Terradynamic Simulation Group (NTSG) at the University of Montana. New developments at BOKU include the consideration of ground water (Pietsch *et al.* 2003), the species-specific parametrization of current tree types of Austria (Pietsch *et al.* 2005) as well as an improvement in the self initialization of the model (Pietsch and Hasenauer 2006). The EM uses a daily time step and performs a simulation of fluxes and storage of energy, water, carbon and nitrogen for the vegetation and soil components of terrestrial ecosystems. The primary model purpose is to study global and regional interactions between climate, disturbance, and biogeochemical cycles. Input parameters include latitude, elevation and albedo of the location, uptake of nitrogen by the soil, soil structure, as well as daily climate data such as maximum and minimum temperature, precipitation, solar irradiance and humidity. The estimated carbon assimilation is distributed into the various compartments of the ecosystem. The mass of leaves is converted into LAI by means of the specific leaf area. LAI is then used for the determination of the photosynthesis, which in turn can be used to determine the carbon uptake. For the present investigation, only the LAI output from the ecosystem model was used.

3.3 Field measurements

3.3.1 Instrumentation. *Fieldspec spectrometer.* Spectro-radiometric measurements in the field were carried out with the FieldSpec Pro FR spectro-radiometer (Analytical Spectral Devices 2002, Boulder CO 80301, USA). This instrument performs measurements from 350 to 2500 nm at wavelength intervals varying between 1,4 nm (visible and near infrared) and 2 nm (mid infrared). The spectral resolution (full width at half maximum) is 3 nm in the visible and near infrared and up to 12 nm in the mid infrared. Reflectance measurements are performed at constant irradiation by first measuring the radiance from a spectralon panel with known reflectance (near 100%) and afterwards from the target. The reflectance factor of the target is then obtained as the ratio of the two measurements at the target and at the spectralon, multiplied by the spectralon reflectance (the reflectance factor will be called 'reflectance' throughout the whole present manuscript). The measurements were performed with a so-called contact probe device, which includes an irradiating lamp. The contact probe is directly placed on the target (e.g. leaf, bark, soil) and allows for reflectance measurements at low levels of natural irradiation and without disturbances from changes in natural irradiation.

Hemispherical photographs. Several studies (Ross 1981, Jonckheere *et al.* 2004, Weiss *et al.* 2004, Leblanc and Fournier 2005) were carried out comparing different LAI measurement techniques. The most accurate method of LAI determination would be the direct measurement on harvested plants. To overcome the limitations of this technique (labour requirement, destructive character, etc.) numerous indirect LAI measurement methods have been developed, based on the estimation of the

contact frequency or the gap fraction (Ross 1981, Weiss *et al.* 2004). LAI determination by hemispherical photographs (e.g. the CAN EYE method (Jonckheere *et al.* 2004, Weiss *et al.* 2004)) seems to perform with a good accuracy and may belong to the most precise methods (Weiss *et al.* 2004). According to Baret and Weiss (http://www.avignon.inra.fr/can_eye/CAN_EYE4.pps), discrepancies between the different LAI determination techniques of up to 1 may occur. The method CAN EYE was used within the scope of the present investigation.

3.3.2 Airborne data. On 21 June 2005, 10:53 UTC, HyMap hyperspectral data of the Rosalia area were acquired. The HyMap sensor was operated aboard a Do 228 aircraft of DLR within the HyMap Europe 2005 campaign. The HyMap sensor collects radiation in 128 spectral bands that cover the wavelength range from 400 nm to 2500 nm. The bandwidth is approximately 15 nm. The mean flight altitude of the aircraft was 1910 m above ground level, which results in a mean pixel size of 4 m. The flight direction was 343° (almost northern direction). The azimuth angle of the sun was 178° , the zenith angle of the sun was 24° . No hot spot effects may occur in this configuration.

3.3.3 Measurements of spectral reflectance for calibration. *Calibration of HyMap data.* Reflectance measurements at 7 reference points in the HyMap scene were taken with the Fieldspec spectroradiometer and the contact probe device. The reference points were selected observing two criteria: a wide range of reflectance values, and isotropic reflectance characteristics. The software 6S (Vermote *et al.* 1997) was used to perform the atmospheric correction. Aerosol optical thickness and water vapour concentration situated in the layer between the airborne platform and the ground was obtained in an iterative way until the best fit between HyMap-retrieved ground reflectance and measured ground reflectance was obtained at the seven reference points. The values that were obtained for water vapour concentration was 1.55 g cm^{-2} and the value for the aerosol optical depth at 550 nm was 0.01. For ozone, column ozone measurements of the next ground station Sonnblick (47.05° N , 12.95° E) were used. The measured ozone concentration was 300 Dobson units on this day. For the remaining atmospheric parameters (vertical temperature and pressure profile) the 6S software automatically selects the values from the US standard atmosphere 1962. The reflectance obtained from the HyMap measurements and shown in the following sections is the reflected radiance after atmospheric correction multiplied by PI and divided by the global irradiance calculated by the 6S software.

Beside the determination of atmospheric turbidity and water vapour concentration, a recalibration function was applied to the data following the procedure of Guanter *et al.* (2004) in order to remove spectral artefacts.

The calibration was cross-checked using the same seven reference points and a second independent calibration method: the empirical line method (Roberts *et al.* 1985, Conel *et al.* 1987). An agreement within 5% of the resulting reflectance obtained by both methods was achieved.

When comparing the atmospherically corrected Hymap data to the modelled reflectance data, slope and aspect of the plots have to be taken into account. We therefore either referred both to horizontal plots or to inclined plots. In order to take into account the inclination of the plots and the fact that the trees are in upright position, the Sun-canopy-sensor (SCS)-correction, suggested by Gu and Gillespie (1998) was applied to the data:

Table 2. Overview of parameters for which best fit with PROSPECT is obtained. These parameters were also used for all the model calculations.

SLW (specific leaf weight)	100 g m ⁻²
<i>N</i> effective number of cell layers	1.68
Water concentration	59 g m ⁻²
Chlorophyll	94 μg cm ⁻²
Dry matter	20 g m ⁻²
Brown pigment	0.2 g m ⁻²

$$L_n = L_0 (\cos(\alpha) \cos(\theta_s)) / \cos(i) \quad (1)$$

L_0 is the radiance arriving at the sensor from pixels on the sloped terrain; L_n is the radiance arriving at the sensor corrected so that it is comparable to radiance reflected from horizontal pixels. α is the slope of the terrain surface, θ_s is the sun zenith angle, i is the sun incidence angle measured from the surface normal.

Some more sophisticated correction procedures based on the SCS method are available (Koukal *et al.* 2005, Soenen and Peddle 2005), which take into account the diffuse irradiance component. Since the slope of the plots is below 30° and the wavelengths of interest are higher than 500 nm, we expect (according to our simulations) the difference between the correction factors of the different procedures to be lower than 1%.

3.4 Determination of model input parameters

Tables 2 and 3 show an overview of the measurements and of the assumptions regarding the model input parameters for the 38 plots.

3.4.1 Determination of leaf model input parameters. The reflectance from 350 nm to 2500 nm of the reflectance of several types of understory vegetation was measured using the ASD FieldSpec spectrometer contact probe (figure 2(a) and (b)). Five samples of each type of plant were measured. The reflectance of grass is with 60% in the near infrared (NIR), around 20% higher than the reflectance of fern, moss, clover and various other types of vegetation. These reflectance spectra were used in the following simulations to determine an average ground reflectance. The reflectance of beech leaves was measured on 11 samples with the spectrometer contact probe. We then compared the measured reflectance values with PROSPECT

Table 3. Model input parameters describing the canopy used for the forward calculations. Average values of leaf inclination, relative leaf size and Markov parameter were assumed according to the observations on-site. LAI was determined using hemispherical photography (CAN-EYE method) and using ecological modelling (EM).

Thm Leaf inclination	0°
Sl, relative leaf size	0.02
Markov parameter	1
LAI determined for each stand separately	
with CAN-EYE method	1.5–3.4
with EM	1.58–2.34

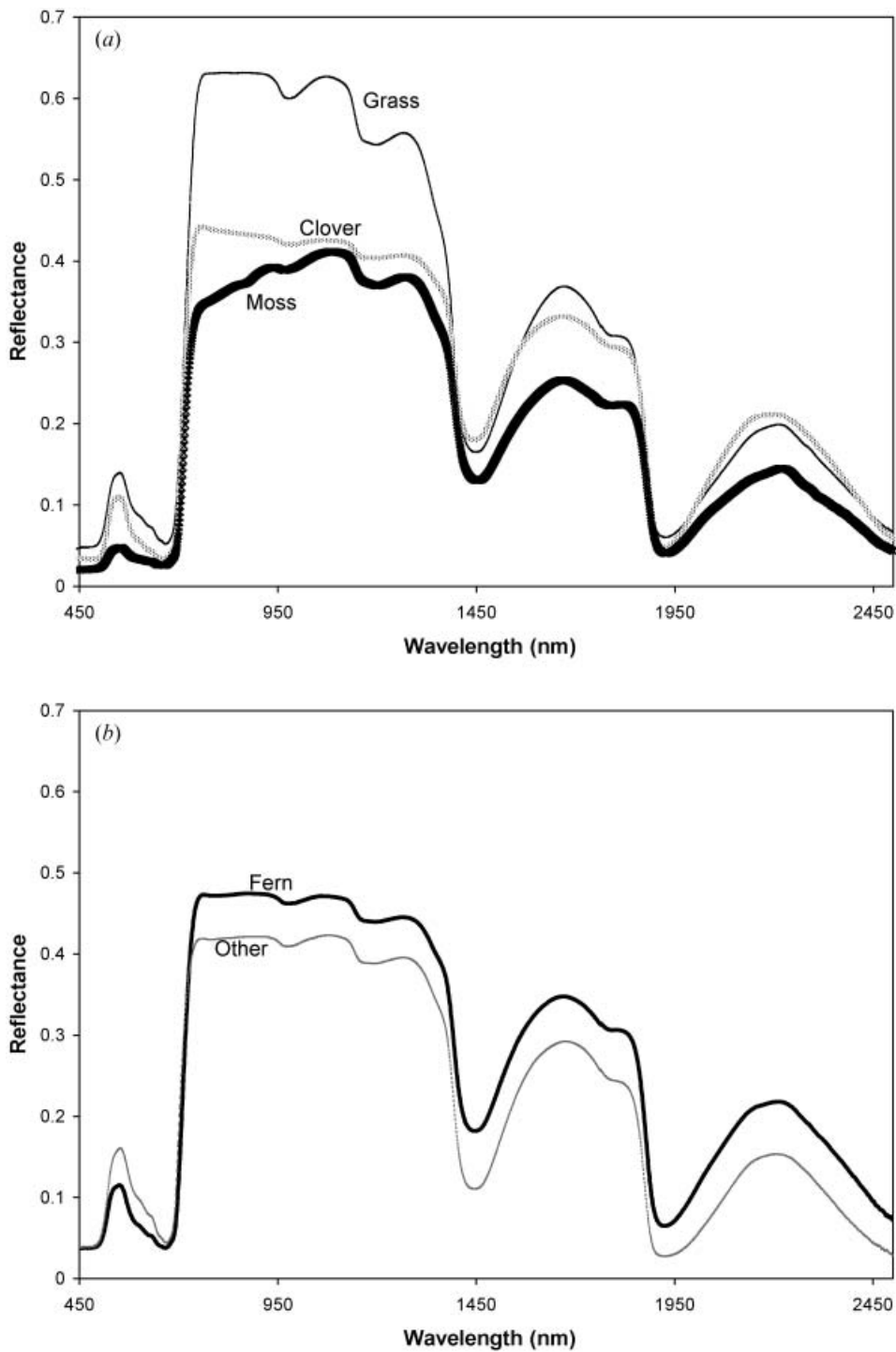


Figure 2. Measured reflectance of different types of understory vegetation (moss, clover, grass (a) and fern and various other types (b)) measured in the field with the contact probe (artificial irradiation).

model simulations (figure 3). The driving parameter, which mostly influences the leaf reflectance, is the parameter N which is an indicator of the compactness of the leaf. The best fit was obtained for N equal to 1.68. The values of all input parameters for which the best fits were obtained are shown in table 2. For the simulations shown in the next sections we used the measured leaf reflectance and we calculated the transmittance using the parameter values resulting in the best fit. The same leaf biochemical parameter values were used for all sites.

3.4.2 Determination of canopy model input parameters. The LAI was estimated using two methods: with hemispherical photographs analysed by the CAN EYE method, and with the ecosystem model (EM). In the following sections comparisons between the two types of ground truth data will be made separately. No corrections were made for clumping or stem influence for the deciduous stands, since these two components show compensatory effects in forest stands (Eriksson *et al.* 2006). The Markov parameter, which is an indicator for clumpiness, was therefore set to 1 for all the stands.

According to the size of the leaves (5–10 cm) and the height of the trees (5–30 m) we used for the relative leaf size the minimum value mentioned in the ACRM program of 0.02. An overview of all the model input parameters is given in table 3.

3.4.3 Ground characteristics. At each stand, detailed photographs of the ground and canopy conditions were taken. Based on the photographs and observations, the average percentage of different ground type was determined for each plot. In most stands, the ground was covered with senescent leaves or with ground vegetation. Figure 4 shows different types of ground reflectance measured with the Fieldspec spectrometer. Ground covered with senescent leaves has a NIR reflectance between

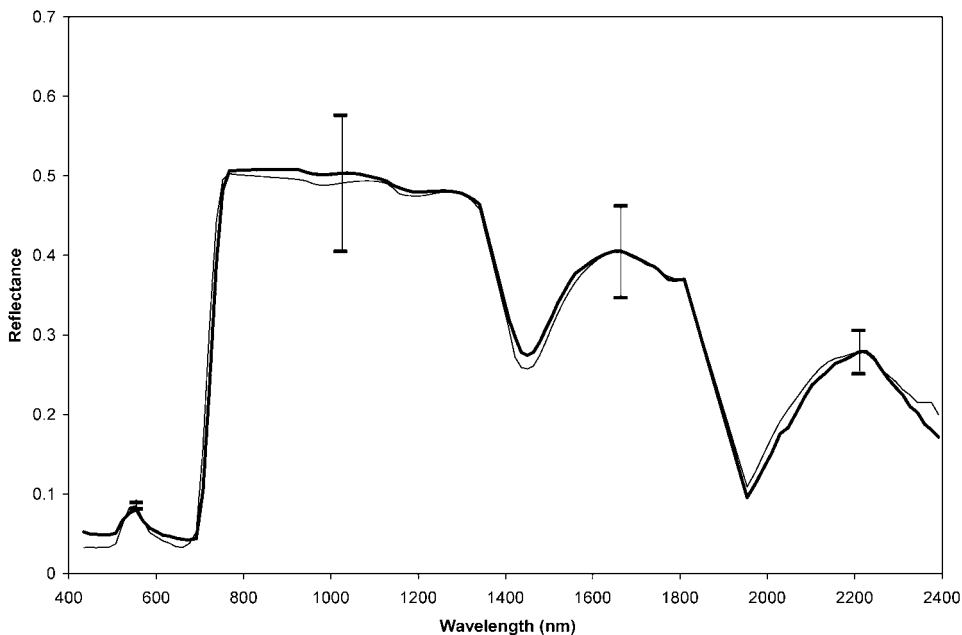


Figure 3. Typical modelled (thin line) and measured (bold line) reflectance of a beech leaf. Error bars show the standard deviation of the measured leaf reflectance. Model simulations were performed with the model PROSPECT.

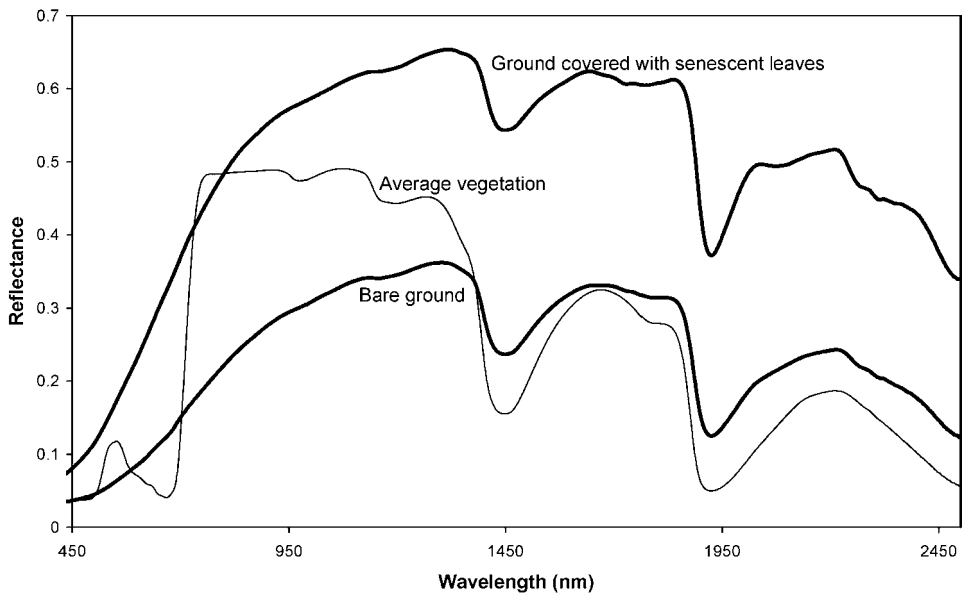


Figure 4. Reflectance of bare ground and ground covered with senescent leaves measured in the field with the contact probe compared to the average reflectance of ground vegetation (average of results shown in figure 2).

60% and 65%, which is twice as high as the reflectance of living ground vegetation, with NIR reflectance of 45% to 50%. The ground reflectance used for modelling the reflectance of each stand was determined by weighted summation of the measured reflectance values. Weighting was performed according to the proportion of the different types of components on the ground. For the forward calculations, the ACRM model was changed so that model input parameters were directly taken from the measured and weighted spectral ground reflectance. No specification of the model ground reflectance using the method by Price (1990) was required.

4. Results and discussion

4.1 Comparison of HyMap data with modelling

For the direct mode, model simulations were performed for the 126 HyMap wavelengths.

For the simulation in inverse mode, 21 'optimum' bands of the 126 HyMap were chosen, following findings of Thenkabail *et al.* (2004) who identified 22 'optimum' hyperspectral narrow wavebands (in the 400–2500 nm range) by means of statistical methods. One of these wavebands did not correspond to any of the HyMap wavelengths. Therefore, in the present study only 21 bands were used for the simulation in inverse mode. Due to their sensitivity to chlorophyll, soil background, biomass, LAI, plant moisture and vegetation stress, these wavebands characterize and classify best vegetation and crops.

The selected bands corresponding to HyMap are located in the visible part (492.7 nm, 554.3 nm, 646.2 nm and 676.5 nm), the red edge region (707.3 nm, 722.4 nm and 737.5 nm), the near infrared (874 nm, 888.5 nm, 911.1 nm, 990.2 nm, 1082.9 nm, 1127.7 nm, 1214.5 nm, 1243.1 nm and 1285.4 nm), the early mid-infrared (1675.7 nm and 1725.4 nm) and the far mid-infrared (2225.7 nm, 2293.7 nm and

2343.1 nm) part of the spectrum. The measurement configuration used for the model represented the actual condition during the sensor overpass with a solar zenith angle of 24° and a view zenith angle to the different stands between 0 and 29° .

Figure 5 shows a comparison, over the whole spectrum, of the average of all 38 plots of HyMap-derived reflectance and modelled reflectance. This comparison is representative for all the plots (see also figures 6, 7 and 8). The standard deviation between the different plots of the HyMap-derived retrieved reflectance is also shown. The uncertainty of the model calculations is shown at the wavelengths 554 nm, 888.5 nm, 1675 nm and 2207 nm. For the estimation of the model uncertainty we took into account an uncertainty in LAI determination of ± 0.03 , a change in relative leaf size from 0.15 to 0.02 and a Markov parameter of 0.6 instead of 1. The error bars show the maximum and minimum values obtained for one combination of the three above mentioned parameters. Besides the dependence on LAI the ACRM model shows a high sensitivity to changes in the Markov parameter. Decreasing the Markov parameter to 0.6 would lead to an increase in the calculated reflectance by approximately 20% and in turn to an increase in the discrepancy between model calculations and measurements. A change in LAI of 0.06 and an increase in relative leaf size of 0.13 (which is completely unrealistic) would result in a change in the reflectance of approximately 0.025% or 6%.

There is agreement between modelled reflectance and HyMap-derived retrieved reflectance only in the visible wavelength range. In the remaining wavelength ranges, the model always overestimates the retrieved reflectance. Even if the model and the measurement uncertainties are taken into account, the discrepancy between both remains. This fact is also confirmed when the reflectance values for the individual plots are compared (figures 6, 7, and 8). For each analysed spectral band we calculated the following parameters shown in the figures: the correlation coefficient

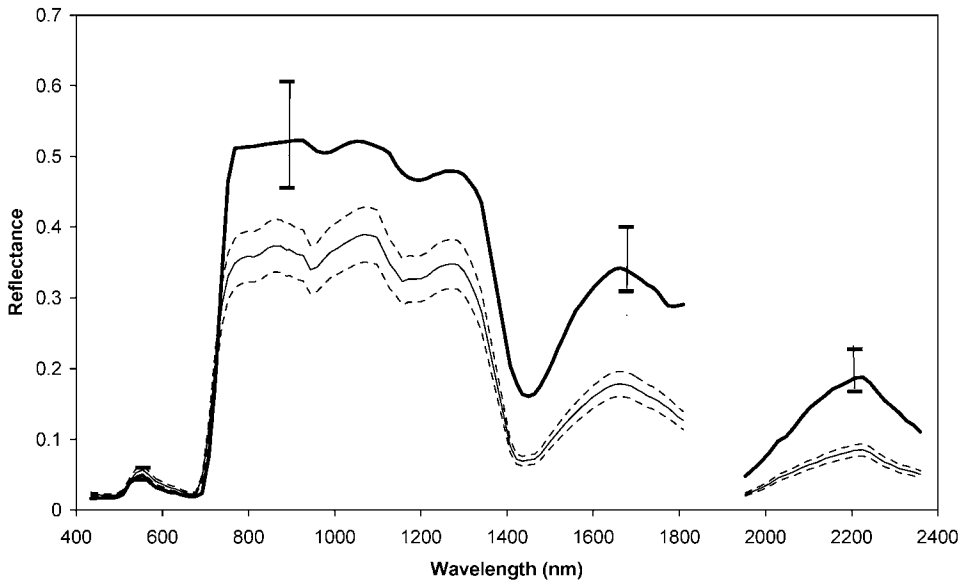


Figure 5. Typical modelled reflectance (thin line) compared with the average reflectance derived from HyMap (bold line) for the 38 beech plots. The error bars show the fluctuations (maximum and minimum values) of the model calculations. The dotted lines indicate the standard deviation of the derived HyMap reflectance of the 38 plots.

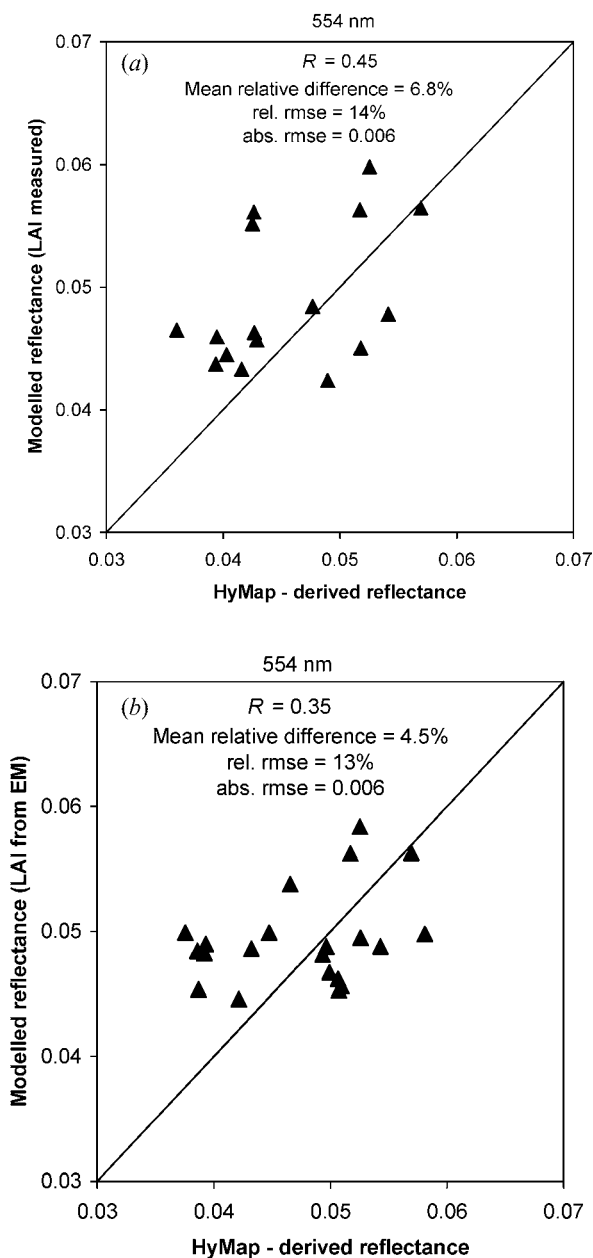


Figure 6. Modelled reflectance for each stand compared with HyMap derived reflectance at 554 nm. For the model simulations the measured leaf area index (LAI) (a) and the LAI from ecosystem modelling (EM) (b) are used.

R , the root mean square error (rmse) and the mean relative difference (mrd), indicating the magnitude of the offset between model retrieved and HyMap retrieved data:

$$\text{mrd} = \frac{1}{n} \sum_{i=1}^n \left(\frac{y_i - x_i}{(x_i + y_i)/2} \right) 100 \quad (\%) \quad (2)$$

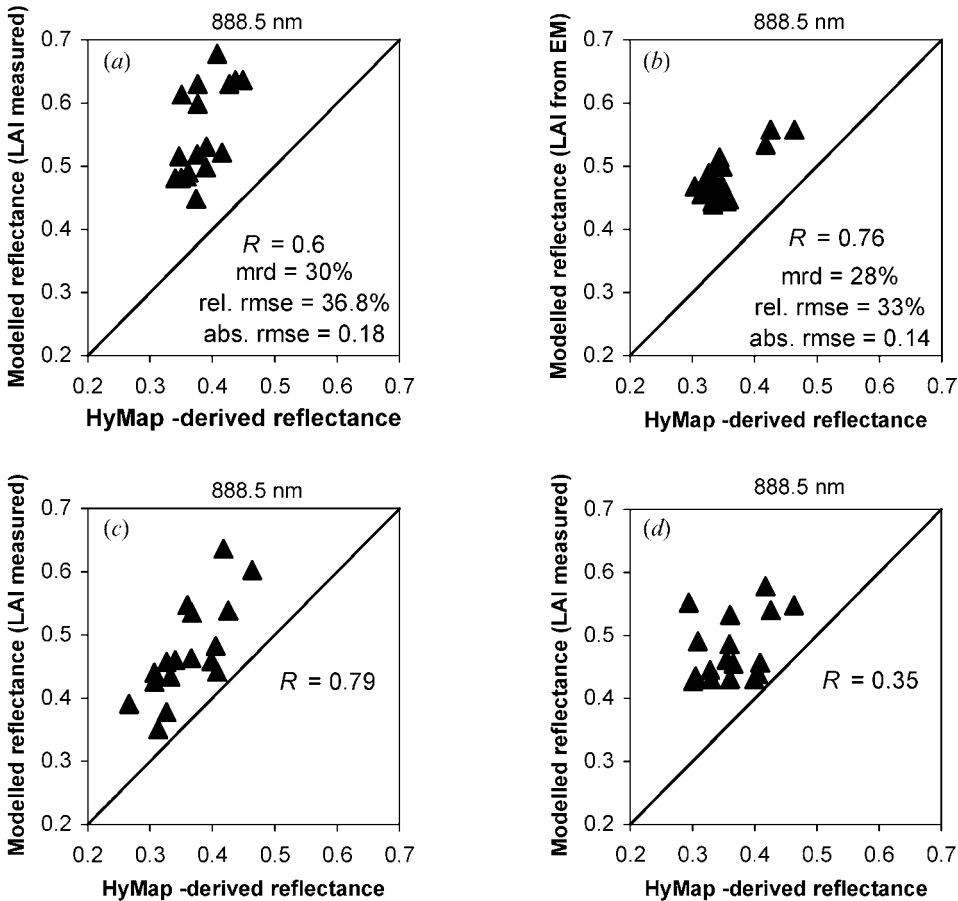


Figure 7. Comparison of modelled reflectance and HyMap derived reflectance at 888.5 nm for various conditions: (a) leaf area index (LAI) input from measured data, Gu and Gillespie correction applied to HyMap derived reflectance; (b) LAI input from ecological modelling, Gu and Gillespie correction applied to HyMap derived reflectance; (c) LAI input from measured data, HyMap data without topographic normalization, reflectance modelling for inclined terrain surface (cosine correction), (d) LAI input from measured data, HyMap data without topographic normalization. Reflectance modelling performed for horizontal surface similar to cases (a) and (b).

where x_i is the reflectance determined from HyMap and y_i is the modelled reflectance. The mrd indicates the magnitude of the offset between model and HyMap retrieved data.

In order to determine the significance of the correlation between modelled reflectance and HyMap-derived reflectance, a t -test was applied at the 95% confidence level to the data.

In the visible wavelength range (554 nm), figures 6(a) and (b) show a mrd of 4% to 7%, which indicates a good agreement between model and retrieved reflectance. The rmse is around 0.001, which represents in both cases a relative rmse around 13% to 14%. Altogether with an R -value between 0.35 and 0.45 and n equal to 17 and 21, respectively, the t -test showed no significance at the 95% level between modelled and HyMap retrieved reflectance.

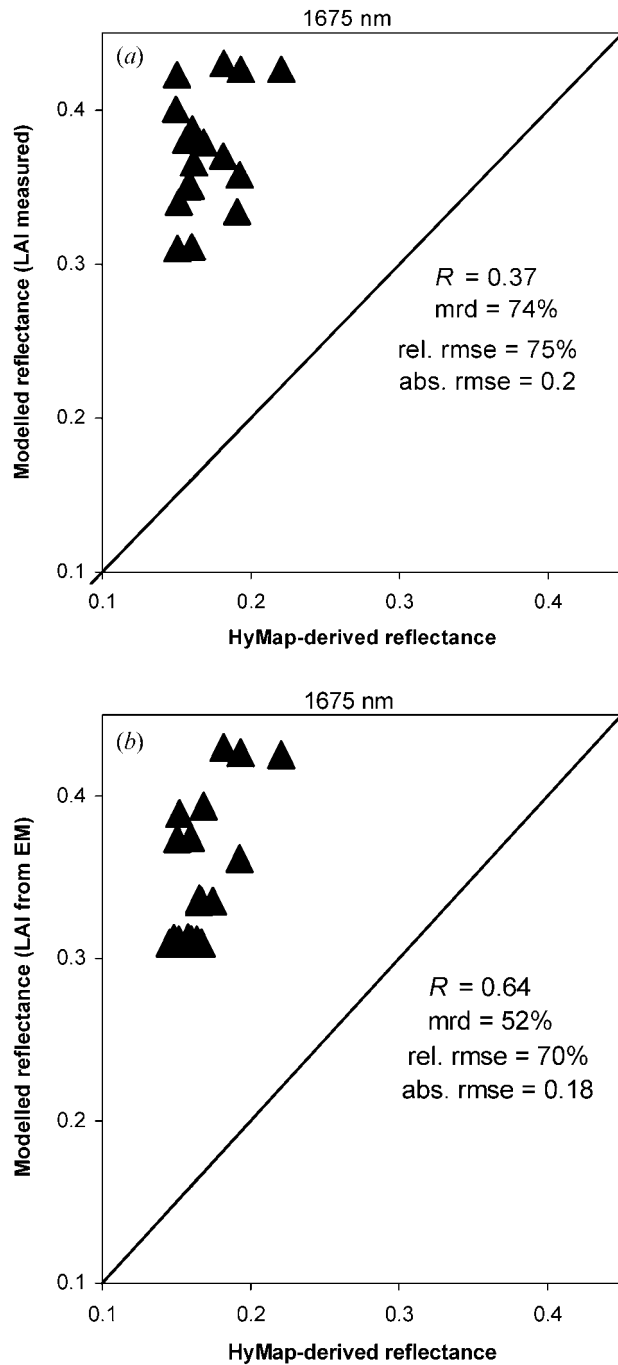


Figure 8. Modelled reflectance for each stand compared with HyMap-derived reflectance at 1675 nm. For the model simulations the measured (a) and the modelled (b) leaf area index (LAI) are used.

The strong dependence of reflectance on chlorophyll in this wavelength range may explain the lack of correlation. The fluctuations in the measured reflectance may probably mainly be caused by inhomogeneities in stand structure (varying stem density and volume, varying crown cover). Besides that, it may also be attributable to varying chlorophyll content between the stands. Our leaf reflectance measurements were not performed at all the sites. We therefore assumed the same biochemical properties of the leaves at all the locations. A small uncertainty may also be added by the relatively low signal-to-noise ratio in this wavelength range and the strong influence of the atmosphere (more scattering and extinction) that may add some noise and scattering to HyMap retrieved reflectance.

In the NIR (888.5 nm) (figure 7(a) and (b)), the correlation R between model calculations and HyMap measurements ranges from 0.6 to 0.76. The t -test shows a statistically significant correlation in both cases. The systematic overestimation of the reflectance by the model is between 28% and 30%. The absolute deviation of the reflectance is approximately 0.14 to 0.18. The rmse is between 37% and 38%.

In figure 7(a) and (b), the HyMap-derived reflectance is topographically corrected with the SCS method, and the modelled reflectance applies to horizontal terrain. In contrast to this, figure 7(c) and (d) show the topographically uncorrected HyMap-derived reflectance. The modelled reflectance applies to inclined terrain (corresponding to the actual plot inclination) in figure 7(c) and to horizontal terrain in figure 7(d). The comparison of these figures illustrates the influence of topography. The variation in the reflectance between the plots can be seen to be much larger in the case of inclined plots, resulting in higher R values. An uncertainty in the topographic correction results from the fact that orientation and inclination may vary within a plot as mentioned in §2.

In the MIR (1675 nm) (figure 8(a) and (b)), the systematic deviation between modelled and measured reflectance is even larger. The model overestimates the reflectance by 74% (with measured LAI input) and 52% (with LAI input from ecosystem modelling). The average absolute deviation is 0.20 and 0.18, respectively. The correlation between model and measurement is, with $R=0.37$ and $R=0.64$, slightly better than in the visible wavelength range. It is significant only for LAI input from ecosystem modelling. A general explanation for the low correlation may be the fact that certain parameters influencing the reflectance, such as LAI and water concentration in the leaves, were kept constant in the model simulations. The explanation for the correlation being lower in the MIR compared to the NIR may lie in the larger dependence of the reflectance on LAI in the NIR as compared to the MIR.

4.2 Estimation of the LAI

4.2.1 Estimation of the LAI using ACRM model. LAI was determined from the HyMap reflectance values using the inversion mode of the ACRM model. Three parameters were left free in this inversion: the LAI and the weighting factors s_1 and s_2 of the Price function. The Markov parameter was set to 1. The leaf parameters were chosen as determined according to §3.4.1. The inversions were performed with measurements at 21 wavelengths corresponding to the wavelength indicated by Thenkabail *et al.* (2004), leaving out the one band not available in HyMap. The results are shown in figure 9(a) and (b). The retrieved LAI shows considerable variation around the values measured using hemispherical photographs. The correlation coefficient is 0.49 for the comparison of the retrieved LAI with the measured LAI and

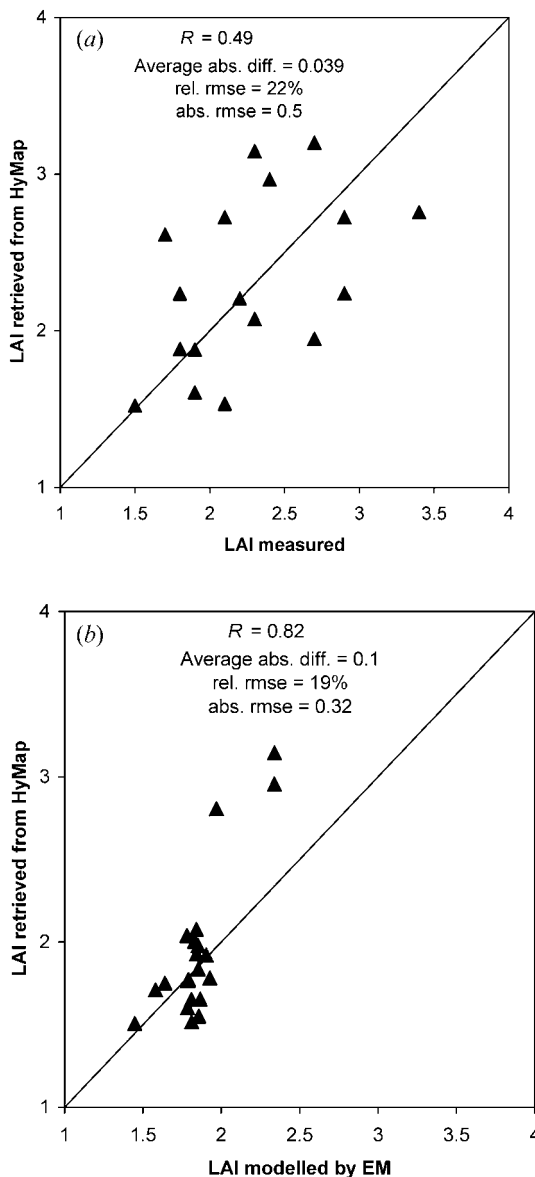


Figure 9. Comparison of the retrieved leaf area index (LAI) with the measured (a) and the modelled (b) LAI.

much better with 0.82 for the comparison of the retrieved with the modelled LAI. In both cases the correlation is significant at the 95% level. The average absolute difference is equal to 0.039 for the comparison with the measured LAI and 0.1 for the comparison with the modelled LAI. The absolute rmse is equal to 0.5 and 0.32, respectively. These last values may be considered as the accuracy achievable when retrieving LAI from the HyMap data. As already indicated in table 3, the LAI value calculated by ecosystem modelling is on average lower than the measured one. The modelled LAI seems to better characterize the investigated pixels, probably because it is less affected by fine-scale inhomogeneities in the forest canopy.

A prerequisite for accurate LAI retrieval is the appropriate choice of the leaf biochemical parameters—dry matter, chlorophyll content, water content and leaf structure N . Our simulations showed that the accuracy of the LAI retrieval may be strongly affected by the wrong choice of these leaf parameters.

4.2.2 Estimation of the LAI using vegetation indices. In order to test the performance of the ACRM model for LAI retrieval, the obtained correlations were compared to the correlations with well known vegetation indices. The vegetation indices that were used are shown in table 4. Indices identified by Schlerf *et al.* (2005) as those showing the highest correlations with the LAI, such as the hyperspectral perpendicular vegetation index (PVI_hyp), the perpendicular vegetation index (PVI), the transformed soil-adjusted vegetation index (TSAVI), the hyperspectral ratio vegetation index (RVI_hyp), or widely used indices such as the simple ratio vegetation index (SR) and the normalized difference vegetation index (NDVI), were chosen for the present study. The TSAVI and PVI indices require a parameter a , which corresponds to the soil line slope, and a parameter b corresponding to the point of intercept (Baret *et al.* 1989). Since, in the present study, the very non-homogeneous soil conditions (senescent leaves, ground vegetation, bare ground, etc.) did not allow the determination of a soil line slope, the soil line parameters were fixed to arbitrary values ($a=1.17$, $b=3.37$ according to Leblon (<http://www.r-s-c-c.org/rscc/Volume4/Leblon/leblon.htm>)). For the TM3 and TM4 channels the average reflectance over the wavelength range of the channels was used for the index calculations.

The correlation coefficients R of these indices with the measured and with the modelled LAI values are shown in table 5. The lowest correlations were obtained with SR, with RVI_hyp and with NDVI. The highest correlations were obtained with PVI_hyp, with PVI and with TSAVI. However, all these correlation coefficients range below the correlation coefficients obtained with the canopy reflectance model (CRM). No significant correlations were obtained between measured LAI and the

Table 4. Overview of the indices used in this study.

Name	Abbreviation	Equation	Reference
Hyperspectral perpendicular vegetation index	PVI_hyp	$\frac{ref1148 - a * ref807 - b}{\sqrt{1 + a^2}}$	Schlerf <i>et al.</i> 2005
Perpendicular vegetation index	PVI	$\frac{refTM4 - a * refTM3 - b}{\sqrt{1 + a^2}}$ $a=1.17, b=3.37$	Richardson and Wiegand 1977
Transformed soil-adjusted vegetation index	TSAVI	$\frac{a(refTM4 - a * refTM3 - b)}{a * refTM4 + a * refTM3 - ab}$ $a=1.17, b=3.37$	Baret <i>et al.</i> 1989
Hyperspectral ratio vegetation index	RVI_hyp	$\frac{ref1088}{ref1148}$	Schlerf <i>et al.</i> 2005
Simple ratio	SR	$\frac{refTM4}{refTM3}$	Pearson and Miller 1972
Normalized difference vegetation index	NDVI	$\frac{refTM4 - refTM3}{refTM4 + refTM3}$	Rouse <i>et al.</i> 1974

ref, reflectance; TM 3, Thematic Mapper channel 3 (630–690 nm); TM 4, Thematic Mapper channel 4 (760–900 nm); *ref*1088, reflectance at 1088 nm; *ref*1148, reflectance at 1148 nm; *ref*807, reflectance at 807 nm.

Table 5. Correlation coefficients R with measured and modelled leaf area index (LAI) of various vegetation indices.

	CRM	PVI_hyp	PVI	TSAVI	RVI_hyp	SR	NDVI
LAI measured	0.49	0.3827	0.4028	0.4625	0.3209	0.2238	0.2509
LAI modelled	0.82	0.7337	0.7329	0.555	0.0377	0.18	0.1758

CRM, canopy reflectance model (ACRM model); PVI_hyp, hyperspectral perpendicular vegetation index; PVI, perpendicular vegetation index; TSAVI, transformed soil-adjusted vegetation index; RVI_hyp, the hyperspectral ratio vegetation index; SR, simple ratio vegetation index;

NDVI, normalized difference vegetation index.

indices. Correlations between modelled LAI and the indices were significant for TSAVI, PVI and PVI_hyp.

5. Conclusions

The PROSPECT leaf reflectance model accurately calculates the reflectance of a leaf in the whole wavelength range, when the model input parameters are carefully chosen. The ACRM did not perform well in the forward mode in the NIR and MIR wavelength ranges, but seems to be a useful tool for LAI retrieval in the inversion mode.

The ACRM strongly overestimates the reflectance in the NIR by approximately 28–30% and in the MIR by 50–74%. The correlation coefficients of 0.60 and 0.76 in the NIR (888.5 nm) show that the model may, with reservations, be used in the forward mode if the systematic offset is taken into account. If the offset is taken into account, an absolute accuracy not better than 0.14 to 0.18 may be expected in the NIR.

The lack of data on fluctuations in chlorophyll and water content between individual trees did not allow the exact sensitivity of the ACRM model to chlorophyll and to water content to be tested. This fact may explain the rather low correlation coefficient in the visible (554 nm) and MIR (1675 nm) wavelength ranges. A low mean relative deviation was, however, obtained between modelled and HyMap retrieved reflectance in the visible wavelength range with an absolute error of 0.006.

The largest mean relative difference as well as the largest relative rmse occur in the MIR (1675 nm). The model strongly overestimates the HyMap-retrieved reflectance by 50–74%.

Since a very good agreement between retrieved and experimentally determined LAI was obtained, we can assume that the effect of LAI on canopy reflectance is properly taken into account by the model. The most probable reason for the overestimation of the canopy reflectance by the ACRM model may lie in an overestimation of multiple scattering and multiple reflectance phenomena within the canopy. ACRM takes into account leaves that have a high reflectance and transmittance only. Stems and branches, which usually show a low reflectance and which do not transmit any radiation are ignored in the ACRM code. Another possible reason for the strong overestimation by the model may also lie in an overestimation of the influence of the ground reflectance by the code. Kuusk and Nilson (2001) compared Boreal Ecosystem Atmosphere Study (BOREAS) data with simulations performed with the semi-homogeneous model MCRM, which includes

geometrical and structural parameters such as the crown radius and the tree height. They also found an overestimation of the modelled signal in the MIR wavelength range. They explained this discrepancy with an overestimation of multiple reflectance phenomena within the canopy by the canopy reflectance model.

Referring to the inverse mode, we compared the retrieval accuracy for LAI obtained with the ACRM to the retrieval accuracy possible with the well-known indices TSAVI, SR, NDVI, PVI, PVI_hyp and RVI_hyp. The correlation coefficients between ACRM-retrieved LAI and LAI measured or determined by ecosystem modelling was higher than the correlation coefficients between any of the indices and the measured or modelled LAI. The ACRM may therefore be used for the determination of LAI with an expected accuracy of 0.32 to 0.5. A prerequisite is the appropriate choice of the leaf biochemical parameters—dry matter, chlorophyll content, water content and leaf structure N . The accuracy of the LAI retrieval may strongly be affected by the wrong choice of these leaf parameters, which may be determined as the set of parameters giving the best fit of measured leaf reflectance and leaf reflectance modelled by PROSPECT.

We can summarize that for the forward modelling of forest canopy reflectance a correction of the offset should be performed. In reverse mode, the ACRM model is well suited for the retrieval of LAI even for complex terrain.

Acknowledgments

These investigations were performed within the scope of the project 'Crop Drought Stress Monitoring by Remote Sensing (DROSMON)', supported by the Austrian Science foundation (FWF), grant number P17647-N04. We thank the reviewers for their most valuable suggestions.

References

- BARET, F., GUYOT, G. and MAJOR, D.J., 1989, Crop biomass evaluation using radiometric measurements. *Photogrammetria (PRS)*, **43**, pp. 241–256.
- CHEN, J.M., PAVLIC, G., BROWN, L., CIHLAR, J., LEBLANC, S.G. and WHITE, H.P., et al. 2002, Derivation and validation of Canada-wide coarse-resolution leaf area index maps using high resolution satellite imagery and ground measurements. *Remote Sensing of Environment*, **80**, pp. 165–184.
- CONEL, J.E., GREEN, R.O., VANE, G., BRUEGGE, C.J., ALLEY, R.E. and CURTISS, B.J., 1987, Airborne imaging spectrometer-2: radiometric spectral characteristics and comparison of ways to compensate for the atmosphere. *Proceedings of SPIE*, **834**, pp. 140–157.
- DEMAREZ, V. and GASTELLU-ETCHEGORRY, J.P., 2000, A modeling approach for studying forest chlorophyll content. *Remote Sensing of Environment*, **71**, pp. 226–238.
- EKLUNDH, L., HALL, K., ERIKSSON, H., ARDÖ, J. and PILESJÖ, P., 2003, Investigating the use of Landsat Thematic Mapper data for estimation of forest leaf area index in southern Sweden. *Canadian Journal of Remote Sensing*, **29**, pp. 349–362.
- ERIKSSON, H.M., EKLUNDH, L., KUUSK, A. and NILSON, J., 2006, Impact of understory vegetation on forest canopy reflectance and remotely sensed LAI estimates. *Remote Sensing of Environment*, **103**, pp. 408–418.
- GOVAERTS, Y. and VERSTRAETE, M.M., 1998, Raytran: a Monte Carlo ray tracing model to compute light scattering in three-dimensional heterogeneous media. *IEEE Transactions on Geoscience and Remote Sensing*, **36**, pp. 493–505.
- GU, D. and GILLESPIE, A., 1998, Topographic normalization of Landsat TM images of forest based on subpixel sun-canopy-sensor geometry. *Remote Sensing of Environment*, **64**, pp. 166–175.

- GUANTER, L., ALONSO, L. and MORENO, J., 2004, Atmospheric correction of CHRIS/Proba data acquired in the SPARC campaign. In *Proceedings of the 2nd CHRIS/Proba Workshop, ESA/ESRIN*, Frascati, Italy, 2004, ESA-SP-578 (Paris: European Space Agency).
- JACQUEMOUD, S. and BARET, F., 1990, a model of leaf optical properties spectra. *Remote Sensing of Environment*, **34**, pp. 75–91.
- JONCKHEERE, I., FLECK, S., NACKAERTS, K., MUYS, B., COPPIN, P., WEISS, M. and BARET, F., 2004, Review of methods for *in situ* leaf area index determination, Part I. Theories, sensors and hemispherical photography. *Agricultural and Forest Meteorology*, **121**, pp. 19–35.
- KIMES, D., GASTELLU-ETCHEGORRY, J. and ESTÈVE, P., 2002, Recovery of forest canopy characteristics through inversion of a complex 3D model. *Remote Sensing of Environment*, **79**, pp. 320–328.
- KOUKAL, T., SCHNEIDER, W. and SUPPAN, F., 2005, Radiometric-topographic normalization in mountainous terrain for Landsat-TM-based forest parameter assessment by the kNN method. In M. Oluic (Ed.), *New Strategies for European Remote Sensing, Proceedings of the 24th Symposium of the European Association of Remote Sensing Laboratories (EARSeL)*, Dubrovnik, Croatia, 25–27 May 2004 (Rotterdam: Millpress).
- KUUSK, A., 1991, Determination of vegetation canopy parameters from optical measurements. *Remote Sensing of Environment*, **37**, pp. 207–218.
- KUUSK, A., 2001, A two-layer canopy reflectance model. *Journal of Quantitative Spectroscopy and Radiative Transfer*, **71**, pp. 1–9.
- KUUSK, A. and NILSON, T., 2001, Testing directional properties of a forest reflectance model. *Journal of Geophysical Research*, **106**, pp. 12011–12021.
- LEBLANC, S.G. and FOURNIER, R.A., 2005, Towards a better understanding of *in-situ* canopy measurements used in the derivation and validation of remote sensing leaf area index products. In *31st International Symposium on Remote Sensing of Environment*, Saint Petersburg, Russia (Saint Petersburg: Russian Federation of Remote Sensing), 20–24 June 2005.
- LI, X., STRAHLER, A.H. and WOODCOCK, C.E., 1995, A hybrid geometric optical radiative transfer approach for modeling albedo and directional reflectance of discontinuous canopies. *IEEE Transactions on Geoscience and Remote Sensing*, **33**, pp. 466–480.
- MERONI, M., COLOMBO, R. and PANIGADA, C., 2004, Inversion of a radiative transfer model with hyperspectral observations for LAI in poplar plantations. *Remote Sensing of Environment*, **92**, pp. 195–206.
- MYNENI, R., HOFFMAN, S., KNYAZIKHIN, Y., PRIVETTE, J., GLASSY, J. and TIAN, Y., et al. 2002, Global products of vegetation leaf area and fraction absorbed PAR from one year of MODIS data. *Remote Sensing of Environment*, **83**, pp. 214–221.
- PEARSON, R.L. and MILLER, L.D., 1972, Remote mapping of standing crop biomass for estimation of the productivity of the short-grass prairie, Pawnee National Grasslands, Colorado. In *Proceedings of the 8th International Symposium on Remote Sensing of Environment* (Ann Arbor, MI: ERIM International), pp. 1357–1381.
- PEDDLE, D.R., JOHNSON, R.L., CIHLAR, J. and LATIFOVIC, R., 2004, Large area forest classification and biophysical parameter estimation using the 5-scale canopy reflectance model in multiple-forward-mode. *Remote Sensing of Environment*, **89**, pp. 252–263.
- PIETSCH, S.A. and HASENAUER, H., 2006, Evaluating the self-initialisation procedure of large scale ecosystem models. *Global Change Biology*, **12**, pp. 1658–1669.
- PIETSCH, S.A., HASENAUER, H., KUCERA, J. and CERMÁK, J., 2003, Modeling effects of hydrological changes on the carbon and nitrogen balance of oak in floodplains. *Tree Physiology*, **23**, pp. 735–746.

- PIETSCH, S.A., HASENAUER, H. and THORNTON, P.E., 2005, BGC-model parameters for tree species growing in central European forests. *Forest Ecology and Management*, **211**, pp. 264–295.
- PINTY, B., et al. 2001, The Radiation Transfer Model Intercomparison (RAMI) exercise. *Journal of Geophysical Research*, **106**, pp. 11937–11956.
- PINTY, B., et al. 2004, Radiation Transfer Model Intercomparison (RAMI) exercise: results from the second phase. *Journal of Geophysical Research*, **109**, pp. D06210, doi:10.1029/2003JD004252.
- PRICE, J.C., 1990, On the information content of soil reflectance spectra. *Remote Sensing of Environment*, **33**, pp. 113–121.
- QIN, W. and GERSTL, S.A.W., 2000, 3-D scene modeling of semi-desert vegetation cover and its radiation regime. *Remote Sensing of Environment*, **74**, pp. 145–162.
- RAUTIAINEN, M., 2005a, The spectral signature of coniferous forests: the role of stand structure and leaf area index. Academic Dissertation, Department of Forest Ecology Faculty of Agriculture and Forestry, University of Helsinki, Finland.
- RAUTIAINEN, M., 2005b, Retrieval of leaf area index for a coniferous forest by inverting a forest reflectance model. *Remote Sensing of Environment*, **99**, pp. 295–303.
- RAUTIAINEN, M., STENBERG, P., NILSON, T. and KUUSK, A., 2004, The effect of crown shape on the reflectance of coniferous stands. *Remote Sensing of Environment*, **89**, pp. 41–52.
- RICHARDSON, A.J. and WIEGAND, C.L., 1977, Distinguishing vegetation from soil background information. *Photogrammetric Engineering and Remote Sensing*, **43**, pp. 1541–1552.
- ROBERTS, D.A., YAMAGUCHI, Y. and LYON, R.J.P., 1985, Calibration of airborne imaging spectrometer data to percent reflectance using field spectral measurements. In *Proceedings of the 19th International Symposium on Remote Sensing of Environment*, pp. 295–298.
- ROSS, J., 1981, *The Radiation Regime and Architecture of Plant Stands*, The Hague: Dr. W. Junk Publishing, 391 pp.
- ROUSE, J.W., HAAS, R.H. and SCHELL, J.A., 1974, Monitoring the vernal advancement of retrogradation of natural vegetation. In *NASAI/GSFC, Type III, Final Report* (pp. 1–371), Greenbelt, MD.
- SCHLERF, M. and ATZBERGER, C., 2006, Inversion of a forest reflectance model to estimate structural canopy variables from hyperspectral remote sensing data. *Remote Sensing of Environment*, **100**, pp. 281–294.
- SCHLERF, M., ATZBERGER, C. and HILL, J., 2005, Remote sensing of forest biophysical variables using HyMap imaging spectrometer data. *Remote Sensing of Environment*, **95**, pp. 177–194.
- SOENEN, S.A. and PEDDLE, D.R., 2005, SCS+C: A modified sun-canopy-sensor topographic correction in forested terrain. *IEEE Transactions on Geoscience and Remote Sensing*, **43**, pp. 2148–2154.
- SOUDANI, K., FRANCOIS, C., LE MAIRE, G., LE DANTEC, V. and DUFRENE, E., 2006, Comparative analysis of IKONOS, SPOT, and ETM+ data for leaf area index estimation in temperate coniferous and deciduous forest stands. *Remote Sensing of Environment*, **102**, pp. 161–175.
- THENKABAIL, P.S., ENCLONA, M.S., ASHTON, B. and VAN DER MEER, 2004, Accuracy assessments of hyperspectral waveband performance for vegetation analysis applications. *Remote Sensing of Environment*, **91**, pp. 354–376.
- THORNTON, P.E., LAW, B.E., GHOLZ, H.L., CLARK, K.L., FALGE, E., ELLSWORTH, D.S., GOLDSTEIN, A.H., MONSON, R.K., HOLLINGER, D., FALK, M., CHEN, J. and SPARKS, J.P., 2002, Modeling and measuring the effects of disturbance history and climate on carbon and water budgets in evergreen needleleaf forests. *Agricultural and Forest Meteorology*, **113**, pp. 185–222.
- VERHOEF, W., 1984, Light scattering by leaf layers with application to canopy reflectance modelling: the SAIL model. *Remote Sensing of Environment*, **16**, pp. 125–141.

- VERMOTE, E.F., TANRÉ, D., DEUZE, J.L., HERMAN, M. and MORCRETTE, J.J., 1997, Second simulation of the satellite signal in the solar spectrum, 6S—an overview. *IEEE Transactions on Geoscience and Remote Sensing*, **35**, pp. 675–686.
- WALTHALL, C.L., NORMAN, J.M., WELLES, J.M., CAMPBELL, G. and BLAD, B.L., 1985, Simple equation to approximate the bidirectional reflectance from vegetative canopies and bare soil surfaces. *Applied Optics*, **24**, pp. 383–387.
- WEISS, M. and BARET, F., 1999, Evaluation of canopy biophysical variable retrieval performances from the accumulation of large swath satellite data. *Remote Sensing of Environment*, **70**, pp. 293–306.
- WEISS, M., BARET, F., SMITH, G.J., JONCKHEERE, I. and COPPIN, P., 2004, Review of methods for in situ leaf area index (LAI) determination Part II. Estimation of LAI, errors and sampling. *Agricultural and Forest Meteorology*, **121**, pp. 37–53.
- ZARCO-TEJADA, P.J., MILLER, J.R., HARRON, J., BAOXIN, H., NOLAND, T.L., GOEL, N., MOHAMMED, G.H. and SAMPSON, P., 2004, Needle chlorophyll content estimation through model inversion using hyperspectral data from boreal conifer forest canopies. *Remote Sensing of Environment*, **89**, pp. 189–199.

4.5 Publikation V

Occurrence of repeated drought events: can repetitive stress situations and recovery from drought be traced with leaf reflectance?

Rita Linke, Katja Richter, Judith Haumann, Werner Schneider, and Philipp Weihs

Periodicum Biologorum 110 (3): 219-229, 2008.



Occurrence of repeated drought events: can repetitive stress situations and recovery from drought be traced with leaf reflectance?

RITA LINKE¹
KATJA RICHTER^{2,3}
JUDITH HAUMANN¹
WERNER SCHNEIDER²
PHILIPP WEIHS³

¹ Department of Ecophysiology and Functional Anatomy of Plants, Faculty of Life Sciences, University of Vienna, Althanstraße 14, 1090 Vienna

² Institute of Surveying, Remote Sensing and Land Information, Department of Landscape, Spatial and Infrastructure Sciences, University of Natural Resources and Applied Life Sciences (BOKU), Peter Jordan Straße 82, 1190 Vienna

³ Institute of Meteorology, Department of Water, Atmosphere and Environment, University of Natural Resources and Applied Life Sciences (BOKU), Peter Jordanstraße 82, 1190 Vienna

Correspondence:

Rita Linke
Department of Ecophysiology and Functional Anatomy of Plants, Faculty of Life Sciences, University of Vienna, Althanstraße 14, 1090 Vienna
E-mail: r.linke@gmx.at

Key words: wheat, drought stress, recovery, leaf reflectance, relative water content, photosynthesis, chlorophyll

Received October 18, 2008.

Abstract

Within the last years a lot of effort has been made to improve irrigation efficiency and early drought stress detection by using various remote sensing techniques. In the present study two different species of wheat (Triticum aestivum and Triticum durum), cultivated in a growth chamber, were used to investigate the effects of drought occurring at different phenological stages. Plant physiological traits and spectral leaf reflectance were used to assess the potential of remote sensing techniques. Drought stress was applied either at flowering and/or at grain filling. Subsequently, a treatment following recovery after drought stress at flowering was set up. The effects of drought were traced by following the changes in plant physiological traits (i.e. photosynthetic rate, leaf conductance, relative and actual leaf water content) as well as in leaf reflectance. Drought resulted in a significant reduction of plant physiological traits and water relations, independently of the time of its occurrence. Rewatering plants after the stress period at flowering resulted in a recovery of plant physiological traits. Single leaf reflectance of plants subjected to drought increased over the entire range of the spectrum. However, five spectral regions with relatively high differences were observed: 520–530 nm, 570–590 nm, 690–710 nm, 1410–1470 nm and 1880–1940 nm. Additionally, three spectral indices were tested towards their applicability for tracing drought stress and subsequent recovery, yielding a reasonable relationship with measured leaf water content, photosynthetic rate and leaf nitrogen content.

INTRODUCTION

Water scarcity is increasingly important in many parts of the world. Within the next centuries global climate change is expected to result in a long-term trend towards higher temperatures, greater evapotranspiration, and an increased incidence of drought in specific regions (1, 2). Moreover, not only changes in the spatial but also in the temporal distribution patterns of precipitation and radiation are to be expected (3); e.g.: in Europe higher precipitation levels are predicted for the winter half-year and drier periods for the summer half-year (2).

Under conditions of drought stress, absorption of radiation by the leaf tends to decrease due to lower leaf water content. Although water absorbs most strongly in the wavelengths of the infrared region of the

TABLE 1

Summary of climatic conditions in the growth chamber.

	Spring	Summer
Temperature	07–14°C day / 06–12°C night	17–26°C day / 14–20°C night
Relative humidity	60–80% day / 75–90% night	50–70% day / 60–90% night
Light (1m above ground)	~ 700 $\mu\text{mol m}^{-2} \text{s}^{-1}$	~ 700 $\mu\text{mol m}^{-2} \text{s}^{-1}$
Day length	13.5 h	15.5 h

spectrum from approximately 1300 nm to 2500 nm (4), some absorption also occurs at lower wavelengths. As water is lost from a leaf, reflectance increases and absorption decreases, primarily as a result of water's radiative properties (5, 6). Even after accounting for the radiative characteristics of water, secondary effects occur. These include the influence of water content on absorption by other substances in the leaves, such as pigments. Also included as secondary are the effects of water content on wavelength-independent processes, particularly multiple reflections inside the leaf (7).

Moreover, drought stress not only causes leaf water content to decline but also affects physiological processes (e.g. leaf conductance, photosynthetic rates, etc.). Furthermore, changes in pigment and nitrogen concentration of plant tissue will occur. For example, chlorophyll and RubisCO contents decline as the leaf remobilizes resources under stress conditions (8). Chlorophyll and accessory pigments absorb strongly in the visible range (9, 10). Carter and Knapp (11) described a consistent stress induced alteration of leaf reflectance at visible wavelengths (~400–720nm) since chlorophyll is the major absorber in the leaf and the metabolic disturbance brought about by stress alters leaf chlorophyll concentrations (9). Leaf reflectance in the visible range of plants experiencing nutrient deficiency was also found to increase since nitrogen (and magnesium) is essential in the formation of chlorophyll. As leaves become more chlorotic, reflectance increases and the reflectance peak, normally centred at about 550 nm, broadens towards the red as absorption of incident light by chlorophyll decreases (12). Plant responses to water deficit therefore include both biochemical and morphological changes that primarily lead to acclimation and later to functional damage and the loss of plant parts (13).

A lot of effort has been made towards the use of spectral reflectance of leaves and canopies for stress detection in agricultural environments. While leaf reflectance is driven by the chemical composition of the leaves, the reflectance of a canopy is influenced by its geometry – the leaf area index, inclination and clumping of the leaves – as well as the reflectance of single leaves. In this study we only concentrate on the reflectance of leaves and not of the whole canopy.

The aim of the present study was, on the one hand, to evaluate the impact of drought stress on plant physiological traits and leaf reflectance of wheat (*Triticum aestivum* and *Triticum durum*) occurring at different phenological

stages (at flowering and/or grain filling). On the other hand, the incidence of two consecutive drought events and recovery of plants after drought was investigated. The analysis of the effect of consecutive stress periods and recovery on changes in leaf reflectance has rarely been performed until now but might gain in importance considering the predicted increased frequency of drought events whereby plants could be exposed to drought repeatedly (2, 14, 15, 16).

MATERIAL AND METHODS

1. Experimental Setup

Plants (*Triticum aestivum* L. cv. Xenos and *Triticum durum* L. cv. Floradur) were grown in 8 litre plastic pots (7). Simulation of seasons in the growth chamber was based upon long-time observation of temperature and relative humidity (past 10 years; meteorological station: 16°29' eastern longitude and 48°15' northern latitude). Illumination of the growth chamber was accomplished by 54 lamp units consisting of a lamp (Powerstar HQI TS 250/NDL UVS, 250W, Osram, Germany) and an appropriate reflector (Osram, Germany) yielding a PPFD of ~1200 $\mu\text{mol m}^{-2} \text{s}^{-1}$ in 1.5m above the ground. Detailed climatic conditions are summarized in Table 1.

For germination, 25 seeds of *T. aestivum* / *T. durum* were placed in each pot (7 replicates) and seedlings were thinned to 20 plants per pot. Nitrogen fertilization (2.11g N per pot; equivalent to 150kg N/ha) with Nitramoncal (27% N) was evenly split in three bits (before sowing, at stem elongation and at heading). P and K were supplied with Hortipray (NPK 0:52:34; 2.05g/pot, equivalent to 180kg K/ha). Prior to sowing the agricultural soil was additionally fertilized with »Flory Basisdünger 10®« (Eufloor GmbH, Germany; trace elements). As cultural substrate, a 2:1 mixture of air-dried and sieved (<4mm) agricultural top soil (6.33kg; A-Horizon; chernozem) and quartz sand (3.17kg; 0.2–2.0 mm) was used.

Four different treatments were set up per species – one control treatment and three treatments exposed to drought at different times during ontogeny:

AC/DC: control plants of *T. aestivum* / *T. durum*;
AF/DF: *T. aestivum* / *T. durum* exposed to drought stress at flowering; recovery after anthesis; AG/DG: *T. aestivum* / *T. durum* exposed to drought stress at grain filling; AFG/DFG: *T. aestivum* / *T. durum* exposed to drought stress at flowering and grain filling.

Soil humidity of control plants was consistently held at 20–23 vol% (AC/DC). Drought stress at flowering was imposed by halving water supply 10 days before the beginning of pollen shedding resulting in a soil humidity of ~10 vol% (TDR Trime, Imko Micromodultechnik GmbH, Germany) at flowering (AF/DF). After flowering, plants receiving a second stress at grain filling were allowed to recover for 8 days (water supply similar to control plants) before the second stress was imposed by halving water supply again (soil humidity during measuring period ~10 vol%; AFG/DFG). Plants receiving drought stress only at grain filling (AG/DG) were treated similar to control plants until after flowering. Drought stress was imposed at the same time as in plants of the treatment stressed twice.

2. Measurements

2.1. Physiological Measurements

Physiological and spectral measurements were made in the mid region of the youngest fully expanded leaves at three developmental stages: vegetative growth, flowering and grain filling.

Gas exchange measurements (A/C_i curves) were made using a CIRAS-I system (PP-Systems, U.K.) with an external air conditioning system. Leaves were placed in a cuvette of 2.5 cm², which was illuminated with a PPF of 1000 $\mu\text{mol m}^{-2} \text{s}^{-1}$. Temperature of the leaf chamber was maintained at 20 °C, air flow was set to 300 ml min⁻¹ and relative humidity of the incoming air was held at 45–55%. Light saturated photosynthetic rates (A_{sat}) refer to measurements at growth conditions under saturating light intensities (CO_2 : 350–370 $\mu\text{mol mol}^{-1}$; light: 1000 $\mu\text{mol m}^{-2} \text{s}^{-1}$).

Actual leaf conductance (g_L) was measured with a steady state porometer (PMR-4, PP-Systems; U.K.). Data were collected separately for both upper (adaxial) and lower (abaxial) leaf surface.

Chlorophyll content (Chl_{tot}) of leaves was determined with a SPAD-502 hand held chlorophyll meter (Minolta, Japan; (18)). For the measurement of absolute chlorophyll content per unit leaf area [$\mu\text{g cm}^{-2}$] small leaf discs of known area were cut and transferred to 5 ml of *N,N*-Dimethylformamide. Samples were stored at –18 °C until spectrophotometer readings of the eluate were taken (DU-7400, Beckman, USA; (19)). A calibration curve of SPAD readings versus absolute chlorophyll content was used to convert the SPAD readings into area based chlorophyll contents.

For calculation of the relative water content (RWC), leaf material was collected and fresh weight was immediately determined. Saturated weight was measured after placing the leaf discs in Petri dishes between wet filter paper for 24 hours (4 °C, dark). Dry weight was determined after drying leaf material to constant weight at 70 °C. Relative water content (20) was then calculated as:

$$\text{RWC} = \frac{(\text{fresh weight} - \text{dry weight})}{(\text{saturated weight} - \text{dry weight})} * 100 [\%]$$

and actual leaf water content was calculated as

$$\text{AWC} = \frac{(\text{fresh weight} - \text{dry weight})}{(\text{fresh weight})} * 100 [\%].$$

Plant material for measuring leaf nitrogen content ([N], expressed as percentage of dry matter) was dried to constant weight (70 °C) and milled (Cyclotec® Sample Mill; Planetary Ball Mill, PM 4000, Retsch). An aliquot of 1–2 mg of each sample (pooled samples) was weighed into tin capsules and analysed by isotope ratio mass spectrometry (IRMS). A continuous-flow IRMS system, consisting of an elemental analyser (EA 1110, CE Instruments, Milan, Italy) which was interfaced to the IRMS (DeltaPLUS, Finnigan MAT, Germany) was used.

2.2. Spectral measurements

Leaf spectral reflectance was measured with a Field-Spec Pro FR in connection with a plant reflectance probe from Analytical Spectral Devices Inc., Boulder, CO. The radiometer operates in the spectral range from 350 to 2500 nm. In the 350 to 1000 nm range, the sampling interval is approximately 1.4 nm and the spectral resolution (full width at half maximum) is 3 nm. In the 1000 to 2500 nm range, the sampling interval is 2 nm and the spectral resolution is 10 to 12 nm. The reflectance probe is equipped with an internal light source and works with a bi-conical measurement geometry. The device was adapted for a sample area of 19 mm by 7 mm to be able to measure the reflectance of individual wheat leaves. The detector field of view subtends an angle of up to 25°, and its axis is inclined by an angle of 25° to the sample normal. Radiance measurements were performed on single leaves (youngest fully expanded) and on a Spectralon panel serving as a white reference. Reflectance values were obtained as ratios of leaf radiances and Spectralon radiances.

Relative difference of reflectance spectra between stress and control treatments ($\Delta R/R$) was calculated as $[(R_{\text{stress}} - R_{\text{control}}) / R_{\text{control}}] * 100; (\%)$.

In addition, three spectral indices were calculated: photochemical reflectance index (PRI), an index for the estimation of relative water content (RWC_i) and an index for the estimation of the actual water content (AWC_i). The PRI is widely used for the estimation of photosynthetic radiation use efficiency. It was proposed according to the finding that the interconversion of xanthophyll cycle pigments in intact leaves can be detected as subtle changes in absorbance at 505–510 nm (21) or the reflectance at 531 nm (22). The photochemical reflectance index (PRI), incorporating reflectance at 531 nm (xanthophyll cycle signal), was then defined as $[(R_{570} - R_{531}) / (R_{570} + R_{531})]$ in the attempt to establish a reflectance-based photosynthetic index (23). Concerning the attempt to trace leaf water content (RWC and AWC) with spectral indices, a lot of effort has been made and a number of different indices have been developed for numerous crop species: among them the water index (WI ; R_{900} / R_{970} ;

TABLE 2

Summary of physiological traits of *T. aestivum* and *T. durum*. Significance levels refer to the differences between control and stress treatments. n=5-30; n.s.: not significant, *: p ≤ 0.05; **: p ≤ 0.01; ***: p ≤ 0.001.

		<i>Triticum aestivum</i> L.				<i>Triticum durum</i> L.			
		AC	AF	AG	AFG	DC	DF	DG	DFG
A _{sat}	vegetative	21.2				17.5			
	flowering	16.9	10.7***			15.6	9.9***		
	grain filling	13.8	12.2 ^{n.s.}	4.4***	6.9***	11.5	14.5**	3.9***	6.1***
g _L US	vegetative	185.0				224.3			
	flowering	453.9	81.2***			342.9	113.3***		
	grain filling	508.2	387.2***	56.9***	93.0***	382.5	370.7 ^{n.s.}	86.8***	125.0***
g _L LS	vegetative	84.0				87.4			
	flowering	164.1	18.4***			129.3	25.7***		
	grain filling	171.8	116.3**	15.3***	20.3***	142.5	101.1*	26.4***	48.1***
RWC	vegetative	86.7				91.3			
	flowering	83.8	74.0**			86.5	82.9 ^{n.s.}		
	grain filling	76.3	81.9*	57.1***	64.0***	81.8	82.0 ^{n.s.}	67.4***	74.2*
AWC	vegetative	81.2				83.1			
	flowering	72.2	68.8**			77.4	76.0 ^{n.s.}		
	grain filling	74.1	74.8 ^{n.s.}	68.3 ^{n.s.}	71.1**	77.8	78.0 ^{n.s.}	75.5**	76.0 ^{n.s.}
Chl _{tot}	vegetative	46.8				53.5			
	flowering	55.0	59.2***			55.7	53.4*		
	grain filling	48.3	50.3**	61.7***	55.6***	49.2	54.0***	52.1**	53.4***
Leaf[N]	vegetative	4.3				4.6			
	flowering	4.4	4.2**			4.2	3.8***		
	grain filling	2.4	2.3 ^{n.s.}	1.9**	2.0**	2.4	2.5 ^{n.s.}	2.1*	2.2 ^{n.s.}

Abbreviations: A: *T. aestivum*; D: *T. durum*; C: control; F: drought at flowering, plants were recovered at grain filling; G: drought stress at grain filling; FG: drought stress at flowering and grain filling. A_{sat}: [$\mu\text{mol m}^{-2} \text{s}^{-1}$], g_L: [$\text{mmol m}^{-2} \text{s}^{-1}$], RWC: [%], AWC [%], Chl_{tot}: [$\mu\text{g cm}^{-2}$]; Leaf[N]: leaf nitrogen content in % dry matter; US: upper leaf surface, LS: lower leaf surface

(24)), the water band index (WBI; R_{905} / R_{980} ; (25)) and some other indices described by Yu *et al.* (26). In the present study, for estimating RWC the ratio $RWC_i = R_{1483} / R_{1650}$ and for estimating AWC the ratio $AWC_i = R_{1121} / R_{1430}$ (26) were used.

2.3. Statistical Analysis

To test the level of significance between control plants and those of the stress treatments, data were subjected to a one-way analysis of variance (ANOVA; Systat 8, SPSS Inc.). For spectral measurements the mean of the five regions showing greatest differences between treatments was calculated (520–530nm, 570–590 nm, 690–710 nm,

1410–1470nm and 1880–1940nm) and used for statistics (ANOVA). All tests were made separately for the different species and phenological stages. Correlation analysis, testing the relationship between physiological parameters and spectral indices, was performed with Statgraphics Plus 5.0 software package (Statistical Graphics Inc.).

RESULTS

Physiological Measurements

Drought stress at flowering substantially reduced light saturated photosynthetic rates (A_{sat}) of both species (AF: –36%, DF: –37%; Table 2). Rewatering caused A_{sat} to re-

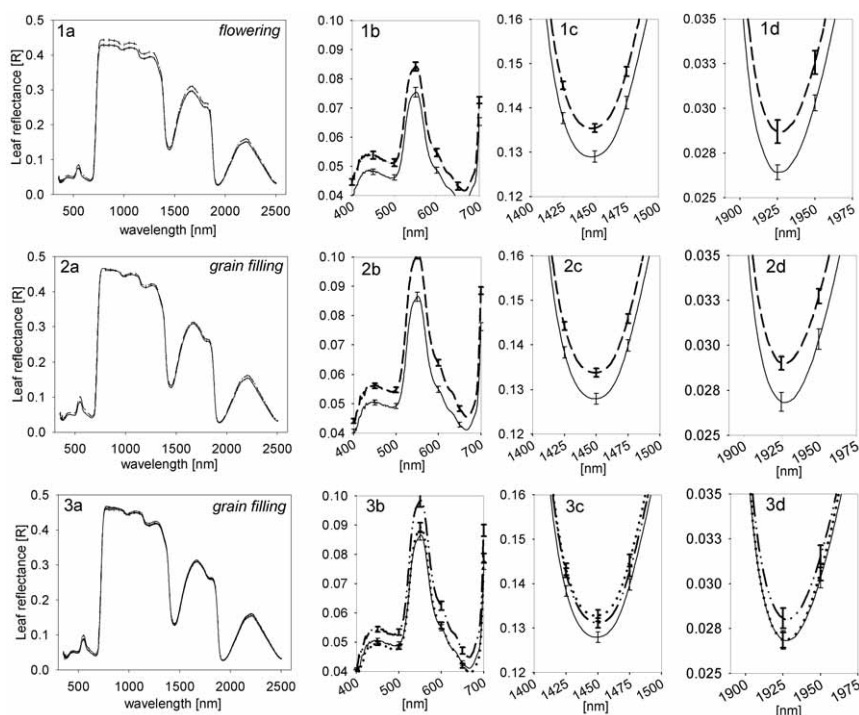


Figure 1. Leaf reflectance of *T. aestivum*. Row 1a-d shows leaf reflectance of control plants (AC; —) and drought stressed (AF; ---) plants at flowering. Row 2a-d represents leaf spectra of control plants (AC; —) and plants rewatered for 15 days (AF; ---; recovery) at grain filling. Row 3a-d shows leaf reflectance of control plants (AC; —) and plants stressed at grain filling either the first time (AG; ···) or the second time (AFG; - · - ·). 1-3a shows the original leaf spectrum and 1-3/b-d show the regions of greatest differences between stress and control treatments in detail. Curves represent the mean of 20-30 leaf spectra \pm standard error.

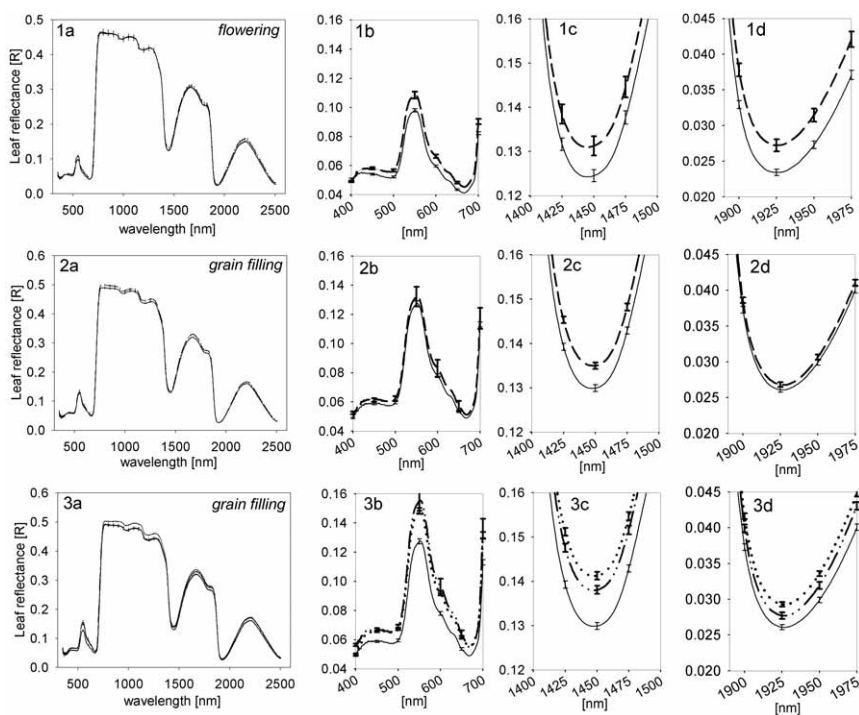


Figure 2. Leaf reflectance of *T. durum*. Row 1a-d shows leaf reflectance of control plants (DC; —) and drought stressed (DF; ---) plants at flowering. Row 2a-d represents leaf spectra of control plants (DC; —) and plants rewatered for 15 days (DF; ---; recovery) at grain filling. Row 3a-d shows leaf reflectance of control plants (DC; —) and plants stressed at grain filling either the first time (DG; ···) or the second time (DFG; - · - ·). 1-3a shows the original leaf spectrum and 1-3/b-d show the regions of greatest differences between stress and control treatments in detail. Curves represent the mean of 20-30 leaf spectra \pm standard error.

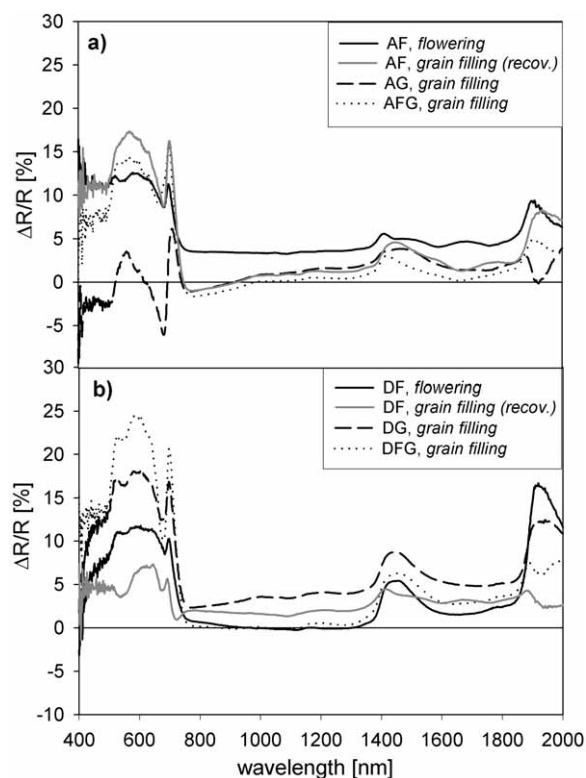


Figure 3. Relative difference ($\Delta R/R$) between reflectance of stressed and control plants of a) *T. aestivum* and b) *T. durum*. Differences were calculated as $[(R_{\text{stress}} - R_{\text{control}}) / R_{\text{control}}] * 100$ (%). Legend: AF: DF: differences between control and plants stressed at flowering, measured at flowering; AF: DF (recov.): differences between control and plants stressed at flowering, measured at grain filling after being rewatered for 15 days; AG: DG: differences between control and plants stressed at grain filling, measured at grain filling; AFG: DFG: differences between control and plants stressed at flowering and grain filling, measured at grain filling; $n=20-30$.

cover to nearly control values until grain filling in *T. aestivum* (−11%). In *T. durum*, values at grain filling even exceeded those of control plants (+25%). At grain filling however, in both species, reductions were more pronounced in plants receiving drought stress only at grain filling (AG: −68%, DG: −66%) than in those already stressed at flowering (AFG: −50%, DFG: −47%).

Regarding leaf conductance (g_L), *T. aestivum* was more susceptible to drought than *T. durum* independently of phenology (Table 2). Rewatering plants after drought stress at flowering restored g_L on the upper surface in *T. durum*. In *T. aestivum*, however, values remained somewhat below values of control plants. Drought at grain filling more strongly affected g_L in AG/DG compared to AFG/DFG.

Relative water content (RWC) of plants stressed at flowering was reduced (AF: −12%, DF: −4%; Table 2). At grain filling, RWC of formerly stressed plants was equal to or even exceeded values of control plants (AF: +7%, DF: +0.3%). Drought at grain filling resulted in an even

stronger reduction of RWC than at flowering (average: A: −21%, D: −14%). In both species, RWC of plants stressed only at grain filling was lower than that of plants already stressed at flowering.

Actual leaf water content (AWC) was also reduced significantly under drought (Table 2). In contrast to RWC the changes of AWC in the course of phenology were more pronounced which is due to the fact that the AWC only represents the water content as percentage of fresh weight whereas the RWC represents the actual water content given with respect to a standard measure (leaves under conditions of water saturation).

Drought at flowering caused an increase of total chlorophyll content (Chl_{tot} ; $\mu\text{g cm}^{-2}$) in AF (+11%) and a decrease in DF (−4%; Table 2). Rewatering resulted in higher Chl_{tot} contents at grain filling (AF: +4%, DF: +10%). Those plants subjected to drought at grain filling, either the first or the second time, also showed higher Chl_{tot} values compared to control plants (AG: +28%, DG: +6% and AFG: +15%, DFG: +8%, respectively).

Leaf nitrogen content (leaf [N], in % of dry matter) was reduced in plants subjected to drought at flowering (AF: −6%, DF: −11%; Table 2). At grain filling, leaf [N] from formerly stressed plants was still lower in *T. aestivum* (−5%) but higher in *T. durum* (+8%) when compared to control plants of either species. Plants subjected to drought stress during grain filling showed a reduction in leaf [N]. However, the reductions were more pronounced in plants stressed only at grain filling (AG: −20%, DG: −11%; AFG: −16%, DFG: −7%).

Spectral Measurements

Subjecting plants to drought stress, either at flowering or at grain filling, resulted in a general increase of single leaf reflectance (R; Figure 1–3). In both species, five spectral regions with relatively high differences were observed: 520–530 nm, 570–590 nm, 690–710 nm, 1410–1470 nm and 1880–1940 nm (Figure 3). Drought at flowering increased R in these spectral regions by up to +12%, +12%, +10%, +5% and +9% in *T. aestivum* and by up to +11%, +12%, +9%, +5% and +15% in *T. durum* (Table 3). Although rewatering plants after the stress period at flowering resulted in a recovery of plant physiological traits and water relations (see above) the effects observed on leaf R were different. Changes in leaf reflectance ($\Delta R/R$, %) between control plants and formerly stressed plants of *T. aestivum* in the range of 520–530 nm, 570–590 nm and 690–710 nm were even greater after recovery than during the stress period (520–530 nm: +15%, 570–590 nm: +17%, 690–710 nm: +15%; Table 3). However, the differences at 1410–1470 nm and 1880–1940 nm decreased during recovery. In contrast, $\Delta R/R$ of *T. durum* decreased during recovery within the entire range of the spectrum. The greatest decrease in $\Delta R/R$ was observed in the 1880–1940 nm range.

At grain filling, *T. aestivum* stressed solely at grain filling (AG) showed the smallest increase of R in comparison to control plants which was surprising since the

TABLE 3

Summary of relative difference (%) for physiological parameters and spectral regions of greatest difference. All data refer to the differences between plants subjected to drought stress either at flowering and/or grain filling and control plants. Bold values highlight the differences between control plants and recovered plants (measured at grain filling). Relative difference (%) was calculated as [(stress – control)/ (control)*100]. Significance levels refer to the differences between stress treatments or recovered plants and control. n=5–30; n.s.: not significant, *: p ≤ 0.05; **: p ≤ 0.01; ***: p ≤ 0.001.

		<i>Triticum aestivum</i> L.			<i>Triticum durum</i> L.		
		AF/AC	AG/AC	AFG/AC	DF/DC	DG/DC	DFG/DC
RWC	flowering	–12%**			–4% ^{n.s.}		
	grain filling	+7%*	–25%***	–16%***	+0,3% ^{n.s.}	–18%***	–16%*
AWC	flowering	–5%**			–2% ^{n.s.}		
	grain filling	+1% ^{n.s.}	–8% ^{n.s.}	–4%**	+0,3% ^{n.s.}	–3%**	–2% ^{n.s.}
Chl _{tot}	flowering	+11%***			–4%*		
	grain filling	+4%**	+28%***	+15%***	+10%***	+6%**	+15%***
Leaf[N]	flowering	–6%**			–11%***		
	grain filling	–5% ^{n.s.}	–20%**	–16%**	+8% ^{n.s.}	–11%*	–16% ^{n.s.}
R ₅₂₀₋₅₃₀	flowering	+12%***			+11%***		
	grain filling	+15%***	+0,2% ^{n.s.}	+13%***	+4% ^{n.s.}	+17%***	+22%***
R ₅₆₀₋₅₉₀	flowering	+12%***			+12%***		
	grain filling	+17%***	+3% ^{n.s.}	+14%***	+5% ^{n.s.}	+18%***	+24%***
R ₆₉₀₋₇₁₀	flowering	+10%***			+9%***		
	grain filling	+15%***	+2% ^{n.s.}	+14%***	+5% ^{n.s.}	+4%***	+19%***
R ₁₄₁₀₋₁₄₇₀	flowering	+5%***			+5%*		
	grain filling	+4%***	+4%**	+3%*	+4%***	+9%***	+6%***
R ₁₈₈₀₋₁₉₄₀	flowering	+9%***			+15%***		
	grain filling	+7%***	+1% ^{n.s.}	+4%*	+3%*	+12%***	+7%***

Abbreviations: see Table 2, R: leaf reflectance.

changes in physiological traits were greatest (Table 2). In *T. durum*, however, $\Delta R/R$ between stressed plants and control was greater than that observed in plants stressed at flowering. (The only exception gave the wavelength range of 1880–1940 nm where the differences were smaller at grain filling compared to flowering.)

Drought not only caused leaf R in the near infrared region (NIR) to increase but also in the visible range of the spectrum. Here, the changes were even greater than in the NIR independently of the occurrence of drought in phenology. Of all stress treatments and stress periods in phenology, the greatest $\Delta R/R$ in the visible range was observed at grain filling in the treatment stressed twice (second stress period; Table 3).

Spectral indices for estimating leaf RWC (RWC_i) and AWC (AWC_i) as well as photochemical reflectance index (PRI) were calculated to follow RWC and AWC as well as A_{sat} and leaf[N] in the course of phenology (Figure 4, 5; Table 4). In both species, RWC_i was less correlated with the measured values (*T. aestivum*: r²=0.079, *T. durum*: r²=0.467) than AWC_i was (*T. aestivum*: r²=0.715, *T. durum*: r²=0.953). Tracing the measured values of RWC using RWC_i was neither possible in *T. aestivum* nor in *T. durum* (Figure 4). Using AWC_i it appeared possible to follow the trend of measured AWC in both *T. aestivum* and *T. durum*, during phenology but only for control plants. At grain filling, the difference in the AWC estimated from leaf R in *T. aestivum* between recovered and

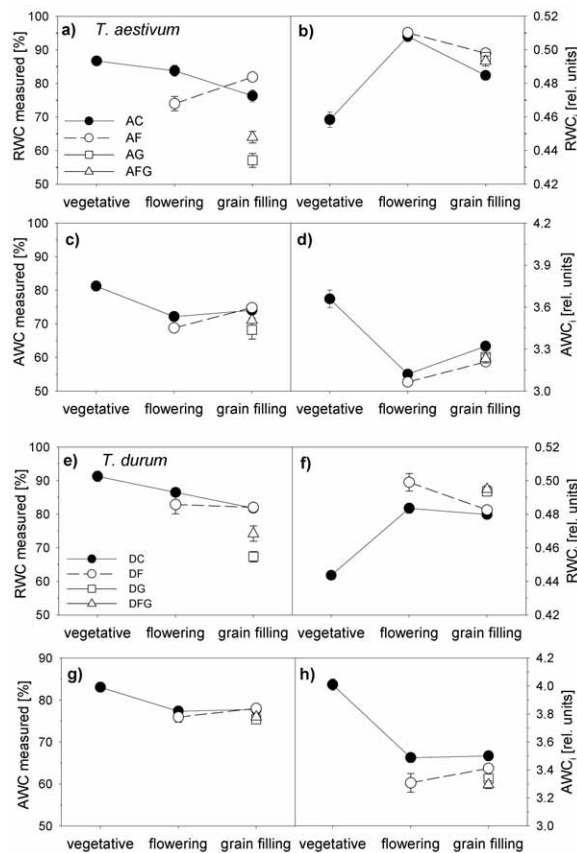


Figure 4. Comparison of the phenological course of measured and estimated RWC and AWC. a-d) *T. aestivum* and e-h) *T. durum*. Legend: A: *T. aestivum*; D: *T. durum*; C: control. F: drought at flowering, recovered at grain filling. G: drought at grain filling. FG: drought at flowering and grain filling. n=6 for measured RWC and AWC. n=20-30 for estimated RWC (RWC_i) and AWC (AWC_i). Errors represent standard error.

TABLE 4

Correlation statistics for the relationship between physiological parameters (RWC, AWC, A_{sat} and leaf [N]) and spectral indices (RWC_i , AWC_i and PRI). In addition to the correlation coefficient (r^2) and the significance level (p), the slope and intercept of the linear equation are given.

	r^2	p	slope	intercept
<i>Triticum aestivum</i> L.				
RWC	0.079	0.542	-4.526	0.526
AWC	0.715	0.017	0.037	0.564
A_{sat}	0.679	0.023	1.096	0.024
leaf[N]	0.774	0.009	5.774	0.019
<i>Triticum durum</i> L.				
RWC	0.467	0.091	-1.611	0.613
AWC	0.953	0.000	0.094	-3.848
A_{sat}	0.514	0.070	1.293	0.020
leaf[N]	0.986	0.000	8.499	8.551

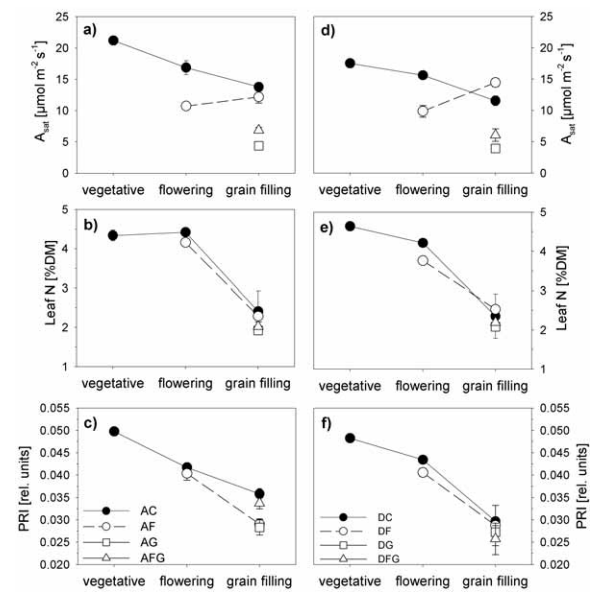


Figure 5. Comparison of the phenological course of light saturated photosynthetic rates (A_{sat}), leaf nitrogen content (leaf [N]) and photochemical reflectance index (PRI). a-c) *T. aestivum* and d-f) *T. durum*. Legend: A: *T. aestivum*; D: *T. durum*; C: control. F: drought at flowering, recovered at grain filling. G: drought at grain filling. FG: drought at flowering and grain filling. n=3-12 for A_{sat} and leaf [N]. n=20-30 for PRI. Errors represent standard error.

control plants give the impression of an even greater reduction than during the stress period at flowering itself, although the measurements of AWC reveal full recovery. In *T. durum* the differences decreased during recovery. However, values of AWC_i remained below control plants despite the complete recovery becoming obvious from measured values (Figure 4; see also $\Delta R/R$, Figure 3).

PRI correlated quite well with A_{sat} but even better with leaf [N] in both species (Table 4). Tracing phenological changes in A_{sat} and leaf [N] using PRI did not give good results for plants subjected to drought stress at any time in ontogeny. Better results for this correlation were only obtained for control plants. Therefore, neither recovery of plants after drought at flowering nor the extent of change in A_{sat} and leaf [N] due to drought could be estimated appropriately.

4. DISCUSSION

Drought stress significantly influenced plant physiological traits independently of the time of its application in phenology. The lowering of the actual leaf conductance (g_L), as observed during all stress periods in the present study, is one of the first processes occurring under decreased soil water availability providing a higher water use efficiency to the plant (27, 28, 29). Moreover, as reviewed by Cornic (30), stomatal closure is mainly responsible for the decline in net photosynthetic rate of C_3 leaves subjected to moderate drought stress. However, at a certain stage of stress, internal CO_2 concentration (C_i)

frequently increases, indicating the predominance of non-stomatal limitations to photosynthesis (31, 32, 33). Reductions of light saturated photosynthetic rates (A_{sat}) in the present experiment were mainly due to stomata limitation since a significantly lower C_i was found (data not shown).

In the present study, drought stress resulted in higher leaf reflectance (R) over the entire spectrum both in *T. aestivum* and in *T. durum*, a response also found elsewhere (*c.f.* 34, 35, 26). However, five regions with relatively high differences were observed: 520–530 nm, 570–590 nm, 690–710 nm, 1410–1470 nm and 1880–1940 nm (Figure 1–3).

Rewatering plants after the stress period at flowering allowed them to restore their physiological traits until grain filling (15 days rewatered). RWC of recovered plants even exceeded that of control in *T. aestivum* (+7%) and was restored to control level in *T. durum* (+0.3%). There-with, A_{sat} also recovered. Only g_L of plants from both species remained somewhat lower than that of control plants. However, the results from leaf R did not follow this trend. In *T. aestivum*, $\Delta R/R$ within the range of 1410–1470 nm and 1880–1940 nm remained nearly as high as during the stress period at flowering despite the 7% higher RWC of recovered plants. Though in *T. durum* a reduction of $\Delta R/R$ was found, leaf R still remained above that of control plants. Within the visible range of leaf spectra $\Delta R/R$ in *T. aestivum* even increased during recovery compared to the actual stress period. In *T. durum* $\Delta R/R$ within the visible range decreased during recovery but R still remained above that of control plants as already observed for the near infrared region. The results of the present study therefore indicate that quantifying the extent of change for either leaf water content or Chl_{tot} and leaf [N] from changes in leaf R is problematic. Especially recovery from drought could not be traced using leaf R since the differences between formerly stressed plants and control plants remained high as observed in *T. aestivum* or decreased only slightly as in *T. durum* but in neither of the species investigated leaf R returned to control level despite the complete recovery of physiological traits.

The reason for the enduring differences in leaf R between fully recovered plants and control plants remains rather unclear and information on leaf R during recovery of plants after a stress period is rare in literature. However, it is assumed that secondary effects following drought stress might be involved. Drought can affect the cell structure and biochemistry (*e.g.*: 36, 37, 38, 39) and is further known to influence the morphology of the leaf surface by means of changes in the content and/or composition of epicuticular waxes (40, 41, 42, 43) or the occurrence of hairs (42). Moreover, drought has the potential to accelerate ontogenetic development (44, 45). Such alterations of leaf morphology and/or biochemical composition could not only have influenced leaf R after recovery but also have attributed to (or might be the reason for) the unexpectedly great differences in leaf R observed in plants subjected to a second stress period at grain filling. This result contrasts again with the observations of

physiological traits since those were more affected by drought in AG and DG compared to AFG and DFG at grain filling. The less pronounced reaction of physiological traits to a second drought period is attributed to some preconditioning of plants already exposed to drought at flowering and/or the higher amount of green biomass (transpiring surface) of plants from the treatment stressed solely at grain filling. Plants of the treatment stressed twice (AFG and DFG) were watered optimally for eight days after drought at flowering before water supply was halved again. Leaf osmotic potential remained below (more negative) that of control plants during these days providing a better initial situation concerning osmotic adjustment (data not shown) for plants already experiencing a first drought period at flowering.

The differences observed in $\Delta R/R$ during recovery between *T. aestivum* and *T. durum* show that no general prediction can be made concerning the potential to trace recovery from a stress situation with leaf reflectance. Apparently, different species and even cultivars respond inconsistently to drought stress with respect to their spectral signature. Especially the cultivar of *T. aestivum* used in this study (cv. Xenos) appears not promising for tracing recovery with leaf reflectance. In *T. durum* (cv. Floradur) $\Delta R/R$ decreased during recovery within the entire range of the spectrum but the greatest decrease in $\Delta R/R$ occurred in the 1880–1940 nm range. Since this spectral range falls into the main atmospheric water bands it is unsuitable for remote sensing by satellite or airplane. However, to test an eventual potential for short distance remote sensing/ precision farming, we performed simulations of the transmittance in these wavelength ranges using the code LOWTRAN 7 (46) assuming the worst case scenario (99% air humidity). Results showed that at distances below 100 m the transmittance was larger than 50% in the wavelength range 1410–1470 nm. At 1880–1940 nm transmittance became larger than 50% only at distances below 15 m. This shows a potential for a short distance (below 100 m) remote sensing mainly in the wavelength range 1410–1470 nm. This remote sensing application would however at least require an accurate determination of the distance between sensor and canopy, an artificial radiation source (since the solar radiation is already totally absorbed) and an accurate determination of air humidity (to apply a correction to the measured transmittance). Other aspects like sensor sensitivity, characteristics of the radiation source, requirements regarding the accuracy of the sensor to determine plant optical path etc... would be needed to be investigated within the scope of a future study.

In contrast to changes in leaf R within the range of 1410–1470 nm and 1880–1940 nm, which can be attributed mainly to differences in leaf water content, the changes within the visible range are not well defined with respect to a certain stressor. As already described by Carter (47) an increased reflectance at visible wavelengths (400–700 nm) is the most consistent response to stress within the 400–2500 nm range. The often made assumption that the chlorophyll content of leaves was propor-

tional to moisture content (*e.g.* 48) may be correct for some species but cannot be generalized to all ecosystems. Variations in chlorophyll content can be caused by water stress but also by phenological status of the plant, atmospheric pollution, nutrient deficiency, toxicity, plant disease, and radiation stress (39, 49). These findings are supported by the results from the present study where different trends for RWC, Chl_{tot} and leaf [N] were found. Due to these adverse effects of leaf [N] (decrease) and Chl_{tot} (increase) an interpretation of the increased leaf R is difficult. At least the specific cause of these differences remains uncertain. However, the increased Chl_{tot} content found might result from leaf shrinkage leading to a seemingly higher chlorophyll content per unit leaf area ($\mu\text{g cm}^{-2}$).

Finally, three spectral indices (RWC_i , AWC_i and PRI) were tested towards their ability in estimating biophysical parameters (RWC, AWC, A_{sat} and leaf [N]; Table 4). Concerning the estimation of leaf water content a better correlation was found for AWC. Unfortunately, the AWC is the less meaningful parameter since it only gives the water content as percentage of fresh weight which might vary greatly between species, phenology and environmental conditions (39). The RWC, however, represents the actual leaf water content with respect to a standard measure (leaves under conditions of water saturation; (39) and is therefore the more appropriate indicator of plant water status. Moreover, following changes in biophysical parameters using these indices was not possible due to the different extent of changes in leaf R compared to physiological traits under drought stress at different phenological stages. From these results it is concluded that a good relationship between spectral indices and biophysical parameters does not necessarily lead to an appropriate estimation of biophysical parameters at a given phenological state and/or physiological status.

5. CONCLUSION

Drought stress occurring at different phenological stages increased leaf R throughout the whole spectrum. Unfortunately, the degree to which plant physiological traits and water relations changed could not be quantified by the extent of change in leaf R, at least when drought occurred at different phenological stages. The main concern of the present study, however, was to test the ability of leaf reflectance to follow recovery of physiological traits after a stress period which may be of essential importance when considering the occurrence of repeated drought events. Distinguishing between a currently occurring stress situation and an already passed one could become crucial in context with the application of spectral measurements in the field to trace stress situations and to make recommendations on fertilization or irrigation. Unfortunately, recovery from drought stress could not be traced by leaf R since the differences between formerly stressed plants and control plants remained either high as observed in *T. aestivum* or decreased only slightly as in *T. durum*. In neither species leaf R returned to control level despite the complete recovery of physiological traits.

These results, however, also indicate that rather big differences between different species might occur and further investigations using different species with different leaf morphology and anatomy would be needed.

Estimating leaf water content (RWC and AWC) as well as Chl_{tot} and leaf [N] from reflectance measurements gave good correlations. For tracing changes in physiological parameters during phenology and stress periods, however, the use of these indices was not promising due to false estimation of stress situations and recovery (Figure 4, 5). An appropriate estimation appeared, if at all, only possible in unstressed control plants. A good correlation between spectral indices and physiological parameters alone is therefore not necessarily sufficient for estimating physiological parameters from leaf spectra appropriately.

Acknowledgement: This research was financially supported by the Fonds zur Förderung der wissenschaftlichen Forschung (FWF; Austria; grant number P17647-N04). Franz Suppan is thanked for performing spectral measurements.

REFERENCES

- HILLEL D, ROSENZWEIG C 2002 Desertification in relation to climate variability and change. *Advances in Agronomy* 77: 1–38
- IPCC 2007 CLIMATE CHANGE 2007: The physical science basis, summary for Policymakers, Contribution of Working Group I to the Fourth Assessment Report of the Intergovernmental Panel on Climate Change, International Panel on Climate Change. WMO UNEP report.; www.ipcc.ch
- LAWLOR D W, MITCHELL R A C 1991 The effects of increasing CO_2 on crop photosynthesis and productivity: a review of field studies. *Plant, Cell & Environment* 14: 807–818
- CURCIO J A, PETTY C C 1951 The near infrared absorption spectrum of liquid water. *Journal of the Optical Society of America* 41: 302–304
- BOWMAN W D 1989 The relationship between leaf water status, gas exchange, and spectral reflectance in cotton leaves. *Remote Sensing of Environment* 30: 249–255
- HUNT E R, ROCK B N 1989 Detection of changes in leaf water content using near- and middle-infrared reflectance. *Remote Sensing of Environment* 30: 43–54
- CARTER G A 1991 Primary and secondary effects of water content on the spectral reflectance of leaves. *American Journal of Botany* 78: 916–924
- PARRY M A J, ANDRALOJC P J, KHAN S, KEYS A J 2002 Rubisco activity: effects of drought stress. *Annals of Botany* 89: 833–839
- KNIPLING E B 1970 Physical and physiological basics for the reflectance of visible and near-infrared radiation from vegetation. *Remote Sensing of Environment* 1: 155–159
- CARTER G A, MITCHELL R J, CHAPPELKA A H, BREWER C H 1992 Response of leaf spectral reflectance in loblolly pine to increased atmospheric ozone and precipitation acidity. *Journal of Experimental Botany* 43: 577–584
- CARTER G A, KNAPP A K 2001 Leaf optical properties in higher plants: Linking spectral characteristics to stress and chlorophyll concentration. *American Journal of Botany* 88(4): 677–684
- AYALA-SILVA T, BEYL C A 2005 Changes in spectral reflectance of wheat leaves in response to specific macronutrient deficiency. *Advances in Space Research* 35: 305–317
- CHAVES M M, PEREIRA J S, MAROCO J, RODRIGUES M L, RICARDO C P P, OSÓRIO M L, CARVALHO I, FARIA T, PINHEIRO C 2002 How plants cope with water stress in the field. Photosynthesis and growth. *Annals of Botany* 89: 907–916
- SCHÄR C, VIDALE P L, LÜTHI D, FREI C, HÄBERLI C, LINIGER M A, APPENZELLER C 2004 The role of increasing temperature variability in European summer heatwaves. *Nature* 427: 332–336

15. VIDALE P L, LÜTHI D, WEGMANN R, SCHÄR C 2007 European climate variability in a heterogeneous multi-model ensemble. *Climatic Change* 81: 209-232
16. SENEVIRATNE S I, LÜTHI D, LITSCHI M, SCHÄR C 2006 Land-atmosphere coupling and climate change in Europe. *Nature* 443: 205-209
17. KICK H, GROSSE-BRAUCKMANN E 1961 Über die Konstruktion eines Vegetationsgefäßes aus Kunststoff. *Zeitschrift für Pflanzenernährung, Düngung und Bodenkunde* 95(140): 52-55
18. MARKWELL J, OSTERMANN J C, MITCHELL J L (1995). Calibration of the Minolta SPAD-502 leaf chlorophyll meter. *Photosynthesis Research* 46: 467-472
19. INSKEEP W P, BLOOM P R 1985 Extinction coefficients of Chlorophyll a and b in N,N-Dimethylformamide and 80% Acetone. *Plant Physiology* 77: 483-485
20. LÖSCH R 2003 Wasserhaushalt der Pflanzen. Vlg. Quelle & Meyer, p 39
21. BILGER W, BJÖRKMANN O, THAYAS S 1989 Light-induced spectral absorbance changes in relation to photosynthesis and the epoxidation state of xanthophylls cycle components in cotton leaves. *Plant Physiology* 91: 542-551
22. GAMON J A, FIELD C B, BILGER W, BJÖRKMANN O, FREDEEN A L, PENUELAS J 1990 Remote sensing of the xanthophylls cycle and chlorophyll fluorescence in sunflower leaves and canopies. *Oecologia* 85: 1-7
23. GAMON J A, SERRANO L, SURFUS J S 1997 The photochemical reflectance index: an optical indicator of photosynthetic radiation use efficiency across species, functional types, and nutrient levels. *Oecologia* 112: 492-501
24. PENUELAS J, FILELLA I 1998 Visible and near infrared reflectance techniques for diagnosing plant physiological status. *Trends in Plant Science* 3(4): 151-156
25. DAVENPORT J R, LANG N S, PERRY F M 2000 Leaf spectral reflectance for early detection of disorders in model annual and perennial crops. ASA-CSSA-SSSA, 677 Segoe Road, Madison, WI 53711, USA. *Proceedings of the Fifth International Conference on Precision Agriculture*.
26. YU G-R, MIWA T, NAKAYAMA K, MATSUOKA N, KON H 2000 A proposal for universal formulas for estimating leaf water status of herbaceous and woody plants based on spectral reflectance properties. *Plant and Soil* 227: 47-58
27. CORNIC G, MASSACCI A 1996 Leaf photosynthesis under drought stress. In: *Photosynthesis and the Environment* (ed. N.R. Baker), Kluwer Academic Press, p 347-366
28. LAWLOR D W, CORNIC G 2002 Photosynthetic carbon assimilation and associated metabolism in relation to water deficit in higher plants. *Plant, Cell & Environment* 25: 275-294
29. FLEXAS J, MEDRANO H 2002 Drought inhibition of photosynthesis in C₃ plants: stomatal versus non-stomatal limitations revisited. *Annals of Botany* 89: 183-189
30. CORNIC G 1994 Drought stress and high light effects on leaf photosynthesis. In: *Photoinhibition of Photosynthesis* (eds N.R. Baker and J.R. Bowyer), BIOS, Scientific Publishers, p 297-313
31. LAWLOR D W 1995 The effects of water deficits on photosynthesis. In: *Environment and plant metabolism* (ed. Smirnov). BIOS Scientific Publishers, Oxford, p 129-160
32. BRODRIBB 1996 Dynamics of changing intercellular CO₂ concentration (Ci) during drought and determination of minimal functioning Ci. *Plant Physiology* 111: 179-185
33. MEDRANO H, ESCALONA J M, BOTA J, GULÍAS J, FLEXAS J 2002 Regulation of photosynthesis of C₃ plants in response to progressive drought: stomatal conductance as a reference parameter. *Annals of Botany* 89: 895-905
34. WOOLLEY 1971 Reflectance and Transmittance of Light by Leaves. *Plant Physiology* 47: 656-662
35. PENUELAS J, INOUE Y 1999 Reflectance indices indicative of changes in water and pigment contents of peanut and wheat leaves. *Photosynthetica* 36(3): 355-360
36. YORDANOVI, VELIKOVA V, TSONEV T 2000 Plant responses to drought stress, and stress tolerance. *Photosynthetica* 38(2): 171-186
37. READ J, STOKES A 2006 Plant biomechanics in an ecological context. *American Journal of Botany* 93(10): 1546-1565
38. LAMBERS H, CHAPIN III FS, PONS T L 1998 »Plant Physiological Ecology«. Springer.
39. LARCHER W 2003 »Physiological Plant Ecology – Ecophysiology and Stress Physiology of Functional Groups«. Springer (4th edition).
40. JORDAN W R, MONK R L, MILLER F R, ROSENOW D T, CLARK L E, SHOUSE P J 1983 Environmental physiology of sorghum. I. Environmental and genetic control of epicuticular wax load. *Crop Science* 23: 552-558
41. JOHNSON D A, RICHARDS R A, TURNER N C 1983 Yield, water relations, gas exchange and surface reflectances of near-isogenic wheat lines differing in glaucousness. *Crop Science* 23: 318-325
42. DENG X-P, SHAN L, INANAGA S, INOUE M 2005 Water-saving approaches for improving wheat production. *Journal of the Science of Food and Agriculture* 85: 1379-1388
43. SEHPERD T, GRIFFITHS D W 2006 The effect of stress on plant cuticular waxes. *New Phytologist* 171: 469-499
44. FOYER C H, DESCOURVIÈRES P, KUNERT K J 1994 Protection against oxygen radicals: an important defence mechanism studied in transgenic plants. *Plant, Cell & Environment* 17: 507-523
45. KIMBALL B A 1995 Productivity and water use of wheat under free air CO₂ enrichment. *Global Change Biology* 1: 429-442
46. KNEIZYS F X, SHETTLE E P, ABREU L W, CHETWYND J H, ANDERSON G P, GALLERY W O, SELBY J E A, CLOUGH S A 1988 Users guide to Lowtran 7. AFGL-TR-88-0177, Air Force Geophysics Laboratory.
47. CARTER G A 1994 Ratios of leaf reflectances in narrow wavebands as indicators of plant stress. *International Journal of Remote Sensing* 15(3): 697-703
48. TUCKER C J 1977 Asymptotic nature of grass canopy spectral reflectance. *Applied Optics* 16(5): 1151-1156
49. CECCATO P, FLASSE S, TARANTOLA S, JACQUEMOUD S, GRÉGOIRE J-M 2001 Detecting vegetation leaf water content using reflectance in the optical domain. *Remote Sensing of Environment* 77: 22-33

5 Anhang (Bestätigung der Publikation I)

03-May-2009

Dear Ms. Richter:

I am pleased to inform you that your manuscript entitled: "Experimental assessment of the Sentinel-2 band setting for RTM-based LAI retrieval of sugar beet and maize" has been accepted as a Research Article for publication in the Canadian Journal of Remote Sensing.

Your manuscript will be forwarded to the National Research Council Research Press for publication and in you should expect to hear from them directly concerning your galley proofs.

If you have not already done so, would you please read the attached Copyright and Publication Charge files, fill out the appropriate parts of these forms and return them to me by mail or by fax as indicated on the forms.

Thank you for your interest in publishing in the Canadian Journal of Remote Sensing.

The AE has prepared a new version of the abstract of the paper in FRENCH. It is attached for your interest and I assume you will be happy with it. If not, please let me know. Else I will pass this new one to NRC Press.

Congratulations

Sincerely,

Prof. Nicholas Coops
Editor in Chief, Canadian Journal of Remote Sensing
editor.cjrs@ubc.ca

6 Lebenslauf/CV

Persönliche Daten

Name	Katja Richter
Geburtstag	06.09.1978
Geburtsort	Dresden
Land	Deutschland
Staatsbürgerschaft	Deutschland

Ausbildung

1985-1997	J. Haydn-Gymnasium Dresden-Striesen (Abschluss Abitur, 15.07. 1997), Dtl.
1997-2003	Studium Geographie, TU Dresden, Dtl., und Universität Wien, Ö. Spezialisierung: Klimatologie und Geoinformatik
Ab 2004	Studium Doktorat, Universität für Bodenkultur Wien (BOKU), Fachrichtung Landwirtschaft/ Fernerkundung

Beruflicher Werdegang

2001-2008	Tutorin, Studienassistentin und Lektorin für zahlreiche Lehrveranstaltungen im Bereich Geographie/Klimatologie/GIS/Fernerkundung an der Universität Wien, BOKU und Universität Federico II di Napoli, Italien.
2004-2005	Mitarbeiterin im Laboratorium für Umweltanalytik GesmbH, Wien, Ö.
2005-2007	Wissenschaftliche Mitarbeiterin am Institut für Vermessung, Fernerkundung und Landinformation (IVFL) der Universität für Bodenkultur, Wien, im Rahmen des Projekts: Crop Drought Stress Monitoring by Remote Sensing (DROSMON).
seit 2007	Wissenschaftliche Mitarbeiterin an der Universität Federico II di Napoli, Italien, im Rahmen des EU Projekts: Participatory multi-Level EO-assisted tools for Irrigation water management and Agricultural Decision-Support (PLEIADeS).

Internationale Aktivitäten

seit 2004	Teilnahme an zahlreichen internationalen Kongressen und Workshops (EGU, SPIE, RAQRS, IGARSS, ISRSE u. a.).
seit 2008	Session Co-Chair, SPIE Europe Remote Sensing.
Wien	Juni 2009